FOSSIL

DOE/PC/89883-30
(DE92008466)

COAL LIQUEFACTION PROCESS STREAMS CHARACTERIZATION AND EVALUATION

Novel Analytical Techniques for Coal Liquefaction: Fluorescence Microscopy

Topical Report

By
R. F. Rathbone
J. C. Hower
F. J. Derbyshire

October 1991

Work Performed Under Contract No. AC22-89PC89883

For
U.S. Department of Energy
Pittsburgh Energy Technology Center
Pittsburgh, Pennsylvania

By
University of Kentucky
Lexington, Kentucky

DISCLAIMER

Printed in the United States of America, Office of Scientific and Technical Information, Oak Ridge , Tennessee

DOE/PC/89883--30

DE92 008466

CONSOLIDATION COAL COMPANY
RESEARCH AND DEVELOPMENT DEPARTMENT
4000 BROWNSVILLE ROAD
LIBRARY, PA 15129

COAL LIQUEFACTION PROCESS STREAMS CHARACTERIZATION AND EVALUATION

NOVEL ANALYTICAL TECHNIQUES FOR COAL LIQUEFACTION: FLUORESCENCE MICROSCOPY

TOPICAL REPORT

Prepared By

University of Kentucky
Center for Applied Energy Research
3572 Iron Works Pike
Lexington, KY 40511-8433

R. F. Rathbone, J. C. Hower, and
F. J. Derbyshire

OCTOBER 1991

U.S. DOE patent clearance was provided by Chicago Operations Office on 8/5/91.

Prepared for
Consolidation Coal Company
Research and Development Department
4000 Brownsville Road
Library, PA 15129

F. P. Burke
R. A. Winschel
S. D. Brandes

Under Contract to:
United States Department of Energy
Contract No. DE-AC22-89PC89883

PROJECT ASSESSMENT

Introduction

Under subcontract to Consolidation Coal Co. (U.S. DOE Contract No. DE-AC22-89PC89883), the University of Kentucky/Center for Applied Research (UK/CAER) studied the use of fluorescence microscopy for analysis of coal-derived materials. The full report authored by the UK/CAER researchers is presented here. The following assessment briefly highlights the major findings of the project, and provides Consol's evaluation of the potential of the method for application to coal-derived materials. These results will be incorporated by Consol into a general overview of the application of novel analytical techniques to coal-derived materials.

Summary

This study demonstrated the feasibility of using fluorescence and reflectance microscopy techniques for the examination of distillation resid materials derived from direct coal liquefaction. Resid, as defined here, is the 850°F$^+$ portion of the process stream, and includes soluble organics, insoluble organics and ash. The technique can be used to determine the degree of hydrogenation and the presence of multiple phases occurring within a resid sample. It can also be used to infer resid reactivity. The technique is rapid, requiring less than one hour for sample preparation and examination, and thus has apparent usefulness for process monitoring. Additionally, the technique can distinguish differences in samples produced under various process conditions. It can, therefore, be considered a potentially useful technique for the process developer. Further development and application of this analytical method as a process development tool is justified based on these results.

Program Description

This report describes the work performed at the University of Kentucky/ Center for Applied Energy Research (UK/CAER) under a subcontract to Consolidation Coal Co., Research and Development. Consol's prime contract to the U.S. Department of Energy (Contract No. DE-AC22-89PC89883, "Coal Liquefaction Process Streams Characterization and Evaluation") established a program for the analysis of direct coal liquefaction derived materials. The program involves a number of participating organizations whose analytical expertise is being applied to these materials. This Participants Program has two main objectives.

The broad objective is to improve our understanding of fundamental coal liquefaction chemistry to facilitate process improvement and new process development. The specific approach to achieving this objective is to provide a bridge between direct coal liquefaction process development and analytical chemistry by demonstrating the application of various advanced analytical methods to coal liquefaction materials. The methodologies (or techniques) of interest are those which are novel in their application for the support of coal liquefaction, and those which have not been fully demonstrated in this application. Consol is providing well-documented samples from different direct coal liquefaction production facilities to the program participants. The participants are required to interpret their analytical data in context to the processing conditions under which the samples were generated. The methodology employed then is evaluated for its usefulness in analyzing direct coal liquefaction derived materials.

Participant's Methodology

UK/CAER used fluorescence and reflectance microscopy to analyze distillation resids ($850°F^+$). These are solids at room temperature, and contain THF-soluble and -insoluble organics and mineral matter. The samples were produced at two different continuous liquefaction facilities: the 6TPD Wilsonville Advanced Coal Liquefaction R&D Facility and the 30-50 lb/day Hydrocarbon Research Inc. (HRI) bench unit. Two major processing parameters were varied among the Wilsonville runs. These were feed coal and reactor configuration (thermal/catalytic vs. catalytic/catalytic). Samples from Wilsonville were taken from two locations: between the reactors and after the second-stage reactor. These samples are expected

to represent different extents of coal liquefaction. The Wilsonville samples were composites of samples taken over long periods of single runs. Samples from HRI were chosen to represent production of material as the catalyst aged during one liquefaction run.

Major Findings Reported by UK/CAER

The following principal observations for the application of fluorescence and reflectance microscopy to coal liquefaction materials were reported by UK/CAER. An expanded discussion can be found in the report, pages 15-33. Fluorescence and reflectance spectra of distillation resids were measured through the use of a microscope photometer system. Wilsonville samples taken at different sampling locations in the plant were found to exhibit distinct variations in fluorescence intensities and spectral distribution. The degree of upgrading the process stream undergoes in the production facility could be evaluated from this information. Relative resid reactivity also could be inferred by direct comparison of the spectral intensities and wavelengths of the fluorescence spectra, and the reflectance spectra, of different samples within a single production run and of samples from different runs. The inferred reactivities are consistent with complementary information such as volatile matter contents, aromaticities and phenolic -OH infrared peak positions, as well as with fundamental factors affecting fluorescence and reflectance. With homogeneous samples, such as the HRI samples, the repeatability of the technique is well within inter-sample variability.

Consol Evaluation

The fluorescence microscopic technique was shown to be potentially useful for the analysis of solid direct coal liquefaction resid samples. A specific and unique advantage of this technique for the analysis of resids is that the whole resid samples can be examined without alteration. This results in a particularly important feature of the technique which is the ability to detect and quantify inhomogeneous components of solid resid samples including unreacted macerals, mineral matter, and multiple resid phases. In addition to qualitative observations, the technique can provide quantitative data. The measured fluorescence intensities provide a relative scale to determine the degree of aromatic condensation found in different samples. The interpretation of these values in the context of coal liquefaction and resid reactivity could indicate which resids are more refractory to upgrading. The determination of red/green quotients (Q), obtained from the fluorescence spectra, is a rapid method to assess the degree of fluorescence heterogeneity of the resids. The fluorescence spectrum apparently is responsive to process trends. The degree of liquefaction or upgrading of coal liquids is discernable among different samples taken at different points in the continuous liquefaction process. In addition, the relative degree of resid hydrogenation can be determined in samples taken consecutively during a liquefaction run in which the major process change is catalyst age.

It is difficult to assess the precision of the technique due to the inherent variabilities of the samples examined here. However, when homogeneous samples, or the portion of heterogeneous samples displaying

only one fluorescence population, are examined, repeatability is good. Long-term reproducibility of fluorescence results can be poor and misleading if spectral changes in the mercury arc lamp emissions, as the lamp ages, are not considered. Inter-laboratory comparisons of data generated outside the scope of this program show that while relative results are consistent, absolute values are not reproducible. An expanded discussion on these points can be found in the report, pages 34-39.

The repeatability of the method and its ability to discern differences and similarities among samples were tested through the use of two "blind" samples. The UK researchers correctly identified that blind sample No. 13 was very similar to sample No. 12 (a homogeneous sample; the pressure filter liquid resid from HRI Run I-27, period 25). In fact, sample Nos. 12 and 13 are aliquots of the same sample. The UK researchers indicated that blind sample No. 14 was most similar to sample No. 1 (the interstage resid from Wilsonville Run 251-II). Actually, sample No. 14 was a separate aliquot of sample No. 2 (the recycle resid from Wilsonville Run 251-II). The Wilsonville Run 251-II samples were highly heterogeneous. Therefore, the UK researchers correctly identified the one homogeneous blind sample and correctly identified the processing run (but not the sampling location) of the one heterogeneous blind sample. Considering the high degree of heterogeneity found in the one blind sample, the fluorescence method proved to be useful for identification of the two unknowns. See page 32 of the report for detailed discussion.

The technique is relatively rapid, requiring about one-half hour for sample preparation and only a few minutes for sample examination. The initial capital investment, including the cost of the microscope, computer, lenses, and ancillary equipment, is approximately $85,000. The labor costs are relatively low. Once the initial system is set up, the sample preparation and examination can be done by a laboratory technician. Data interpretation is minimal for samples taken within a single process in which variables, such as catalyst age, are changed systematically. Data can be quantified and interpreted based on an established calibration.

Further Development

There are a number of avenues for further development of this technique for coal liquefaction materials. Additional chemical information may be obtainable from a more sophisticated analysis of the fluorescence spectra. Quantification of the qualitative observations may be possible through the use of a calibration that is based on well-controlled liquefaction experiments in which process variables are systematically changed. Sample preparation times can be substantially reduced if faster setting epoxy resins can be found which do not interfere with the microscopic analysis. The automation of the technique may lead to an at-site, or near-line, method for process monitoring.

NOVEL ANALYTICAL TECHNIQUES FOR COAL LIQUEFACTION: FLUORESCENCE MICROSCOPY

by:
R.F. Rathbone
J.C. Hower
F.J. Derbyshire

UNIVERSITY OF KENTUCKY
CENTER FOR APPLIED ENERGY RESEARCH

March 1991

Executive Summary

Under U.S. Department of Energy Contract No. DE-AC22-89PC89883, it is the intent of the Consolidation Coal Company, Pittsburgh, PA, to investigate and develop existing analytical techniques which could potentially lead to more effective liquefaction process control. In this context, it is the goal of this subcontract to evaluate the usefulness of a fluorescence microscopy methodology for the analysis of coal-derived resids and interpret the data in light of liquefaction processing conditions, process response, the inferred resid reactivity, and in relation to results of other analytical data. The fluorescence technique utilized in this study, has been widely applied to coal and kerogen characterization, albeit with some modifications, but is novel in its application to the characterization of coal liquids.

Fluorescence spectra (ultraviolet-violet light), and reflectances (white light) of non-distillable (850°F$^+$, or 454°C$^+$) coal liquids (resid) were measured by a microscope spectrophotometer system. The fluorescence emission, from 470 to 700nm, was taken from a polished resid sample surface by scanning at least 5 resid particles per sample, with the spectrum for each particle representing the average of 20 scans. The proportion of white light reflected of a polished resid surface (% reflectance), in air immersion, was measured for 25 resid particles per sample, and reported as a mean value. Volatile matter yield was also obtained for each sample, as an approximate indicator of resid reactivity.

Well-documented resid samples from the Wilsonville CC-ITSL pilot plant and HRI CTSL ebullated bed bench unit were provided by Consolidation Coal Company,

Pittsburgh, PA. Fluorescence, reflectance, and chemical data for Wilsonville Runs 250, 251-II, 257, and 259 were interpreted in relation to reactor modes (catalytic/catalytic vs. thermal/catalytic), sample location (interstage vs. recycle), and coal feedstock, although other processing parameters were varied over the course of these runs. Pressure filter liquid resids from HRI Run I-27 were instantaneous samples, produced under more stable operating conditions, with monotonic changes in catalyst age, reactor temperatures, solvent cut-point, and the solvent/coal ratio as the run progressed. Two (2) unidentified resid samples were provided for experimental control.

It was concluded from an evaluation of the fluorescence microscopical technique that experimental precision was difficult to assess for the Wilsonville resids because of the inherent sample fluorescence variability. The interstage and recycle resids from Run 257 (Illinois #6 coal, C/C) exhibited distinct, usually inter-particle, variations in fluorescence intensities and spectral distributions. The Run 251-II (Wyodak coal, T/C) recycle resid contained an intensely yellow fluorescing component whose fluorescence properties were distinctly different to the majority of the resid. Although the origin of this material is problematical, its presence may indicate that the resid contains two or more incompatible phases, and illustrates a distinct advantage of the fluorescence microscopy technique: the ability to resolve inhomogeneities within resid samples. The analytical precision of the technique was evaluated with more homogeneous resid samples, such as the Wilsonville Run 250 (Illinois #6 coal, T/C) resids and, particularly, the pressure filter liquids from HRI Run I-27, which revealed that spectral intensities are repeatable within 3 to 4 nm.

Within the precision limits of the microscopical techniques, it was concluded that resids from Wilsonville Runs 251-II (Wyodak coal, T/C), 250 (Illinois #6 coal, T/C), and 257 (Illinois #6 coal, C/C) had been upgraded to less condensed, lower molecular weight products in the second stage when compared to the interstage resids. This is based on a shift of the average fluorescence spectra to shorter wavelengths, concomitant with an intensity increase and reflectance decrease, from the interstage to recycle resid samples. Fluorescence spectra for Run 259 (Pittsburgh coal, C/C) interstage and recycle resids were nearly identical, suggesting that the second catalytic stage provided only minor additional hydrogenation.

Interpretations of fluorescence in the context of resid reactivity were founded on the supposition that resids comprised of more highly condensed aromatics are relatively refractory to upgrading and would exhibit relatively high reflectance values, low fluorescence intensities, and maximum fluorescence intensities shifted to longer wavelengths. It was therefore concluded that the Run 257 resids (Illinois #6 coal, C/C) were probably the most reactive, as evidenced by lower reflectances, high volatile matter yields, and shorter fluorescence spectral peak wavelengths than the other Wilsonville resids investigated, followed by resids from Run 250 (Illinois #6 coal, T/C) and 251-II (Wyodak coal, T/C). Resids produced in Run 259 (Pittsburgh coal, C/C) would probably be the least reactive, based on relatively high reflectances, low volatile matter yields, and fluorescence spectra shifted to longer wavelengths than the other Wilsonville resids studied.

Fluorescence and reflectance data suggest that during HRI Run I-27 (Illinois #6 coal, C/C), there was progressively less hydrogenation of the resid with increasing

catalyst age, reactor temperature, and solvent cut-point, and a decrease in the solvent/coal ratio. This was supported by proton nmr data and phenol peak location shifts, which indicated an increased condensation of aromatic structures during the run. A decrease in the volatile matter yield of resids from run day 2 to day 25 suggests that a decrease in resid reactivity occurred over the course of HRI Run I-27.

It is concluded that quantitative fluorescence microscopy is potentially a rapid, inexpensive technique which can provide new insight into the structure and composition of coal-derived resid. Consequently, an automated fluorescence micrscopical technique, as an integral component of a liquefaction process monitoring scheme, could lead to more effective process control. Perhaps the greatest strength of quantitative fluorescence microscopy lies in its ability to resolve inhomogeneities within coal-derived resid samples, including, but not limited to, minerals, unreacted macerals, and multiple resid phases (as determined by reflectance and fluorescence properties). This capability is not possible with most other analytical techniques which typically require dissolution of the resid in a solvent prior to analysis. Whereas these analytical techniques provide chemical and structural information on a homogenized resid sample, and only on the solvent-soluble portion, inherent variability within the coal liquids can be identified and measured with fluorescence microscopical methods.

Table of Contents

I. Introduction

A. Description and Goals

A.1. Purpose

Under U.S. Department of Energy Contract No. DE-AC22-89PC89883, it is the intent of the Consolidation Coal Company, Pittsburgh, PA, to fully exploit existing analytical techniques which could potentially bring new insight into the structure and composition of coal products, and possibly lead to more effective process control. Techniques of interest to this project are those that are novel only in that they have not been fully applied to coal liquefaction process development, and so are potentially under-utilized in this area of research. In this context, it is the goal of this subcontract to evaluate the usefulness of a fluorescence microscopical methodology for the analysis of coal-derived resid and interpret the data in the context of the liquefaction processing conditions and resid reactivity. The fluorescence technique utilized in this study, has been widely applied in coal and kerogen characterization, albeit with some modifications, but is novel in it application to the characterization of coal liquids.

A.2. Background

Fluorescence microscopy has been employed as an analytical tool in organic petrology for approximately 25 to 30 years and has been used extensively in plant biological research since the 1920's and 30's (1). It is reported by George (1989) that luminescence has been an important analytical tool in polymer characterization for over 25 years. Although optical microscopy has also been employed to characterize hydrogenation residues from microautoclave experiments (3,4,5), fluorescence has

played a relatively minor, and qualitative role.

Shiboaka and Russell (1983) described how qualitative fluorescence microscopical techniques can be utilized to "permit the clear observation of very low reflectance material" in hydrogenation residues, and provide a rough estimate of the relative reactivity of macerals during hydrogenation. Fluorescence microscopy has also been employed to characterize vitrinite before and after hydrogenation (7). Davis et. al. (1986) report that with an increase in reactor temperature and/or reaction time, the fluorescence intensity of catalytically hydrogenated vitrinite increased markedly, concomitant with an increase in extractable liquid yield, while the wavelength of maximum intensity (herein referred to as Lmax) exhibited a progressive shift to longer wavelengths. The authors considered this to be a result of the liberation of extractable liquids from a breakdown of the macromolecular structure of coal (intensity increase), while the proportion of condensed aromatics increased with increasing liquid yield (shift to longer wavelengths). Analyses of the oil and asphaltene fractions from these experiments showed that the oils had greater fluorescence intensity and shorter peak wavelengths than the highly aromatic asphaltenes (7). Lin et. al. (1987), also studying vitrinite hydrogenation, observed a fluorescence intensity increase compared to non-hydrogenated vitrinite, corresponding to an increase in the proportion of chloroform soluble material within the coal. This was attributed to the generation of smaller molecular fragments within the vitrinite macerals.

Although previous research efforts discussed above have applied fluorescence microscopy techniques to hydrogenation residues (sometimes solvent extracted) from

microautoclave experiments, the present study attempts to apply similar techniques to high molecular weight coal liquids, specifically, the non-distillable liquids at 850°F$^+$ (454°C$^+$). Well-documented samples from the Wilsonville CC-ITSL coal liquefaction pilot plant and the HRI CTSL bench unit provide an opportunity to evaluate fluorescence microscopical techniques as indicators of liquefaction process performance. However, the interpretation of results is complicated by the numerous changes in operating conditions which occurred during the Wilsonville runs, in addition to differences in processing modes and coal feedstocks between the different runs. Therefore, fluorescence data from the Wilsonville samples were not interpreted in the context of specific processing variables, such as temperature, but in a more general context e.g. interstage vs. recycle sample locations, catalytic/catalytic vs. thermal/catalytic reactor modes, and different coal types. In contrast, fluorescence analyses of HRI resids are interpretable in terms of more specific variables, such as catalyst age. Before discussing the fluorescence experimental methods employed, it is worthwhile to briefly discuss the fluorescence of organic molecules, especially in the solid state.

B. Fluorescence of Organic Molecules

Luminescence is the emission of light energy which occurs when electrons, having been excited to a higher energy orbital, return to their lower energy ground state. Two types of luminescence are distinguished by their radiative lifetimes; fluorescence, which occurs from an excited singlet state (S1), has a radiative lifetime on the order of 10^{-9} to 10^{-6} seconds, whereas for phosphorescence, occurring from an

excited triplet state via intersystem crossing, radiative lifetimes are on the order of 10^{-4} secs and longer (9). The long radiative lifetimes of phosphorescence are such that bi-molecular quenching (discussed below) of the triplet state is encouraged, making phosphorescence in air at room temperature either very weak or totally absent (10).

The majority of organic molecules that fluoresce are those with conjugated double bonds, such as aromatics and alkenes, characterised by pi-electrons less strongly bound within the molecule than sigma electrons, that can be excited to anti-bonding pi-orbitals (10,11). The absence of these bonds, which are referred to as chromophores (12), in aliphatic and saturated cyclic organic compounds dictates that few of these molecules fluoresce (10,11). Furthermore, since alkenes are practically non-existent in sedimentary organic matter due to their relative instability, fluorescence of coal occurs primarily from aromatic structures (12).

Figure 1 is a schematic energy level diagram for unimolecular photophysical processes, occurring from isolated chromphores (i.e. in dilute solution), and include energy absorption, internal conversions, intersystem crossing, and luminescence. Fluorescence spectra from these isolated chromophores consist of bands corresponding to transitions from S1 to the vibrational levels of the ground state (Figure 1). Internal conversions and intersystem crossing convert some electronic energy into vibrational energy, and so decrease the radiating power of the system (13).

Increasing the extent of pi-bond conjugation (i.e. larger molecular size) generally imparts a shift in absorption and emission spectra to longer wavelengths,

resulting from a lower energy difference between S1 and the ground state (14). For example, in liquid solution, benzene and naphthalene fluoresce in the ultraviolet, whereas anthracence exhibits blue, and pentacene red, fluorescence (11).

Substituents on aromatic rings have varying effects on fluorescence, although in general, those which decrease pi-electron mobility in the aromatic ring(s) tend to diminish fluorescence (10). For example, mono-substituted aromatics containing C=O and COOH substituents are weakly to non-fluorescent, whereas benzene itself is fluorescent. This is due to a partial deactivation of the ring by the C=O and COOH groups via withdrawal of pi-electrons (11,14). Conversely, electron donating substituents such as -OH generally cause an intensity increase, although the effects of other interactions associated with hydroxyl groups, such as hydrogen bonding, are complex and very difficult to predict (11).

The fine structure of fluorescence spectra obtained from isolated chromophores is replaced by broad, featureless spectra when fluorescence emission is measured from concentrated solutions, due to bimolecular photophysical processes. These processes involve the energy transfer from an excited "donor" molecule to another molecule ("acceptor") with lower-lying energy levels, through re-absorption of fluorescence emission and dipole-dipole interactions (2,10,11). Re-absorption of fluorescence emission is especially severe in concentrated solutions of chromophores where there is overlap between donor emission and acceptor absorption (2,10). The result is typically a red shift and intensity reduction of measured fluorescence. This phenomenon has been investigated in organic petrology using crude oil

chromatographic fractions (12). The fluorescence spectrum of a 100% aromatic fraction was initially measured, followed by successive dilution of this material in a non-fluorescing paraffin oil. The results, shown in figure 2 reveal that a progressive "blue shift" and intensity increase results with increasing dilution of the aromatic chromophores.

Another common process which quenches monomer fluorescence is the interaction of an electronically excited molecule with an identical unexcited molecule to form a transitory excited state dimer (or "excimer"), from which fluorescence is emitted (2,10). Excimer formation is of great importance when there are high local concentrations of aromatic chromophores. Figure 3 shows the low energy, structureless fluorescence emission of a relatively high concentration of pyrene in methanol (compared with that from a more dilute solution), attributed to excimer formation. An exciplex is much like an excimer, except the ground state molecule is different than the excited species; a structureless emission or radiationless transition commonly results, along with an intensity reduction (2,10,14).

The bimolecular processes described above are important in solid state fluorescence, and so are of particular interest to this study. In solid polymers, singlet excitation energy is de-localized through dipole-dipole intermolecular interactions between identical and non-identical chromophores, such that the excitation is considered to occur over many chromophores (2). As with solutions, exciplex formation, and energy re-absorption by molecules with lower lying energy levels are considered important (2). The expression of these processes in solid state

fluorescence is usually a loss of spectral resolution (Figure 4), a shift of fluorescence spectra to longer wavelengths, and a loss of intensity (2).

The implications of the foregoing discussion to the study of complex, high molecular weight materials such as coal and derived liquids, is that there are likely to be many chromophore species at relatively high local concentrations in a solid medium. Therefore, the fluorescence spectra acquired from such materials are expected to be broad and rather structureless, with relatively low intensities, since there is a higher probability for quenching processes and complex formation to occur. In this respect, Lin and Davis (1988) proposed that the highly aromatic macromolecular network of vitrinite is too condensed to display visible fluorescence, and cited extensive delocalization of pi-electrons as the cause of the fluorescence quenching.

The importance of bimolecular processes to resid fluorescence will depend largely on the concentration and degree of conjugation of aromatic chromophores in the high molecular weight liquids, possibly with ancillary effects from oxygen functionalities. It is evident from these considerations that fluorescence analysis of liquefaction resids has the potential to evaluate process performance, since direct liquefaction processes endeavor to break down the macromolecular structure of coal, and reduce the molecular weight of polycondensed aromatics through hydrogenation, the opening of ring structures, and removal of heteroatoms. In this context, the hydrogenation of a simple condensed aromatic molecule, anthracene, to 9,10 dihydroanthracene results in a shift of the blue anthracene fluorescence into the

ultraviolet (14), and provides an illustration of the changes which might be observed due to different degrees of hydrotreatment.

II. Materials and Methods

A. Description of Samples

Composited resid samples (combined samples from an entire liquefaction run) received from Consolidation Coal Co. consisted of eight (8) non-distillable (at 850°F$^+$ or 454°C$^+$), coal liquids (resid) from Wilsonville CC-ITSL runs 251-II, 259, 250, and 257, four (4) pressure filter liquids (PFL) from the HRI ITSL bench unit (Run I-27), and two samples unidentified for experimental control (Table 1). All samples were brittle solids at room temperature, with a top size of approximately 8 mesh.

Generalized flow sheets from the close coupled integrated two stage liquefaction (CC-ITSL) system at Wilsonville, AL, and the HRI CTSL ebullated bed bench unit are provided in Appendix I. Included on the flow sheets are the sampling locations for resids analyzed in this study.

Wilsonville Run 251-II was operated in the thermal/catalytic mode (although disposable iron oxide was added to the first stage) with a subbituminous (Wyodak) feedstock. Run 259 was operated with a cleaned high volatile A bituminous coal (Pittsburgh) in a catalytic/catalytic configuration. Wilsonville Runs 250 and 257 utilized a high volatile C-B bituminous coal (Illinois #6). However, Run 250 was a thermal/catalytic run, whereas Run 257 was operated with supported catalyst in both stages (Appendix II). HRI Run I-27, also used an Illinois #6 feedstock, and was a

catalytic/catalytic run. Samples from HRI Run I-27 are pressure filter liquid resids, and so consist almost entirely of residual coal liquids, whereas the Wilsonville samples are comprised of unreacted macerals and inorganic matter in addition to the resid.

B. Sample Preparation

Approximately .5 g of resid for each sample was added to several drops of cold setting epoxy resin (with hardener), which had been allowed to set for 10 min. prior to sample preparation, in order to increase the resin viscosity and reduce its ability to dissolve and penetrate the resid. The mixture of resid and epoxy was then placed into a cavity (.25 in. diameter) that was drilled in an epoxy pellet of 1.5 in. diameter, and allowed to harden. After setting, the sample surface was ground and polished by hand on a rotating lap using a series of grinding papers and alumina polishing compounds.

C. Fluorescence Equipment

Fluorescence emission from the resids was observed and measured with a Leitz MPV Compact microscope photometer system, schematically shown in figure 5. Within the photometer is a photomultiplier tube (Hamamatsu) with a relatively strong response in the red region of the electromagnetic spectrum. Intense ultraviolet and violet radiation for fluorescence excitation is obtained with a 100 watt high pressure mercury arc lamp (Figure 6) powered by a stabilized supply.

Illumination of the resid sample was achieved through a Leitz Ploemopak vertical illuminator, which houses the excitation filter, dichromatic beam splitter (dichroic mirror), and barrier filter shown in figure 5. For this study, a filter set was

employed which isolated 355 to 425 nm excitation, and utilized a 455 nm dichroic mirror to reflect light of wavelengths shorter than 455 nm (excitation) down through a 50x air immersion objective to the sample surface. Fluorescence emission from the sample, along with any reflected excitation then passes up through the objective and encounters the 455 nm dichroic mirror. Excitation is mostly reflected out of the emission path, whereas light of wavelengths greater than 455 nm (fluorescence) is permitted to pass. A 460 nm barrier filter ensures that any remaining excitation is filtered from the fluorescence emission.

Fluorescence emission is diffracted by a grating monochromator (ISA Inc.) into a series of beams, each with a narrow bandwidth (8 nm in this study, with ± 1 nm resolution). The monochromator is interfaced with a scanning controller and stepping motor (ISA) such that fluorescence spectra were scanned from 470 to 700 nm at a speed of 300 nm/min.. Intensity readings were taken every 2.5 nm, with a nominal resolution of 5 nm. The microscope photometer and scanning controller were interfaced with a Digital Equipment Corp. computer for data acquisition.

D. Reflectance Equipment

The proportion of light reflected off a polished resid surface was determined utilizing the same microscope photometer employed for fluorescence analysis, except that for reflectance analysis, a 546 nm bandpass filter replaced the scanning monochromator. A 100 W tungsten-halogen lamp, equipped with a stabilized power supply was employed as the illuminant. Collimated light from the source is directed to the sample by a series of lenses and a Berek prism within a vertical illuminator, and

then through a 50x air immersion objective.

E. Reflectance Methods

Initial observations revealed that the resids were optically isotropic, therefore, random reflectance measurements (as opposed to mean maximum) were obtained. It was also noted that some of the resids apparently interacted with the immersion oil, usually lowering the reflectance and dissolving a portion of the surface material. As a consequence, reflectance analyses were conducted in air immersion.

An epoxy mounted sample was placed on a glass slide and levelled, using modelling clay as the mounting material. The microscope photometer system was then calibrated using isotropic glasses, of known index of refraction and percent reflectance, as standards. After placing the sample onto the microscope stage, a suitable area of resid was located, free from inorganics or macerals, and a reflectance measurement was recorded manually from a 10 micron (diam.) spot of the resid. Twenty five measurements were acquired per sample, each on a separate particle. The mean of these twenty five readings is reported, along with the standard deviation.

F. Fluorescence Methods

Before fluorescence analyses were conducted, the microscope photometer was calibrated for the optics, filters, and photomultiplier response. To accomplish this, the emission spectrum from a 3400 K tungsten halogen lamp was measured from 470 to 700 nm, at 2.5 nm intervals, and then normalized. The known (or actual) normalized intensities of the tungsten spectrum were then divided by the measured intensities to obtain a correction factor at each wavelength interval.

Samples were mounted on glass slides, as per the reflectance procedure, in order to have a level working surface. A latex sleeve, fitted on one end around the objective (Figure 7), was fastened to the pellet surface with a plastic ring (glued to the latex sleeve) and a small amount of silicone vacuum grease for an air-tight seal. A flow of argon gas through this apparatus was utilized in order to inhibit photo-oxidation.

Under incident white light, an area of resid was selected for measurement which contained a minimum of unreacted coal macerals and inorganic material. The microscope was then set-up for ultraviolet (uv)-violet illumination, and the selected resid area examined for fluorescent particles (e.g. liptinites), which were avoided as much as possible. Under uv-violet illumination, there was a thin (<5 micron) rim of partially dissolved resid, in addition to a halo of relatively intense yellow fluorescence in the surrounding epoxy. These observations suggest that only a thin outer portion of resid was dissolved by the epoxy. Consequently, measurements were conducted away from resid-epoxy boundaries, and only on resid particles larger than approximately 150 microns (smallest dimension).

A measuring spot of 100 microns in diameter was employed in order to maximize the fluorescence signal. Although this rather large area occasionally encompassed unreacted macerals along with resid (mainly for the Run 251-II resids), the majority of these macerals were either non-fluorescent or very weakly fluorescent and so exerted a negligible influence on spectral distribution, although an intensity reduction was an expected result.

After qualitative observations, the fluorescence emission from a selected area of resid was scanned twenty times, the high and low values discarded, and the remaining 18 spectra averaged to get one spectrum per resid particle. This was repeated on four additional particles in each sample (for a total of 5 spectra per sample), with separate fluorescent populations (identified qualitatively) represented if present. However, for the Run 251-II resids, 8 spectra were obtained on the interstage sample, and 6 spectra on the recycle sample because of the relative optical variability exhibited by these resids (discussed below). Raw spectral data were normalized, the correction factor applied, and then re-normalized such that the maximum intensity equaled 100%. The uncorrected spectra were used to assess fluorescence intensity differences between samples, by calculation of the area beneath the spectra.

In order to standardize the system with respect to fluorescence intensity, a simple procedure was developed, because there is currently no standard method for fluorescence microscopy. Using a filter set that permits viewing of a sample in white-light, the emission from the mercury arc lamp was reflected off an isotropic glass reflectance standard of 1.025% reflectance. Reflected mercury arc emission passed through the grating monochromator set for 436 (± 4 nm) corresponding to a mercury emission peak (Figure 6). With the photomultiplier gain held constant at approximately 825 volts, the mercury arc lamp focus was adjusted until the digital readout from the photometer electronics consol read 1.025 volts. Although this procedure probably would not yield reproducible results in other laboratories, it does allow for comparable fluorescence intensities of resid samples in this study. The goal of this procedure

development was to determine if the fluorescence intensity of resids is a potentially useful parameter in evaluating process conditions. If the method appears promising, then a reproducible technique will be pursued in future work.

G. Fluorescence Quotient

In order to ascertain the variability of resid fluorescence properties within each sample, a fluorescence point count was initiated by measuring the fluorescence intensities at 700 nm (red) and 525 nm (green) for twenty resid particles, and calculating the ratio of the 700 nm intensity to that at 525 nm. A low red:green ratio indicates that the resid fluorescence emission is shifted to shorter wavelengths than that which exhibits a comparatively high ratio. This type of ratio is commonly referred to as a red:green quotient (Q). Red:green quotients calculated from the five raw spectra obtained on each sample were also used, giving a total of twenty five (25) particles examined per sample (with the exception of the Run 251-II interstage and recycle resids, in which 28 particles and 26 particles, respectively, were examined, due to the additional spectra acquired on these resids). Data are reported as frequency histograms. Variations of this ratio have been commonly employed in fluorescence studies of macerals, although previous studies typically obtain the ratio from normalized spectra (e.g. 15,16). The purpose of this technique development was to rapidly assess the degree of fluorescence heterogeneity of Wilsonville resid samples; resids from HRI Run I-27 were not included in this analysis because they consisted of homogeneous pressure filter liquids.

H. Proximate Analysis

Volatile matter yield, employed here as an indicator of reactivity, was determined for each resid composite as part of a proximate analysis. This test was performed at the CAER Fuel Characterization Laboratories, using a thermal gravimetric analyzer (DuPont TGA 2950). Percent volatile matter are presented on a moisture and ash free basis (m.a.f.).

III. Results and Discussion

A. Wilsonville Resids, Interstage vs. Recycle

A.1. Run 251-II (Wyodak Coal, T/C)

The interstage and recycle resid composites both contained large amounts of unreacted macerals (huminite and inertinite), as well as inorganics. Some material resembling vitroplast (see ref. 3) was observed, as well as a small concentration of cenospheres, and spherical optically anisotropic semicoke (Plate Ia), which is indicative of unfavorable hydrogenation conditions (17).

Under uv-violet illumination, a relative abundance of green fluorescing liptinite fragments were observed, often less than 5 microns in size (Plate Ib), making definitive identification difficult. Some particles contained a sufficient number of these liptinite fragments that a reliable fluorescence spectrum could not be obtained.

Most of the interstage resid fluoresced with an intensity maximum at wavelengths longer than 700 nm (Figure 8a), although there was a subordinate amount of material with a wavelength of maximum intensity (Lmax) at shorter wavelengths (approx. 680 nm). The recycle resid composite from the V131B surge

tank contained a population resembling that from the interstage sample, although this material is subordinate to a more intensely fluorescing resid with an Lmax at approximately 685 nm (Figure 8b, popl. 1 of Table 2). Furthermore, a portion of the recycle resid displayed extremely intense fluorescence with an Lmax of 578 nm (Figure 8b, popl. 2 of Table 2). This intensely fluorescing material was often observed with distinct particles of the darker orange fluorescing resid included within it (Plate IIa), although a more gradational boundary was occasionally observed between the two (Plate IIb).

The source of fluorescence variability for Run 251-II resids, expressed in figure 8, is essentially two-fold, resulting from fluorescent liptinite fragments within the resid, and variations within the resid itself. In the interstage sample, most fluorescence heterogeneity was accounted for as inter-particle variability. Liptinite-rich portions of resid were often observed as discrete particles, as were areas with distinctly different fluorescence properties. This may indicate that much of the variability is derived from the composited nature of the sample and that instantaneous samples would be more homogeneous, although fluorescing liptinite fragments may still exert an effect on fluorescence properties. However, inter-particle variability could also be produced when the resid was removed from the distillation vessel; boundaries between two resid fluorescent populations could possibly be mechanically weak, causing fracturing to occur at these boundaries.

Variability within the recycle resid is similar to the interstage, with the exception of the intense yellow fluorescing population in the recycle resid. As was mentioned

above, this material was always observed within the same particles as the dominant population of orange fluorescing resid, suggesting that it is not an artefact of resid compositing.

Due to the high fluorescence variability of the Run 251-II samples, it is difficult to compare the red:green quotient (Q) histograms (Figure 9) with those from other runs. The variability primarily arises from the fluorescing liptinite fragments in many of the resid particles and, in addition, a generally low fluorescence intensity (imparting a low signal:noise ratio). For the interstage sample, a combination of brightly fluorescing liptinite particles and a low fluorescence intensity of the surrounding resid accounts for most of the Q values below the 0.60 range, depending largely on the concentration of the liptinites in the resid particle. An example of the effects of liptinite "contaminants" on measured fluorescence properties is given in figure 8a; the dashed spectrum was acquired from a particle of resid with a rather high concentration of liptinite fragments, and has a Q of 0.394. The majority of the interstage resid, however, had ratios in the range 0.40 to 0.70 (Figure 9a), with a few particles in the 0.30 and 0.80 range.

For the recycle sample, similar problems were encountered as for the interstage resid, although in this sample the overall intensities were higher than for the interstage composite. Red:green quotients obtained from particles with relatively high concentrations of liptinite fragments were typically in the 0.20 to 0.30 range (Figure 9b), while the intense, yellow fluorescing resid yielded the quotients in the 0.10 column.

The mean random reflectance of resids from Run 251-II was observed to

decrease slightly (within one std. dev. of mean values) from interstage to recycle resid, corresponding to the fluorescence shift to shorter wavelengths (Table 2). A decrease in vitrinite reflectance is considered to be the result of a decrease in the degree of aromatization and condensation of the vitrinite structural units (18). Accompanying the fluorescence "blue shift" of recycle resids compared to the interstage counterparts, is a decrease in the percentage of aromatic protons, an increase in beta+gamma protons, a shift of the phenol peak location to higher wavenumbers (smaller ring size), and a lower concentration of phenols in the recycle sample (Table 2).

Average fluorescence spectra (calculated from the five individual spectra in figure 8) from the interstage sample and the recycle sample (excluding the very intensely fluorescing portion) are shown in figure 10. The fluorescence properties of the recycle resid compared to the interstage sample are consistent with the effects of catalytic upgrading. However, the selective rejection of preasphaltenes in the critical solvent deasher (CSD) might also have exerted an effect on the observed fluorescence properties of the Run 251-II resids; a preferential removal of condensed, high molecular weight aromatics would contribute to a fluorescence intensity increase and spectral blue shift of the recycle resid.

The origin of the brightly fluorescing material in the recycle resid is problematical. Assuming that this material is not an artefact of the various sample preparation techniques, such as distillation, it is possible that it represents one of the three pasting solvent components (Appendix I) that was incompatible with the other two components. Incompatibilties involving coal liquids have been reported by Mobil

Research and Development (19), who suggested that upgrading over small pore catalysts can produce a distillate that is incompatible with the residual fraction. That this highly fluorescent resid would be amenable to further conversion in the Run 251-II first stage is suggested by its absence (or rare occurrence) in the interstage sample. It is possible that this material is largely converted to a distillable product in the first stage, and therefore is not present in the non-distillable interstage resid sample.

A.2. Run 259 (Pittsburgh Coal, C/C)

The interstage and recycle resid samples from Run 259 (catalytic/catalytic mode) had an abundance of inertinite macerals, but very little distinguishable unreacted vitrinite or liptinite, probably due to the preferential conversion of the reactive macerals in Run 259. Inorganic material was in low abundance compared to resids from Run 251-II (Wyodak coal, T/C). No coke particles were observed, nor were there any anisotropic semi-coke spheres, which is similar to results reported by Davis et. al. (1991). These authors observed negligible concentrations of anisotropic semi-coke in hydrogenation residues generated from a high volatile A bituminous coal in the presence of distillate process solvent and a molybdenum catalyst. This was attributed to the separation and dispersion of free radicals by the solvent, thus reducing the probability of their recombination.

Under uv-violet illumination, the Run 259 resids exhibited a low incidence of fluorescent particles (e.g. liptinite fragments). Fluorescence spectra from the interstage composite exhibited maxima close to 700 nm or greater (Figure 11a), with an average of 696 nm as indicated in Table 3 (this may not reflect the true average

since some residue may have had a maximum beyond the 700 nm instrumental limit). The recycle resid fluorescence spectra were almost identical to those from the interstage sample, again with an apparent average of 696 nm (Table 3).

The red:green quotient histograms (Figure 12) help to show that, despite the apparent homogeneity of the fluorescence spectra (the resid fluorescence was also apparently visually homogeneous), there is variability within the Run 259 resids. However, because Lmax of the Run 259 resids were at 700 nm and longer, the fluorescence analysis could not fully record the spectral changes.

Reflectance data (Table 3) reveal that the recycle resid exhibited a mean reflectance slightly lower than that of the interstage sample, although the reflectance values were nearly within one standard deviation of each sample. The minor changes in fluorescence and reflectance properties between the interstage and recycle samples corresponds to other chemical properties. The recycle sample data reveals a slight decrease in aromatic proton percentages (although there is a relative increase in the proportion of uncondensed aromatic protons), an increase in beta+gamma proton content (4.6 %), a small increase in hydrogen content, and small increases in volatile matter yields and heating value (Table 3).

Close similarities in the average fluorescence spectra (Figure 13) and intensities of the interstage and recycle samples suggest that the second catalytic stage in Run 259 did not substantially alter the overall molecular size or concentration of aromatics in the resid after this material had been through a catalytic first stage. The slight fluorescence intensity increase and reflectance decrease of the recycle sample relative

to the interstage sample is probably a reflection of the decrease in total aromatic concentration. Although there is also evidence for a significant decrease in oxygen content (from ultimate analysis and phenolic -OH concentration), its influence on the resid fluorescence properties is not known, because different functionalities exert different effects.

A.3. Run 250 (Illinois #6 Coal, T/C)

The interstage resid composite from Run 250 contained abundant inertinites and a moderate amount of inorganic material. No coke was observed in the sample, nor were there many identifiable unreacted vitrinite particles. The recycle resid composite was similar in appearance to the interstage sample, except that there was a substantial reduction in inertinite and inorganic proportions in the recycle resid (sampled after the de-ashing step), as reflected by significant decreases in ash (5.9 %) and insoluble organic matter (4.4 %).

The resids displayed a relatively homogeneous fluorescence, although some intensity variations were observed. All five spectra from the interstage resid are practically superimpositions (Figure 14a), with an average Lmax at 684 nm (Table 4). The homogeneity of the fluorescence properties of this resid, is inferred from the small standard deviations in both Lmax and intensity. As figure 14b shows, four spectra from the recycle resid are similar, with an average Lmax of approximately 652 nm, while the fifth spectrum has an intensity maximum at 690 nm, similar to the interstage samples. The recycle resid generally exhibited a higher fluorescence intensity and shorter Lmax (Table 4) than its interstage counterpart.

Red:green quotients for Run 250 samples (Figure 15) support the spectral data in recording a blue shift and slightly greater heterogeneity of the recycle resid compared to the interstage sample. The five (5) fluorescence spectra encompass the entire range of red:green quotients in figure 15, suggesting that they provide a good representation of the sample fluorescence properties.

Mean reflectances of the Run 250 resids decreased by 0.54% from the interstage to recycle sample (Table 4). The difference is significant, as it is greater than 3 standard deviations from the mean values of each sample.

The greater average fluorescence intensity, spectral "blue shift" (Figure 16), and reflectance decrease of the recycle resid composite is accompanied by a lower aromatic proton percentage and a higher concentration of beta+gamma protons, a greater hydrogen content, and a shift in the phenol peak to higher wavenumbers. The substantial increase in volatile matter yield (Table 4), indicates a potentially increased reactivity of the recycle resid.

Despite the small portion of recycle resid with fluorescence spectra similar to the interstage sample (Figure 14), the average fluorescence and chemical data suggest that the catalytic second stage provided considerable upgrading of resid produced in the thermal liquefaction unit (TLU). This is not unexpected since it is generally considered that the primary role of the first stage TLU is to dissolve the coal (and recycled resid), whereas the second stage upgrades the first stage products (20). In Run 250 (and other Wilsonville runs), resid from the first stage is derived from the recycle solvent, and coal that has been processed for the first time, whereas resid

sampled after the second stage catalytic reactor is mainly derived from coal liquids and a much smaller proportion of unreacted coal. It is therefore plausible that the catalytically hydrogenated recycle resid sample displayed a more intense fluorescence, at shorter wavelengths than the interstage sample, indicating the presence of less condensed, lower molecular weight aromatic chromophores. In addition, there is some preferential rejection of preasphaltenes in the CSD, which could also contribute to the differences in fluorescence and chemical properties.

A.4. Run 257 (Illinois #6 Coal, C/C)

The interstage resid from Run 257, contained abundant inertinites, some inorganic material, cenospheres, and cenosphere wall fragments (Plate IIIa). It has been suggested that cenospheres have resulted during direct liquefaction processes from the development of gas bubbles in spherical vitroplast, which exert sufficient pressure on the plastic material to cause expansion, subsequently forming the reticulated structures (3). In comparison with the interstage sample, the recycle resid contained a smaller proportion of inertinites, cenospheres, and mineral matter, also expressed as lower percentages of i.o.m. and ash. Negligible coke particles were observed in resids from Run 257.

Qualitative observations of resid fluorescence revealed substantial variations in the Run 257 samples. Fluorescence colors of the resids exhibited a rather wide range, as is shown in Plate IIIa through IVb. Variations in fluorescence spectral distributions within the interstage resid were quantitatively expressed as one resid population fluorescing with an average Lmax of 646 nm, and the other with an

average at 604 nm (Table 5 and Figure 17a). The general fluorescence characteristics of the interstage resid were also displayed by the recycle resid (Figure 17b), although in this sample, both populations are apparently shifted to shorter wavelengths relative to the interstage resid, with average peak intensity wavelengths of 633 nm and 585 nm (Table 5).

Particle to particle differences were the major source of fluorescence variability, with the two generalized populations usually occurring as more-or-less discrete particles, although there were occasionally fluorescence gradations within particles (Plate IIIa). Within the interstage and recycle samples there were several examples of more than one fluorescence population within a single particle. One such particle, observed in the Run 257 recycle resid exhibited a fluorescence variation from orange to greenish yellow observed within the particle. It was noted that the orange fluorescing resid contained a relative abundance of large minerals and inertinites, whereas the greenish yellow portion had smaller i.o.m. particles included, consisting mainly of small inertinites and cenosphere wall fragments. This is perhaps suggestive of a density gradient from the orange fluorescing (more condensed aromatics = greater density) to the greenish-yellow fluorescing (less condensed aromatics = lower density) resid. Whether the different fluorescence populations were segregated during Run 257 or merely during the distillation process is not known at this time.

Histograms of the red:green quotients exhibited by the Run 257 resids (Figure 18), give an impression of the fluorescence variations within each sample when compared with the Q values of the spectra. The interstage resid had a range of 0.2 to

0.4 (Figure 18a), which is the same range of Q values exhibited by the five spectra in figure 17a. Apparently, the spectra provide a good approximation as to the range of fluorescence variability within the interstage sample. However, fluorescence spectra from the recycle sample have red:green quotients only within the 0.2 to 0.3 range, although the corresponding histogram covers a range of 0.2 to 0.4; apparently the spectra have not adequately represented resid with fluorescence properties slightly shifted to longer wavelengths.

The mean reflectances of resids from Run 257 decreased by 0.34% from interstage to recycle (Table 5), similar to trends exhibited by resids from the other Wilsonville runs. Chemically, the interstage sample is more aromatic and less aliphatic (in general indicated by beta+gamma percentages) than the recycle resid, and apparently is composed of more condensed aromatics as evidenced by the phenol peak frequency shift to lower wavenumbers. The recycle sample also had a slightly higher hydrogen content than the interstage resid. However, unlike the Wilsonville resids discussed previously, the recycle resid yielded a smaller proportion of volatile matter than the interstage sample, suggesting that the former might be less reactive than the latter, despite its higher concentration of I.O.M. and slightly lower heating value.

As with Runs 251-II and 250, the catalytic second stage of Run 257 has clearly upgraded the products from the catalytic first stage. The orange fluorescing (Lmax = 646 nm) portion of the interstage sample might be primarily derived from the coal feedstock, whereas the more intensely fluorescing yellowish resid could represent

slightly upgraded recycle resid from the second stage reactor. The average fluorescence properties of the resid sampled after the second stage reactor (Figure 19) are consistent with the suggestion that some aromatics from the first stage reactor resid product have been hydrogenated to less condensed structures, although at least part of the fluorescence differences could result from selective rejection of preasphaltenes in the CSD. The resid upgrading provided by the second stage is also suggested by analytical data.

B. Comparisons Between Wilsonville Runs

The comparisons of the interstage and recycle resid fluorescence properties suggest that the spectral distribution and intensity are potential indicators of liquefaction process performance. Strongly bonded high molecular weight condensed aromatic structures, that are likely to be more refractory to upgrading than lower molecular weight, less condensed aromatic compounds, would exhibit fluorescence with low intensity, at comparatively long wavelengths. It is suggested, therefore, that intensely fluorescing resids with spectral distributions at shorter wavelengths would be relatively reactive to further upgrading, a property which should also be expressed as an increased volatile matter yield.

B.1. Interstage Resids

The fluorescence spectra of the interstage resids (Figure 20) suggest that the products from Run 259 (Pittsburgh coal, C/C) and Run 251-II (Wyodak coal, T/C) are apparently the least reactive, with relatively low fluorescence intensities, and fluorescence peaks at 700nm or greater. The Run 259 resid is assumed to be

comprised of larger, more condensed aromatic structural units than the resid produced in Run 251-II (although liptinitic fragments in the Run 251-II resids complicate interpretation), as indicated by a low fluorescence emission in the 470nm to approximately 600nm region. Proton NMR data indicate that the interstage resid from Run 259 has approximately the same percentage of total aromatics as the Run 251-II counterpart, although the latter has relatively more uncondensed aromatics than Run 259 resid, which is not unexpected considering the differences between the two feedstocks: product derived from the subbituminous Wyodak coal is expected to contain smaller, less condensed aromatic structural units than the bituminous-rank Pittsburgh coal.

Despite the similarities in aromatic concentrations between the two interstage resids, the proton NMR data suggest that there are differences in the predominant non-aromatic structures. The resid from Run 251-II (Wyodak coal, T/C) has a higher percentage of alkyl beta protons (interior of chains) and slightly lower proportions of total cyclic protons and alkyl alpha protons than the Run 259 (Pittsburgh coal, C/C) interstage resid, although both have similar terminal methyl (gamma) proton concentrations. This indicates that the aromatic structures in the Run 251-II resid (subbituminous feed) have longer alkyl side chains than the Run 259 (high volatile A bituminous feed) resid, whereas the latter has more naphthenic rings disrupting conjugation of the aromatic rings. The interpretation of the significance of the fluorescence intensities from the Run 251-II resid is tentative, due to the relative abundance of non-fluorescent unreacted macerals. In addition, fluorescent liptinite

fragments in the Run 251-II interstage resid also probably affected the fluorescence intensity and caused a slight increase in spectral intensity at the shorter wavelengths.

The Run 250 (Illinois #6 coal, T/C) interstage resid has a fluorescence spectrum that is shifted to shorter wavelengths than that of the Run 251-II (Wyodak coal, T/C) or Run 259 (Pittsburgh coal C/C), with an average intensity that is slightly greater than or equal to Run 251-II, but significantly lower than that of the Run 259 resid. Relative to Run 259, interstage resid from Run 250 was slightly more aromatic (from NMR data in Table 8), which would contribute to a reduction in fluorescence intensity. However, it contains relatively fewer condensed aromatics and more uncondensed aromatics than the interstage resid from Run 259 (hvAb feedstock), probably causing the observed spectral "blue-shift" of the Run 250 resid. That the resid from Run 250 is likely to be more reactive than that from Run 259 is also suggested by its greater volatile matter content (Table 8).

Despite the variability in fluorescence properties of the Run 257 (Illinois #6 coal, C/C) interstage resid (Figure 17), it is evident that the fluorescence emission of this product is substantially shifted to shorter wavelengths relative to the other Wilsonville interstage samples investigated. The average fluorescence intensity of "population 1" (row 8, Table 6) is slightly greater than that from the Run 251-II (Wyodak coal, T/C) and Run 250 (Illinois #6 coal, T/C) interstage composites, although it is approximately the same as that from Run 259 (Pittsburgh coal, C/C). However, "population 2" (Row 9, Table 6) fluoresces at much shorter wavelengths than other resids, with an intensity approximately 2-3 times higher. In addition, the total interstage resid composite is

substantially less aromatic than the other Wilsonville interstage resids (>10% difference in aromatic protons), with evidence of overall smaller aromatics (phenol peak shifted to higher wavenumbers), and a relatively high hydrogen content (7.70%). The reflectance percent is also significantly lower than that of the other Wilsonville resids (Table 7), probably a consequence of the lower aromatic percent and reduced condensation of the aromatic molecules. The reactivity is probably comparatively high, based on a high volatile matter yield of 94.3 % (Table 6), which is at least 20 percent higher than any other Wilsonville resid.

Compared with Run 250 (Illinois #6 coal, T/C), the fluorescence properties of the Run 257 (Illinois #6 coal, C/C) interstage resid suggest that operating the first stage reactor in the catalytic mode produced a resid with a relatively low concentration of aromatic chromophores, and an overall lower molecular weight. The resid is therefore likely to be particularly amenable to further upgrading and conversion. This is in agreement with NMR results which indicate that more extensive hydrogenation and opening of aromatic rings has occurred in the Run 257 first stage, as indicated by greater concentrations of cyclic, alkyl beta, and gamma protons (Appendix III).

B.2. Recycle Resids

Between the different runs, similar relationships hold for the fluorescence properties of the recycle resids as for their interstage equivalents, figure 21, with minor exceptions. As is evident in figure 21, the average fluorescence spectrum from the Run 251-II (Wyodak coal, T/C) recycle resid is similar to that from Run 250 (Illinois #6 coal, T/C): note that this does not include the intensely fluorescing component of the

Run 251-II recycle sample. Apparently, after the products of the thermal first stages (in both runs) are catalytically hydrotreated, their average fluorescence properties become more alike, although they become more internally heterogeneous, possibly caused by the different pasting solvent components (Appendix I), partial fractionation of the resid in the CSD process, and/or by catalytic hydrotreating.

The recycle resid from Run 259 (Pittsburgh coal, C/C) is, as mentioned earlier, very much like its interstage counterpart, and has an average fluorescence emission shifted to the red region of the visible spectrum compared to the other recycle resids, corresponding to its relative abundance of aromatic molecules (as indicated by the proton NMR spectra). A relatively low volatile matter yield implies low resid reactivity, despite the two catalytic stages employed in this run.

Similar to its interstage counterpart, the recycle resid from Run 257 (Illinois #6 coal, C/C) exhibits a fluorescence intensity higher than that of the other recycle samples from Wilsonville, as well as a spectral distribution that is shifted to shorter wavelengths. The mean reflectance percent of the Run 257 recycle resid is also significantly lower than the corresponding resids from the other three Wilsonville runs. In addition, this sample contains the lowest concentration of aromatic protons, while it also has the highest percentage of beta+gamma protons and the phenol peak at a higher wavenumber (3302 cm^{-1}) than the other recycle resids. The relatively high volatile matter content suggests that the resid produced from the second stage reactor in Run 257 is probably the most reactive of all the recycle resids investigated.

C. HRI Run I-27 Resids

The pressure filter liquids from HRI Run I-27 (Illinois #6 coal, two-stage catalytic) proved to be microscopically homogeneous, both in white light and ultraviolet-violet illumination. There was a progressive increase of resid reflectance from PFL P2 to P25 (Table 9). Fluorescence spectra within each sample were, for the most part, very similar (Figure 22): sample #11 (PFL P18) and #12 (PFL P25) each displayed one spectrum that was slightly different from the other four, although the peak wavelength was apparently similar. The wavelength of maximum intensity (Lmax) was substantially shifted to longer wavelengths in samples PFL P2 to PFL P18 (Figure 23), along with a monotonic reduction in relative intensity at the shorter wavelengths, indicating that aromatic ring condensation increased as the run progressed. Table 9 and figure 24 indicate that sample PFL P2 had the greatest average fluorescence intensity, whereas sample PFL P25 had the lowest intensity, suggesting that an increased concentration of aromatic chromophores (causing an increase in energy delocalisation) occurred over the course of the run.

The trends exhibited by the fluorescence and reflectance properties are accompanied by systematic chemical changes. From sample PFL P2 to P25, there is a monotonic increase in percent aromatics, a decrease in beta+gamma proton concentrations and hydrogen content, an increase in phenol concentration, and a shift in phenol peak frequency from 3305 to 3296 cm^{-1} (Table 9), indicative of increasing ring condensation. The volatile matter yield decreased, from PFL P2 to P25, in this sample set.

The fluorescence "red-shift", intensity decrease, and increase in resid

reflectance percent over the course of Run I-27 suggest that the catalyst had become less effective in upgrading the non-distillable fraction of coal liquids to low molecular weight, less aromatic products. With increasing run time, the proportion of uncondensed aromatics decreased from approximately 17%, to 12.5%, as did the concentrations of cyclic and alkyl beta protons, and gamma (terminal methyl) protons (Appendix III), intimating that aromatic ring hydrogenation became less pronounced as Run I-27 progressed. A possible cause of these deleterious changes in resid properties is the partial deactivation of catalyst from deposition of carbonaceous materials onto the catalyst surface, which is believed to occur most rapidly in the early stages of the liquefaction run (21). Other process variables that have been suggested to have influenced resid chemical properties include increased reactor temperatures, a reduction in the solvent/coal ratio, and an increase in the solvent cut-point (the temperature end-point of the net distillate product was increased with time to maintain the desired conversion level, with a result that the initial boiling point of the recycled oils also increased). These changes could also have contributed to the fluorescence spectral red-shift, intensity decrease, and reflectance increase observed from PFL P2 to P25.

D. Unidentified Samples

D.1. Sample #13

Qualitatively, the control sample with reference number 13 was microscopically very homogeneous, both in white light and fluorescence mode, and was similar to the HRI Run I-27 samples. As shown in figure 25, the fluorescence spectrum of this

sample is very similar to that from the Run I-27 resid sampled on day 25. The wavelength of maximum intensity as well as overall intensity is similar to samples PFL P18 and P25, although the overall intensity standard deviation is small and most similar to PFL P25. In addition, the mean reflectance in air is 8.12 % (Table 10), which is within .06% of sample #12 (PFL P25).

D.2. Sample #14

Sample reference #14 was observed to contain an abundance of inertinites and inorganic material. In addition, anisotropic particles of coke and spheres of semi-coke were observed, as with the resids from Run 251-II. The fluorescence was typically orange to brownish-orange, with very small liptinite fragments observed throughout many of the resid particles. Only rarely was intense, yellow-fluorescing resid observed, and this was restricted to relatively small (<200 microns), somewhat circular particles.

Figure 26 and Table 10 reveal that the fluorescence spectra and reflectances are most similar to those recorded for the Run 251-II interstage resid. Additionally, compared to the Run 251-II resids, the red:green quotients of sample #14 had ranges most similar to the interstage composite, although the overall range of values was less for the blind sample (Figure 27). However, it is concluded that sample #14 is most similar to the interstage resid from Run 251-II.

IV. Evaluation of Method

A. Within-Sample Variability

Unlike the other chemical analysis methods employed to characterize the liquefaction resids, the precision of the fluorescence microscopical technique employed here is difficult to evaluate due to inherent variabilities within the solid resid samples. Proton NMR and FTIR analytical techniques first dissolve the resid in a solvent such as THF or pyridine, followed by filtering (22,23), which produces a homogeneous sample representing a more-or-less average composition of the resid, and also removes any filterable insoluble coal liquids. Replicate analyses on this type of sample provide a good indication of the precision of the analytical technique. Unfortunately, these techniques are not able to identify sample heterogeneities, or resolve multiple phases within a resid.

The preparation techniques utilized in this study probably altered only a thin rim of the resid particles. The fluorescence analyses were, therefore, responsive to differences inherent in the solid resid samples. A possible advantage of this "population" distinction is illustrated with the recycle sample of Run 251-II, in which a portion of the resid exhibited distinctly different fluorescence properties than the majority of the sample. Assuming that this material was generated in the liquefaction process, with more detailed sampling it may be possible to determine the origin of the population, and its fate in the Run 251-II loop. On the other hand, it is very time consuming to characterize a resid with very large, gradational variations in fluorescence properties. In this case, dissolving the resid in a solvent, and filtering out

the solids (e.g. fluorescing liptinites in Run 251-II resids) might prove to be a better sample preparation method, although any fluorescence population distinctions will disappear.

Evaluations of sample variability based on Lmax standard deviations (i.e. Table 6 and Table 9) are misleading for samples displaying an apparent maximum near or at 700nm, because it is likely that some of the spectra have an actual Lmax at longer wavelengths, and so were not recorded by the method used in this study. A more accurate depiction of sample variability is given in Table 11, which gives the wavelengths where the fluorescence relative intensities of 25, 50, 75, and 100 % (Lmax) occur, and the associated standard deviation. Where no standard deviation was calculated (denoted by -), fewer than three spectra were acquired on the material.

It is evident from Table 11 that the fluorescence variability of resids from Runs 251-II and 259 is greater than the standard deviation of Lmax implied, as indicated by the larger deviations at 25, 50, and 75 % relative intensities. Low fluorescence intensities exhibited by these resids also contributed to the fluorescence variations within the Run 251-II and 259 resids. Conversely, despite the large deviation for the Run 250 recycle resid, four of the five spectra were practically superimpositions (with an average Lmax of 652 nm), whereas the fifth was significantly different (Lmax = 690 nm) and caused a deceptively large increase in the Lmax standard deviation for this sample.

Samples which provided the best measure of the precision of the fluorescence technique were the homogeneous pressure filter liquids from HRI Run I-27, which

indicate that fluorescence spectra can be repeated within 3 to 4 nm. The large standard deviation at 25% relative intensity for samples PFL P18 and P25 (in the 500 to 525 nm region, as shown in Table 11 and Figure 22) were probably caused by the very low intensities at these short wavelengths. The HRI Run I-27 resids also displayed relatively small deviations in fluorescence intensity and reflectance percentages, as shown in Tables 6 and 9. Although the variability in fluorescence intensity of sample PFL 2 appears to be large, it is minor (1,477) relative to the overall intensity of 18,184 counts. Data from Run I-27 resids indicate that the fluorescence method yields repeatable results (within one laboratory) when homogeneous samples are analysed.

B. Repeatability

In addition to evaluating the variability within any one analysis, replicate pellets were prepared from four samples displaying only one fluorescence population; specifically, samples # 1 (Run 251-II, interstage), #4 (Run 259, recycle), #6 (Run 250, recycle), and #10 (Run I-27, PFL 8). Three fluorescence spectra were acquired from each of these replicate samples.

Figures 28a & b show the spectra of the replicate analysis of the Run 251-II interstage resid, with data presented in tabular form in Tables 11 and 12. The results revealed that the repeated spectra were very similar to the first analyses. However, the average intensity of the replicate sample was clearly higher than the original, as is shown in Table 12. The two sets of analyses for the Run 259 recycle resid had similar intensities, although the average replicate intensity was slightly lower. Unlike the Run

251-II interstage sample, the replicate fluorescence spectrum of the recycle resid from Run 259 is shifted approximately 10 nm to shorter wavelengths (Figure 29), and has small standard deviations at each relative intensity (Table 11). This 10 nm shift occurs in replicate analyses for the other two samples analysed (Figures 30 and 31), again with small standard deviations. Similar to the trend observed for the Run 251-II interstage resid, the intensities of the replicate analyses for sample #6 (Run 250 recycle) and sample #10 (Run I-27 PFL P8) are significantly higher than the first analyses (Table 12).

In order to determine the cause of the discrepancies between the original and repeated analyses, experimental parameters were altered one at a time, and additional fluorescence spectra obtained from the replicate and original samples. For example, when the original pellets of the four samples in question were re-polished and scanned, the fluorescence spectra were nearly identical to those acquired on the replicate samples, indicating that it was not the sample preparation method that was responsible for the discrepancies. Through further experimentation, it was concluded that the spectral characteristics of the mercury arc lamp emission had changed significantly during the lifetime of the bulb. Specifically, the ultraviolet region (e.g. the 365 nm peak) preferentially decayed relative to the violet radiation (e.g. the 405 nm peak), due to deposits which form on the interior surface of the bulb (24). The result is that for chemically heterogeneous samples such as coal liquids, the intense ultraviolet region emitted by a new bulb causes the lower molecular weight, less condensed aromatic chromophores to emit at relatively high intensities because it is

these molecules which will have the stronger absorption in the ultraviolet relative to more highly condensed polynuclear aromatic molecules.

An intensity increase occurred in the replicate analyses because the 365 nm peak was not employed in the intensity standardization procedure, due to the presence of a filter within the vertical illuminator which prohibits ultraviolet radiation from passing through the photometer. Since the intensity standardization procedure utilized a peak in the violet region of the electromagnetic spectrum (436 nm), this region may be rather stable during the bulb's life while the ultraviolet rapidly decayed; a reduction in measured intensity resulted. Replicate analysis of the Run 259 recycle resid did not exhibit a fluorescence intensity increase, probably because of a paucity of low molecular weight, less condensed aromatics in this resid. The relatively high fluorescence intensity that resulted from the use of a newer bulb, is probably the cause of the small standard deviations observed in the replicate fluorescence analyses, as a result of an increased signal:noise ratio.

In order to eliminate the changes in fluorescence spectra with bulb life, it is probably necessary to limit the excitation to a narrower wavelength range. Figure 32 shows the fluorescence spectrum of HRI sample PFL P8 obtained with the "old" mercury arc bulb (used in original analyses) and the newer bulb with fewer operating hours. It is evident from figure 32, that when a wide range of excitation was employed (355-425nm), the afformentioned spectral shift to shorter wavelengths was observed with the newer bulb, whereas when a much narrower ultraviolet excitation band was used (350-380nm), the spectra acquired with the two bulbs were practically identical.

However, a disadvantage of this solution is that resids with relatively high concentrations of condensed aromatic molecules will display very weak fluorescence emission, which necessitates an increase in the photomultiplier gain, causing an amplification of dark current signal.

V. Further Research

Prior to the analysis of additional samples, improvements in the fluorescence techniques, including those discussed in Section III, will be completed. Procedures will be developed for fluorescence analysis employing a narrower band of excitation, and improved system standardization. In addition, spectral scanning at wavelengths greater than 700 nm will be pursued. A standardized intensity calibration procedure has not yet been established for fluorescence microscopy, primarily because of a lack of fluorescing standards which are resistant to environment induced changes (e.g. oxidation), have fluorescence properties similar to coal macerals, and produce a stable, homogeneous, reproducible emission. The commercially available fluorescence standard most commonly utilized in organic petrology is uranyl glass, which emits an intense green fluorescence and is radioactive. Therefore, the CAER petrography laboratory is actively researching methods of fluorescence intensity standardization.

Investigation into the origin of the fluorescence variability observed in the Wilsonville Run 251-II and 257 resids would dictate fluorescence analysis of the different pasting solvent components, to evaluate possible incompatibilities between

the components, and of instantaneous resid samples acquired at selected periods during a run, to determine if fluorescence variations are a function of changes in processing conditions which occurred during the run. However, if fluorescence variability in the resids was produced during distillation, then it is not a function of the processing conditions. In this context, a potentially informative experiment would consist of distilling coal liquids (from Run 251-II, and Run 257) in a small, disposable vessel, followed by sectioning of the vessel along its vertical axis, and polishing the resid surface. Examination of this section could reveal whether fractionation (e.g. by density) of the liquids has occurred during distillation, and if this is a source of fluorescence variability within the resid.

Critical solvent de-ashing effects on Wilsonville resid fluorescence characteristics could be investigated with resid samples obtained before and after the de-ashing step. As discussed in Section III, selective preasphaltene rejection in the CSD processing step may have contributed to the observed fluorescence "blue shift" exhibited by the recycle resids, compared to their interstage equivalents. White-light and fluorescence microscopical analysis (initially, only qualitative observations) of ash the concentrates, would directly reveal the optical characteristics of the rejected organic fraction.

It is evident from the preceeding discussion that further research is required on the Wilsonville Run 250, 251-II, 257, and 259 resids, to identify the factors which exerted a significant influence the resid fluorescence properties. However, this may be a difficult task for resid samples containing relatively high concentrations of minerals

and unreacted macerals (e.g. Run 251-II resids with an abundance of fluorescing liptinite fragments, and unreacted vitrinite and inertinite). Conversely, the HRI Run I-27 pressure filter liquids are optically homogeneous, and produced under more controlled processing conditions than the Wilsonville resids. Consequently, it is possible for the fluorescence and chemical properties of resids sampled from additional HRI liquefaction runs to be interpreted in light of different processing variables such as coal rank, and/or catalyst type.

VI. Summary and Conclusions

Fluorescence spectra (ultraviolet-violet light) and percent reflectance (white light) of non-distillable (at 850°F$^+$ or 454°C$^+$) coal-derived resids were measured utilizing a microscope photometer system. Volatile matter yield was also obtained for each sample, as an approximate indicator of resid reactivity.

Fluorescence and chemical data for Wilsonville CC-ITSL Runs 250 (Illinois #6 coal, T/C), 251-II (Wyodak coal, T/C), 257 (Illinois #6 coal, C/C), and 259 (Pittsburgh coal, C/C) were interpreted with regard to reactor modes (catalytic/catalytic vs. thermal/catalytic) sample location (interstage vs. recycle), and coal feedstock, although other processing conditions were varied during these runs. Pressure filter liquids from the HRI CTSL ebullated bed bench unit (Run I-27, Illinois #6 coal, C/C) were instantaneous samples, produced under more controlled conditions, with monotonic changes in catalyst age, reactor temperatures, solvent cut-point, and the solvent/coal ratio as the run progressed. Two (2) unidentified resid samples were provided for experimental control.

It was concluded from an evaluation of the fluorescence microscopical technique employed that precision of the technique was difficult to assess for the Wilsonville resids because of the inherent sample fluorescence variability. The interstage and recycle resids from Run 257 (Illinois #6 coal, C/C) exhibited distinct, usually inter-particle, variations in fluorescence intensities and spectral distributions. Resids from Run 251-II (Wyodak coal, T/C) also exhibited pronounced fluorescence variations, typically particle-to-particle, often with high concentrations of fluorescing liptinite fragments within the resid. The Run 251-II recycle resid also contained an intensely yellow fluorescing component whose fluorescence properties were distinctly different than the majority of the resid. Although the origin of this material is problematical, its occurrence may indicate that the resid contains two or more incompatible phases, and illustrates a distinct advantage of the fluorescence microscopy technique: the ability to resolve inhomogeneities within resid samples. The analytical precision of the technique was evaluated with more homogeneous resid samples, specifically, the Wilsonville Run 250 resids (Illinois #6 coal, T/C) and the pressure filter liquids from HRI Run I-27 (Illinois #6 coal, C/C), which revealed that spectral intensities are repeatable within 3 to 4 nm.

Fluorescence results are reproducible only if a narrow range of excitation (e.g. 350 to 380 nm) is employed, or the analyses are conducted within approximately 20 mercury arc lamp ignition hours using a wider excitation band (e.g. 355 to 425nm). This is due to spectral changes in the mercury arc lamp emission as the lamp is burned.

Within the limits of precision of the microscopical techniques employed, it was concluded that resids from Wilsonville Runs 251-II (Wyodak coal, T/C), 250 (Illinois #6 coal, T/C), and 257 (Illinois #6 coal, C/C) have been upgraded to less condensed, lower molecular weight products in the second stage when compared to interstage samples. This is based on a shift of the average fluorescence spectra to shorter wavelengths, concomitant with an intensity increase and reflectance decrease, from the interstage to recycle resid. Fluorescence spectra for resids produced in Run 259 (Pittsburgh coal, C/C) were nearly identical, suggesting that the second catalytic stage provided only minor additional hydrogenation.

Interpretations of fluorescence in the context of resid reactivity were founded on the supposition that resids comprised of more highly condensed aromatics are relatively refactory to upgrading and would exhibit relatively high reflectance values, low fluorescence intensities, and maximum fluorescence intensities shifted to longer wavelengths. It was therefore concluded that Run 257 resids (Illinois #6 coal, C/C) were probably the most reactive, as evidenced by lower reflectances, high yields of volatile matter, and shorter fluorescence spectral peak wavelengths than the other Wilsonville resids investigated, followed by resids from Run 250 (Illinois #6 coal, T/C) and 251-II (Wyodak coal, T/C). Resids produced from Run 259 (Pittsburgh coal, C/C) would probably the least reactive, based on relatively high reflectances, low volatile matter yields, and fluorescence spectra shifted to longer wavelengths than the other Wilsonville resids studied.

Fluorescence and reflectance data suggest that during HRI Run I-27 there was

progressively less hydrogenation of the resid, corresponding to increases in catalyst age, reactor temperatures, and solvent cut-point, and a decrease in the solvent/coal ratio. This was supported by proton nmr data and phenol peak location shifts, which also indicated an increased condensation of aromatic structures during the run. A decrease in the volatile matter content of resids from run day 2 to day 25 suggests that a decrease in resid reactivity occurred over the course of HRI Run I-27.

The unidentified samples numbered 13 and 14 exhibited reflectance and fluorescence properties most similar to Run I-27 PFL 25 and Run 251-II interstage resids, respectively.

It is concluded that quantitative fluorescence microscopy is potentially a rapid, inexpensive technique which can provide new insight into the structure and composition of coal-derived resid. Consequently, an automated fluorescence microscopical technique, as an integral component of a liquefaction process monitoring scheme, could lead to more effective process control. Perhaps the greatest strength of quantitative fluorescence microscopy lies in its ability to resolve inhomogeneities within coal-derived resid samples, including, but not limited to, minerals, unreacted macerals, and multiple resid phases (as determined by reflectance and fluorescence properties). This capability is not possible with most other analytical techniques which typically require dissolution of the resid in a solvent prior to analysis. Whereas these analytical techniques provide chemical and structural information on a homogenized resid sample, and only on the soluble portion, inherent variability within the coal liquids can be identified and measured with fluorescence microscopical methods.

VII. References

(1) Lin, R., Unpublished PhD Thesis, 1988, The Pennsylvania State University, 273 pp.
(2) George, G., In Luminescence Techniques in Solid State Polymer Research (Ed. L. Zlatkevich), Marcel Dekker, 1989, 318 pp.
(3) Mitchell, G.D., Davis, A. and Spackman, W., In Liquid Fuels from Coal (Ed. T.R. Ellington), Academic Press, 1977, pp. 245-270.
(4) Ng, N., Journ. Microscopy, 1983, 132(3), pp. 289-296.
(5) Davis, A., Mitchell, G.D., Derbyshire, F.J., Rathbone, R.F. and Lin, R., Fuel, 1991, 70(3), pp. 352-360.
(6) Shiboaka, M. and Russell, N.J., Fuel, 1983, 62(5), pp. 607-610.
(7) Davis, A., Derbyshire, F.J., Finseth, D.H., Lin, R., Stansberry, P.G. and Terrer, M.-T., Fuel, 1986, 65, pp. 500-506.
(8) Lin, R., Davis, A., Bensley, D.F. and Derbyshire, F.J., Org. Geochem., 1987, 11(5), pp. 393-399.
(9) Jaffee, H.H. and Orchin, M., Theory and Application of Ultra-Violet Spectroscopy, Wiley and Sons, 1965, 624 pp.
(10) Bridges, J.W., In Luminescence in Chemistry (Ed. E.J. Bowen), D. Van Nostrand Co., 1968, pp. 77-115.
(11) Wehry, E.L., In Fluorescence: Theory, Instrumentation and Practice (Ed. G.G. Guilbault), Marcel Dekker, 1967, pp. 37-132.
(12) Bertrand, P., Pittion, J.-L. and Bernaud, C., Org. Geochem., 1986, 10, pp. 641-647.
(13) Bowen, E.J., In Luminescence in Chemistry (Ed. E.J. Bowen), D. Van Nostrand Co., 1968, pp. 1-15.
(14) Becker, R.S., Theory and Interpretation of Fluorescence and Phosphorescence, Wiley Interscience, 1969, 283 pp.
(15) Teichmuller, M. and Durand, B., Int. Journ. Coal Geol., 1983, 2, pp. 197-230.
(16) Pradier, B., Bertrand, P., Martinez, L., Laggoun, F. and Pittion, J.L., In Adv. Org. Geochem. (Eds. L. Mattevelli and L. Novelli), Org. Geochem., 1987, 13(4-6), pp. 1163-1167.
(17) Stellar, M., 1987, Hydrogenation Behavior of Coal Maceral Association. Int. Journ. Coal Geol., 9, pp. 109-127.
(18) McCartney J.T. and Teichmuller, M., Fuel, 1972, 51, pp. 64-68.
(19) Stein, T.R., Cabal, A.V., Callen, R.B., Dabkowski, M.J., Heck, R.H., Simpson, C.A. and Shih, S.S., Upgrading of Coal Liquids for Use as Power Generation Fuels, EPRI Annual Rept., AF-873, Res. Proj. 361-2, 1978, 126 pp.
(20) Derbyshire, F.J., Varghese, P. and Whitehurst, D.D., Fuel, 1983, 62, pp. 491-497.
(21) Derbyshire, F.J., Catalysis in Coal Liquefaction: New Directions for Research, IEA Coal Research, 1988, 69 pp.
(22) Robbins, G.A., Winschel, R.A. and Burke, F.P., Am. Chem. Soc. Div. Fuel Chem. Prepr., 1985, 30(4), pp. 155-163.
(23) Winchel, R.A., Robbins, G.A. and Burke, F.P., Fuel, 1986, 65, pp. 526-532.
(24) Oriel Corp., Light Sources, Monochromators, Detection Systems, 1988 Catalog.

Table 1

Resid Samples

Ref. No.	Coal Feed	Source/Conditions	Comments
1.	Wyodak	W; Run 251-II T/C	interstage
2.	Wyodak	W; Run 251-II T/C	recycle
3.	Pittsburgh	W; Run 259 C/C	interstage
4.	Pittsburgh	W; Run 259 C/C	recycle
5.	Illinois #6	W; Run 250 T/C	interstage
6.	Illinois #6	W; Run 250 T/C	recycle
7.	Illinois #6	W; Run 257 C/C	interstage
8.	Illinois #6	W; Run 257 C/C	recycle
9.	Illinois #6	HRI; Run I-27	PFL P 2
10.	Illinois #6	HRI; Run I-27	PFL P 8
11.	Illinois #6	HRI; Run I-27	PFL P 18
12.	Illinois #6	HRI; Run I-27	PFL P 25
13.	Blind Sample		
14.	Blind Sample		

Note: T/C = thermal/catalytic; C/C = catalytic/catalytic;
PFL = pressure filter liquid; P = period; W = Wilsonville

Table 2

Run 251-II (Wyodak coal, T/C)

Property	Interstage	Recycle Popl. 1	Recycle Popl. 2
Lmax (nm)[a]	696	682	578
Intensity (counts)[b]	3880	7700	18268
Mean Reflectance (%)	7.80	7.66	
Ash (%, a.r.)	25.22	27.01	
Carbon %	88.27	87.81	
Hydrogen %	6.07	6.85	
Aromatics (%)	33.2	26.8	
Alpha (%)	29.1	28.4	
Beta+Gamma (%)	37.6	44.8	
Phenol Conc. (meq/g)	1.10	0.74	
Phenol Peak (cm^{-1})	3294	3298	
Volatile Matter (%,maf)	60.6	73.4	
IOM (%)	16.0	13.4	
Heating Value (Btu/lb)	15653	16125	

(a) Lmax = wavelength of maximum intensity, average of six (6) spectra, except popl. 2, which is from only one spectrum.
(b) Intensity is calculated as the area beneath uncorrected spectra, and represents averaged data as for Lmax.

Table 3

Run 259 (Pittsburgh coal, C/C)

Property	Interstage	Recycle
Lmax (nm)[a]	696	696
Intensity (counts)[b]	6658	8497
Mean Reflectance (%)	7.82	7.70
Ash (%, a.r.)	8.74	8.51
Carbon %	90.12	91.01
Hydrogen %	6.19	6.50
Aromatics (%)	33.3	31.5
Alpha (%)	31.1	28.3
Beta+Gamma (%)	35.6	40.2
Phenol Conc. (meq/g)	0.92	0.69
Phenol Peak (cm^{-1})		
Volatile Matter (%,maf)	62.6	68.3
IOM (%)		
Heating Value (Btu/lb)	14896	15177

(a) Lmax = wavelength of maximum intensity, average of five (5) spectra.
(b) Intensity is calculated as the area beneath uncorrected spectra, and represents averaged data as for Lmax.

Table 4

Run 250 (Illinois #6 coal, T/C)

Property	Interstage	Recycle
Lmax (nm)[a]	684	660
Intensity (counts)[b]	4746	6150
Mean Reflectance (%)	7.84	7.30
Ash (%, a.r.)	6.13	0.20
Carbon %	89.65	89.73
Hydrogen %	6.33	7.43
Aromatics (%)	34.5	26.1
Alpha (%)	30.3	28.7
Beta+Gamma (%)	35.3	45.2
Phenol Conc. (meq/g)	1.07	0.74
Phenol Peak (cm^{-1})	3292	3299
Volatile Matter (%,maf)	74.0	85.2
IOM (%)	4.6	0.2
Heating Value (Btu/lb)	16255	16537

(a) Lmax = wavelength of maximum intensity, average of five (5) spectra.
(b) Intensity is calculated as the area beneath uncorrected spectra, and represents averaged data as for Lmax.

Table 5

Run 257 (Illinois #6 coal, C/C)

Property	Interstage Popl.1	Interstage Popl.2	Recycle Popl.1	Recycle Popl.2
Lmax (nm)	646	604	633	585
Intensity (counts)	6714	12666	9284	32108
Mean Reflectance (%)	6.82		6.48	
Ash (%, a.r.)	12.52		9.28	
Carbon %	88.05		88.64	
Hydrogen %	7.70		8.08	
Aromatics (%)	21.8		19.9	
Alpha (%)	28.8		28.0	
Beta+Gamma (%)	49.5		52.0	
Phenol Conc. (meq/g)	0.68		0.50	
Phenol Peak (cm^{-1})	3300		3302	
Volatile Matter (%,maf)	94.3		88.2	
IOM (%)	21.3		14.8	
Heating Value (Btu/lb)	16708		17056	

Table 6

Fluorescence Data for Wilsonville Resids

Run No.	Sample Type	Intensity[c] (counts)	Std.Dev.	Lmax[b] (nm)	Std.Dev.
251-II	T/C, Int[a]	3880	1249	696	7
251-II	T/C, Rec	7700	2068	682	11
251-II	T/C, Rec	18268	-	578	-
259	C/C, Int	6658	887	696	2
259	C/C, Rec	8497	2032	696	3
250	T/C, Int	4746	361	684	5
250	T/C, Rec	6150	1206	660	17
257	C/C, Int	6714	1534	646	7
257	C/C, Int	12666	-	604	-
257	C/C, Rec	9284	1055	633	8
257	C/C, Rec	32108	-	585	-

(a) T/C = Thermal/Catalytic, C/C = Catalytic/Catalytic
Int = Interstage, Rec = Recycle
(b) Values are averages of multiple (>=3) spectra; exceptions are those w/o std. dev., which were obtained from two or less spectra.
(c) Values are in computer counts (arbitrary units), and are calculated as areas beneath uncorrected spectra.

Table 7

Reflectance Data for Wilsonville Resids

Run No.	Sample Type	Reflectance (%, random)	Std. Dev.
251-II	T/C, Int	7.80	0.22
251-II	T/C, Rec	7.66	0.25
259	C/C, Int	7.82	0.11
259	C/C, Rec	7.70	0.26
250	T/C, Int	7.84	0.13
250	T/C, Rec	7.30	0.15
257	C/C, Int	6.82	0.20
257	C/C, Rec	6.48	0.19

Table 8

Chemical Data for Resids

Run No.	Coal	Sample Type	C (%)	H (%)	Proton NMR Data Arom.[b] (%)	Alpha (%)	B + G (%)
251-II	Wyodak	T/C, Int[a]	88.27	6.07	33.2	29.1	37.6
251-II	Wyodak	T/C, Rec	87.81	6.85	26.8	28.4	44.8
259	Pitt	C/C, Int	90.12	6.19	33.3	31.1	35.6
259	Pitt	C/C, Rec	91.01	6.50	31.5	28.3	40.2
250	Ill #6	T/C, Int	89.65	6.33	34.5	30.3	35.3
250	Ill #6	T/C, Rec	89.73	7.43	26.1	28.7	45.2
257	Ill #6	C/C, Int	88.05	7.70	21.8	28.8	49.5
257	Ill #6	C/C, Rec	88.64	8.08	19.9	28.0	52.0
I-27	Ill #6	C/C, P2	88.06	9.14	14.5	28.1	57.3
I-27	Ill #6	C/C, P8	88.25	8.18	20.7	28.3	51.0
I-27	Ill #6	C/C, P18	89.58	7.12	29.2	30.2	40.5
I-27	Ill #6	C/C, P25	90.31	6.50	38.3	28.8	32.8

Run No.	Coal	Sample Type	Phenols (meq/g)	Peak[c] (cm^{-1})	V.M. (% maf)	IOM[d] (%)	H.V.[e] (BTU/lb)
251-II	Wyodak	T/C, Int	1.10	3294	60.6	16.0	15653
251-II	Wyodak	T/C, Rec	0.74	3298	73.4	13.4	16125
259	Pitt	C/C, Int	0.92		62.6		14896
259	Pitt	C/C, Rec	0.69		68.3		15177
250	Ill #6	T/C, Int	1.07	3292	74.0	4.6	16255
250	Ill #6	T/C, Rec	0.74	3299	85.2	0.2	16537
257	Ill #6	C/C, Int	0.68	3300	94.3	21.3	16708
257	Ill #6	C/C, Rec	0.50	3302	88.2	14.8	17056
I-27	Ill #6	C/C, P2	0.25	3305	94.7		
I-27	Ill #6	C/C, P8	0.41	3301	97.6		
I-27	Ill #6	C/C, P18	0.66	3297	82.1		
I-27	Ill #6	C/C, P25	0.71	3296	73.8		

a. T/C = thermal/catalytic, Int = Interstage, Rec = Recycle
b. Arom. = Aromatic, B + G = Beta + Gamma
c. Peak = FTIR Phenol Peak
d. IOM = Insoluble Organic Matter
e. H.V. = Heating Value

Table 9

Run I-27 (Illinois #6 coal, C/C)

Property	PFL Sample Designation (run days) 2	8	18	25
Lmax (nm)[a]	621	652	696	696
Std. Dev.	3	3	4	3
Intensity (counts)[b]	18184	6903	4660	3470
Std. Dev.	1477	874	802	431
Mean Reflectance (%)	6.21	6.80	7.57	8.06
Std. Dev.	0.12	0.07	0.14	0.08
Carbon %	88.06	88.25	89.58	90.31
Hydrogen %	9.14	8.18	7.12	6.50
Aromatics (%)	14.5	20.7	29.2	38.3
Alpha (%)	28.1	28.3	30.2	28.8
Beta+Gamma (%)	57.3	51.0	40.5	32.8
Phenol Conc. (meq/g)	0.25	0.41	0.66	0.71
Phenol Peak (cm^{-1})	3305	3301	3297	3296
Volatile Matter (%,maf)	94.7	97.6	82.1	73.8

(a) Lmax = wavelength of maximum intensity, average of five (5) spectra.
(b) Intensity is calculated as the area beneath uncorrected spectra, and represents averaged data as for Lmax.

Table 10

Fluorescence and Reflectance Data for Unknown Samples

Sample	Lmax (nm)	s.d. (nm)	Intensity (cts)[a]	s.d.[b] (cts)	Reflectance (%, random)	s.d. (%)
#13	699	3	4201	363	8.12	0.11
#14	695	5	4075	1129	7.51	0.45

(a) Refers to computer counts (arbitrary units)
(b) Standard deviation

Table 11

Fluorescence Spectral Data For Resid Composites

Run No.	Sample Type[a]	Wavelength w/ Relative Intensity Equal To:[b] 25% x[c]	25% s.d.	50% x	50% s.d.	75% x	75% s.d.	100% x	100% s.d.
251-II	T/C, Int	499	11	567	12	619	13	696	7
251-II	T/C, Rec	<470	-[d]	545	24	596	22	682	11
251-II	T/C, Rec	<470	-	<470	-	500&675[e]		578	-
259	C/C, Int	531	12	584	9	627	9	696	2
259	C/C, Rec	528	13	581	9	624	7	696	3
250	T/C, Int	501	3	558	2	600	2	684	5
250	T/C, Rec	486	4	542	6	586	6	660	17
257	C/C, Int	<470	-	520	4	572	1	646	7
257	C/C, Int	<470	-	<470	-	515&700		604	-
257	C/C, Rec	<470	-	503	3	553	3	633	8
257	C/C, Rec	<470	-	<470	-	508&668		585	-
I27	C/C, P2	<470	-	495	3	541	2	621	3
I27	C/C, P8	<470	-	512	4	565	4	652	3
I27	C/C, P18	504	10	568	4	615	3	696	4
I27	C/C, P25	525	13	584	4	629	3	696	3
Unknown	#13	532	4	587	2	631	3	699	3
Unknown	#14	501	6	562	10	613	8	695	5
251R[f]	T/C, Int	495	14	562	12	615	9	696	6
259R	C/C, Rec	514	4	570	2	615	2	688	0
250R	T/C, Rec	473	5	531	3	576	3	643	0
I27R	C/C, P8	<470	-	493	1	543	1	640	2

(a) T/C = Thermal/Catalytic, C/C = Catalytic/Catalytic
Int = Interstage, Rec = Recycle
(b) Wavelength(s) with relative intensities of 25,50,75, or 100%
(c) x = avg. wavelength (nm) from multiple spectra
s.d. = standard deviation
(d) Std. Dev. not calculated because <3 spectra were acquired, or else all intensities in spectra were greater than the specified relative intensity
(e) Spectra had 75% relative intensity at two wavelengths
(f) Replicate analyses

Table 12

Replicate Analyses for Resids

Run No.	Sample Type	First Analysis Lmax (nm)	s.d.	Intensity (counts)	Replicate[b] Lmax (nm)	s.d.	Intensity (counts)
251-II	T/C, Int[a]	696	7	3880	696	6	7107
259	C/C, Rec	696	3	8497	688	0	7136
250	T/C, Rec	660	17	6150	643	0	8108
I27	C/C, P8	652	6	6903	640	2	8193

(a) T/C = Thermal/Catalytic, C/C = Catalytic/Catalytic
Int = Interstage, Rec = Recycle
(b) Replicate data represents mean values of 3 spectra

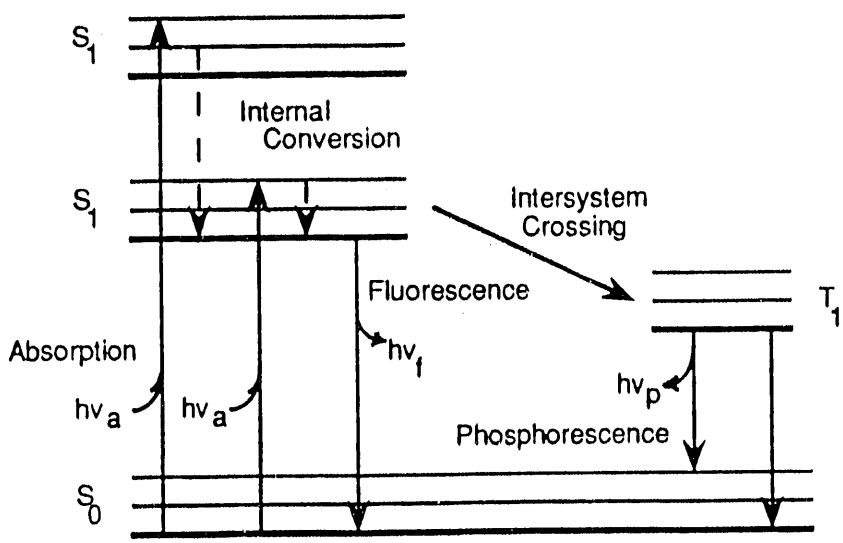

Figure 1. Energy level diagram for absorption and emission of light (from Lakowicz, 1983). hv_a = *absorption*, hv_f = *fluorescence*, hv_p = *phosphorescence*, S_1 *and* T_1 represent singlet and triplet excited states, respectively, and S_0 is the ground state

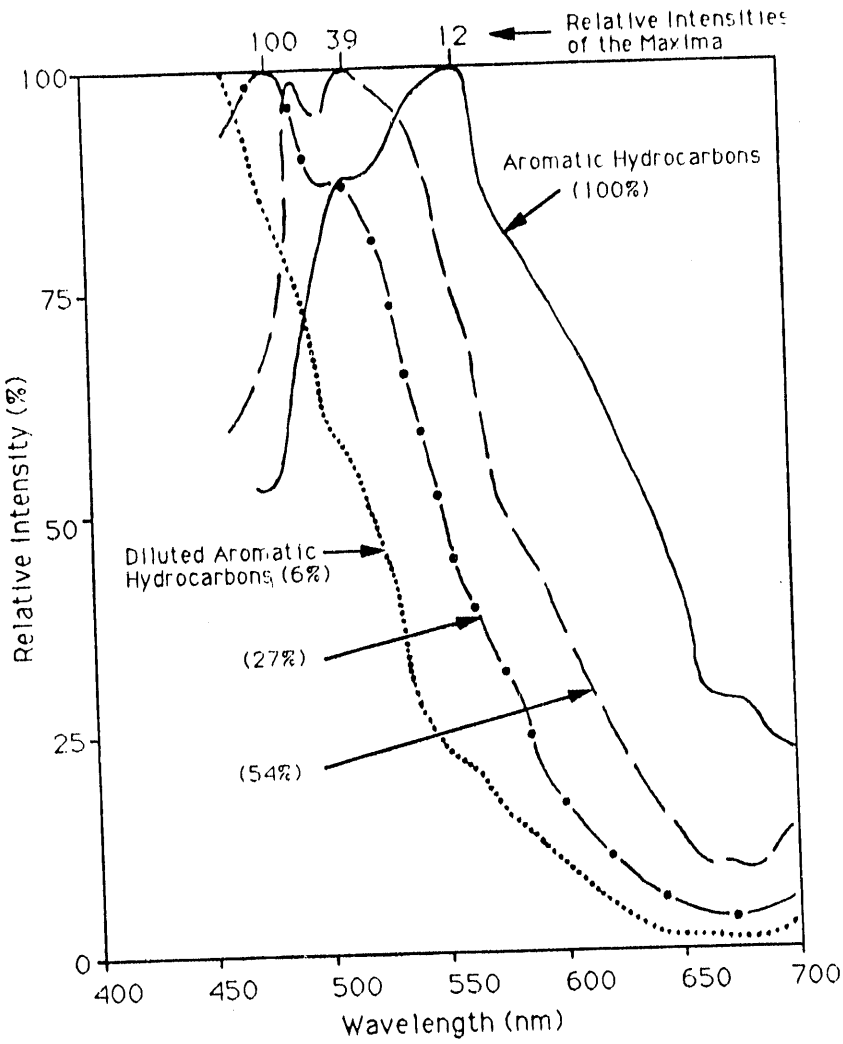

Figure 2. The effects of dilution of aromatic hydrocarbons in a non-fluorescing paraffin oil on the fluorescence emission (modified from ref. 12)

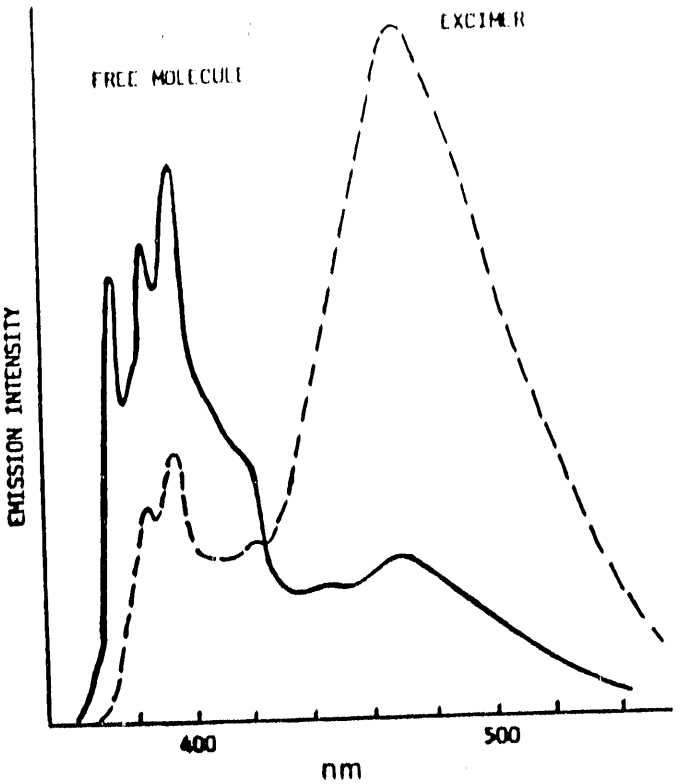

Figure 3. Excimer fluorescence from pyrene, caused by an increased concentration of chromophores (from ref. 2)

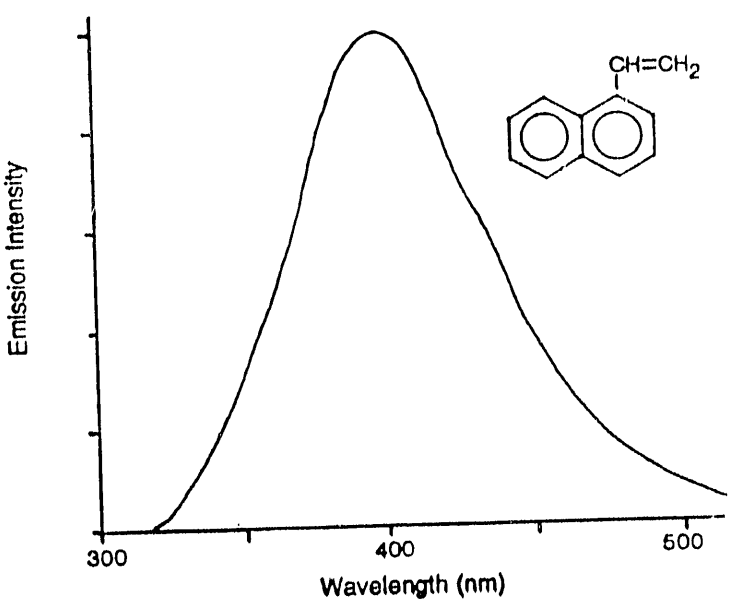

Figure 4. Excimer fluorescence from 1-vinylnaphthalene in the solid state (modified from ref. 2)

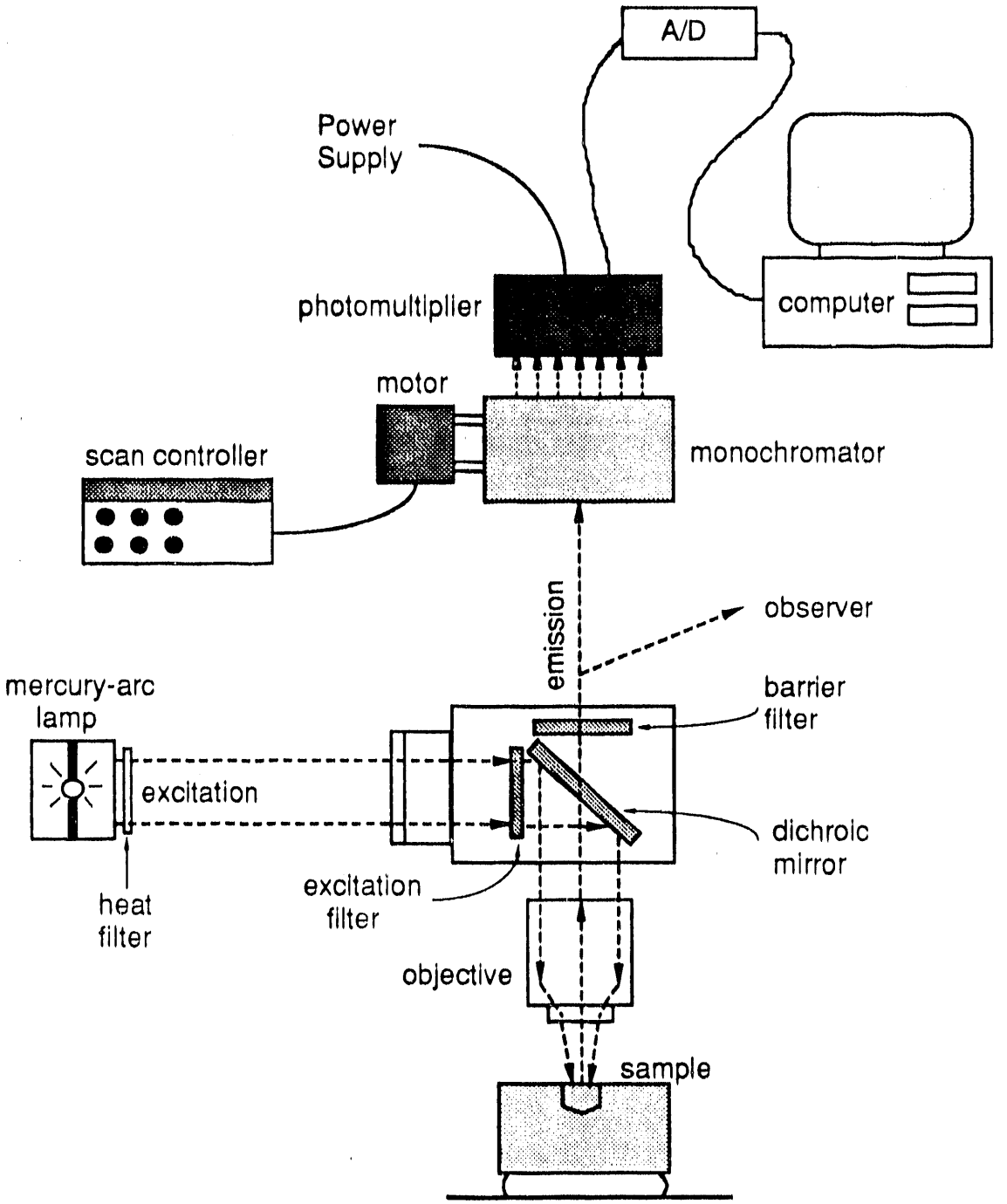

Figure 5. Schematic optical and electronic configuration of a Leitz spectral fluorescence microscope photometer

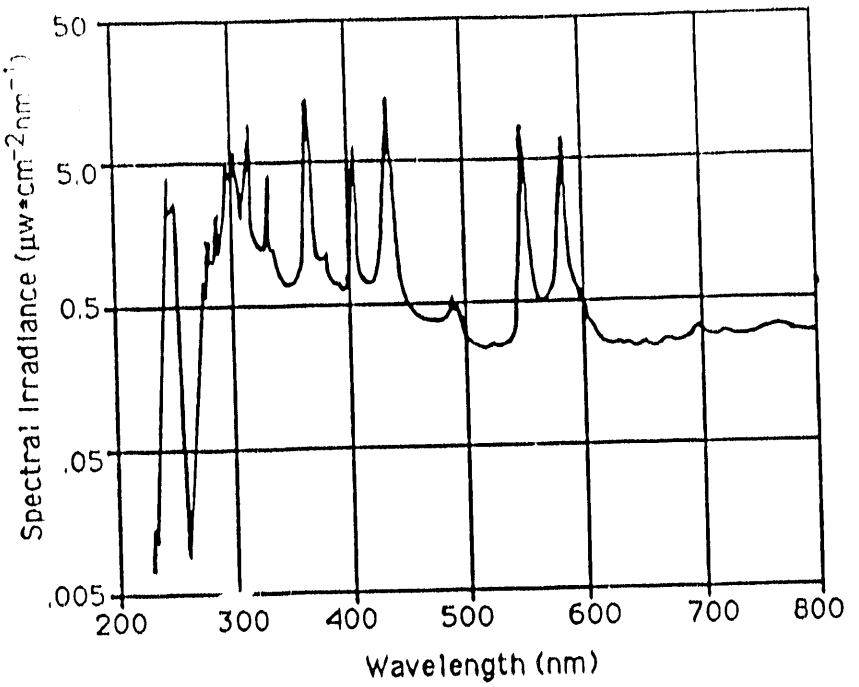

Figure 6. Spectral irradiance of a 100 W mercury arc lamp

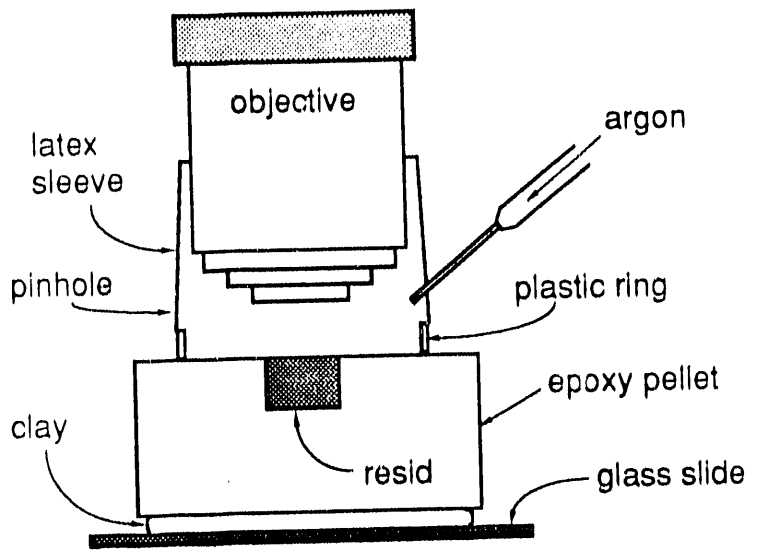

Figure 7. Apparatus for measurement of resid fluorescence in an inert atmosphere

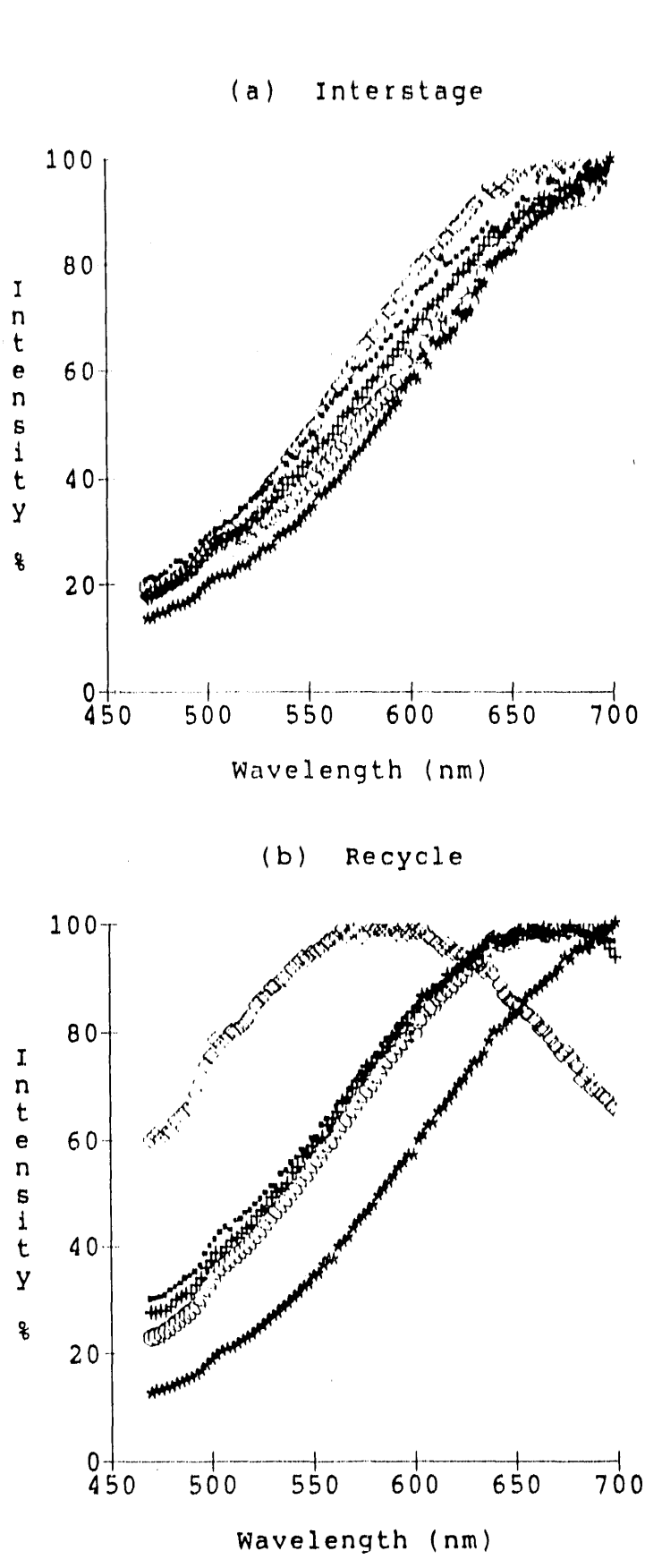

Figure 8. Corrected fluorescence spectra for Run 251-II resids. Each curve represents the fluorescence spectrum from a different resid particle.

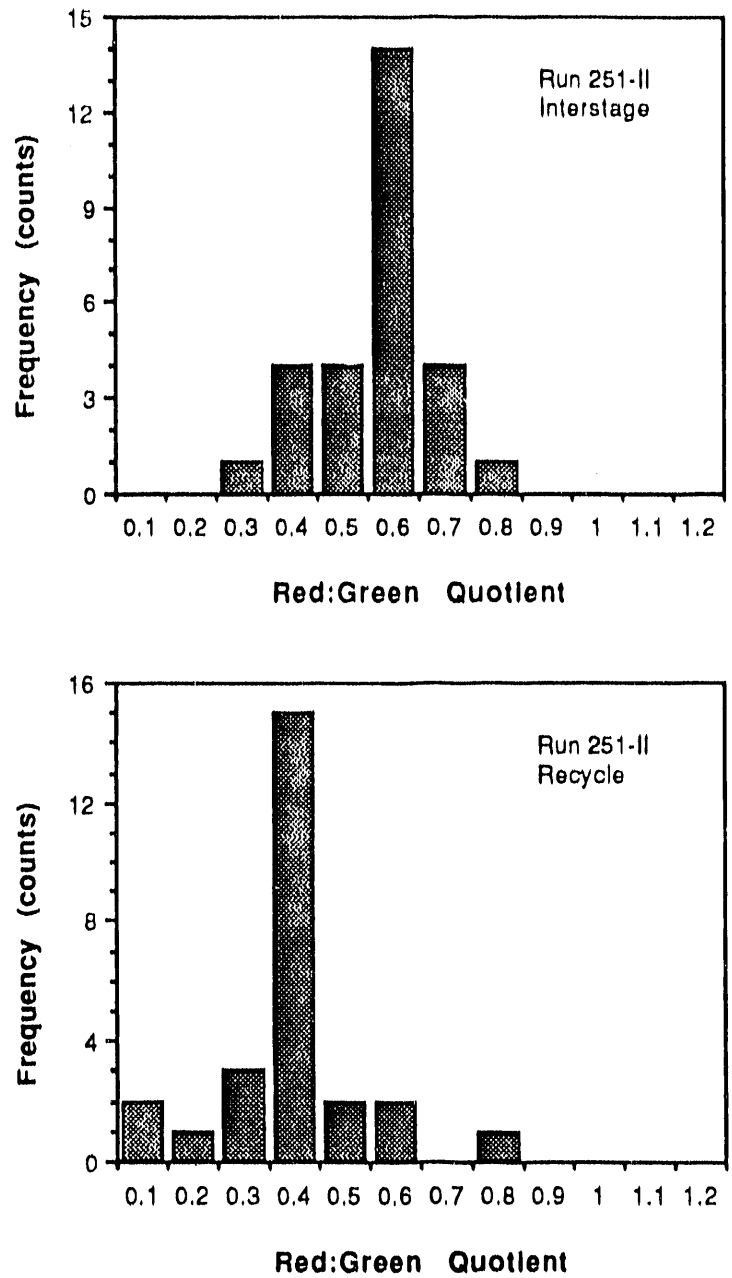

Figure 9. Red:Green quotient histograms for Run 251-II resids

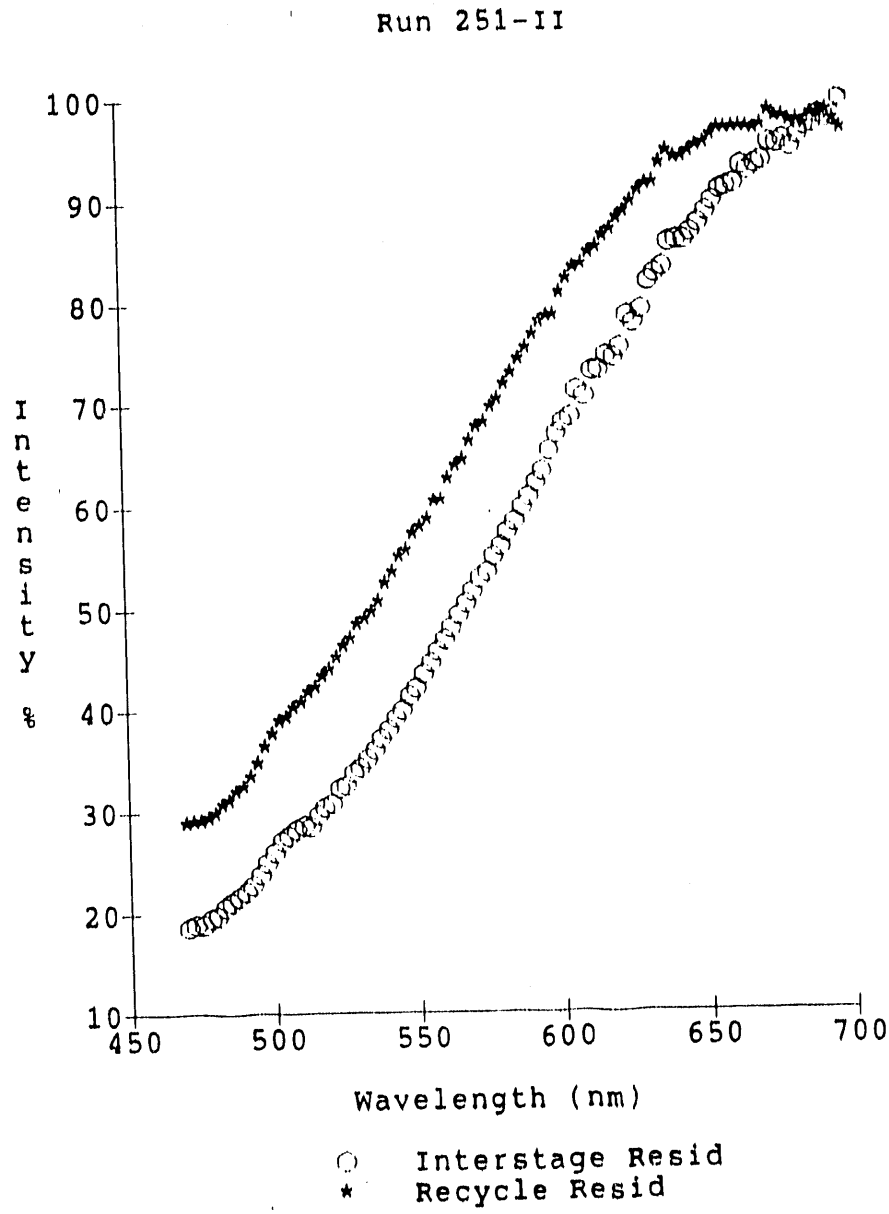

Figure 10. Averaged corrected spectra for Run 251-II resids. Recycle sample average did not include the resid population with Lmax at 578 nm.

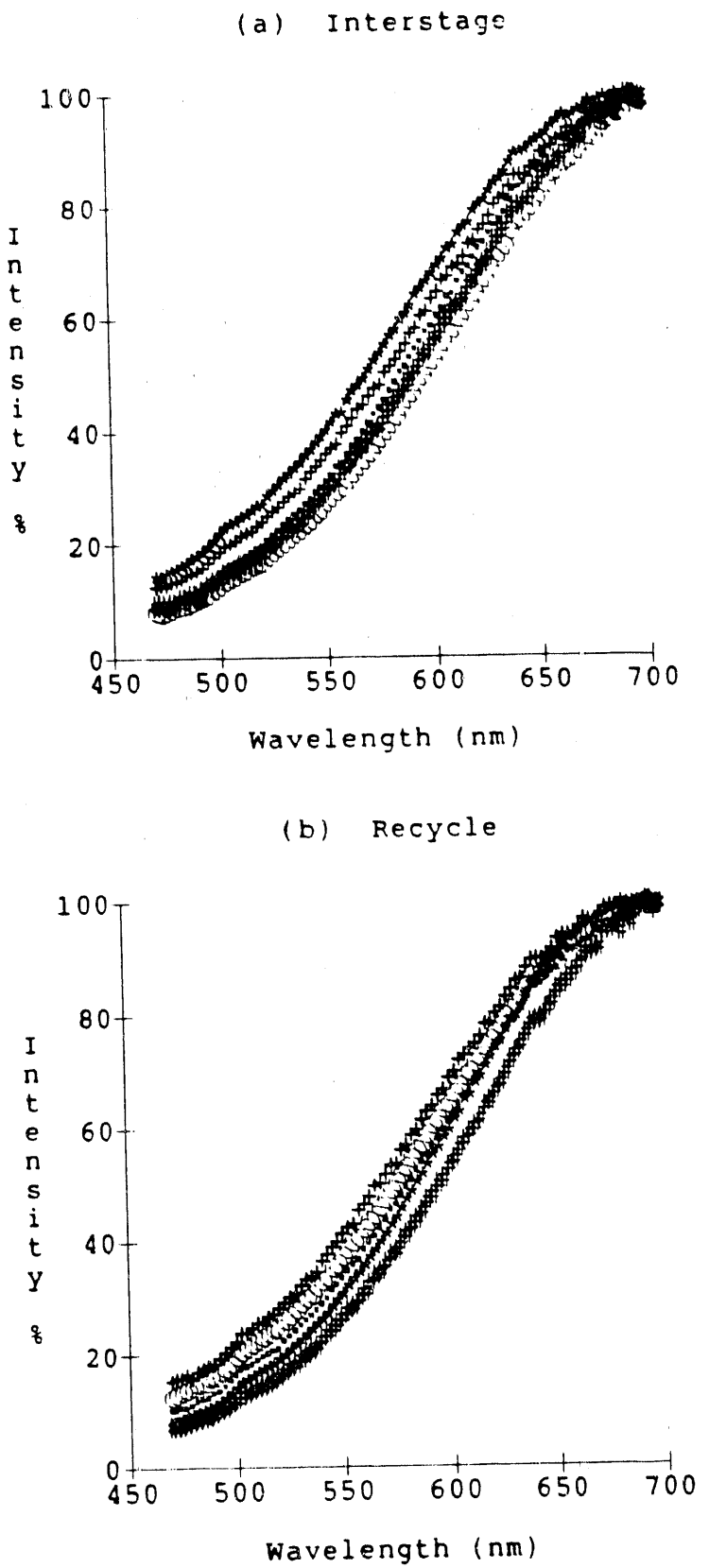

Figure 11. Corrected fluorescence spectra for Run 259 resids.

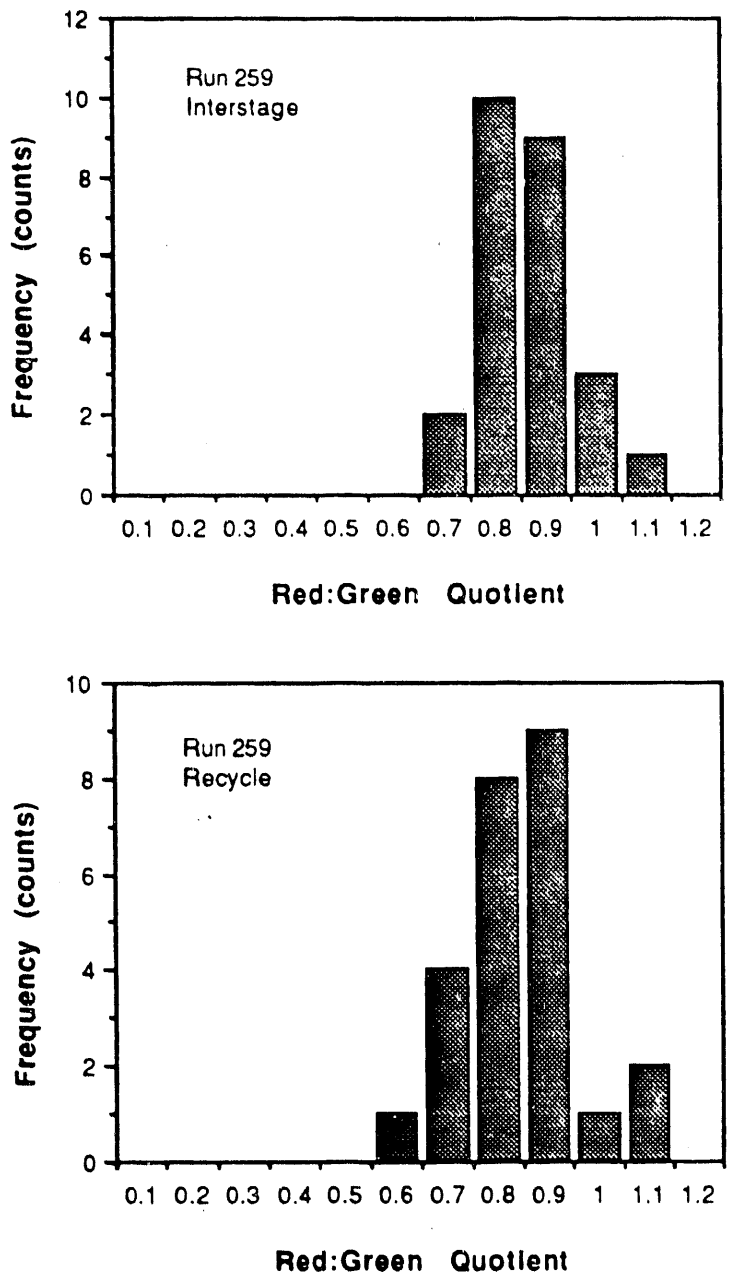

Figure 12. Red:Green quotient histograms for Run 259 resids

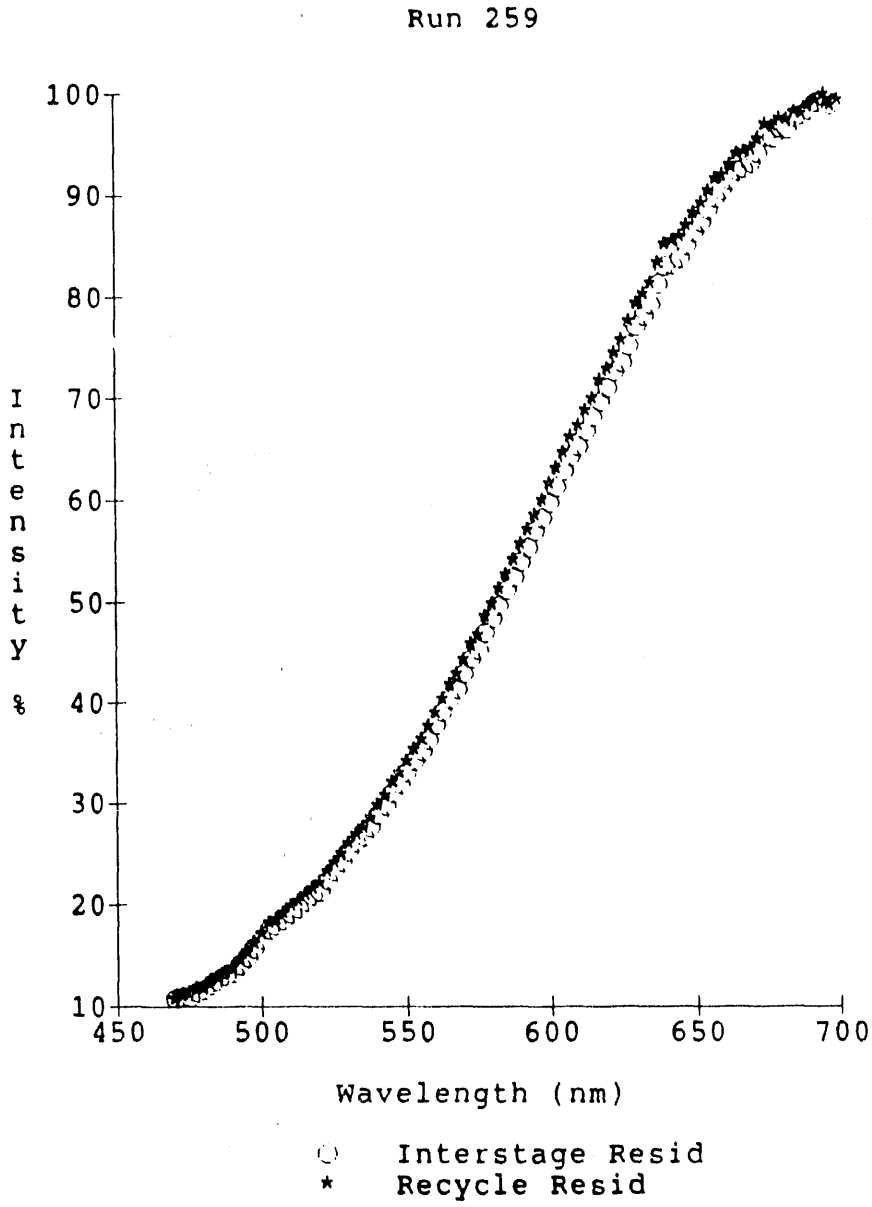

Figure 13. Averaged corrected spectra for Run 259 resids

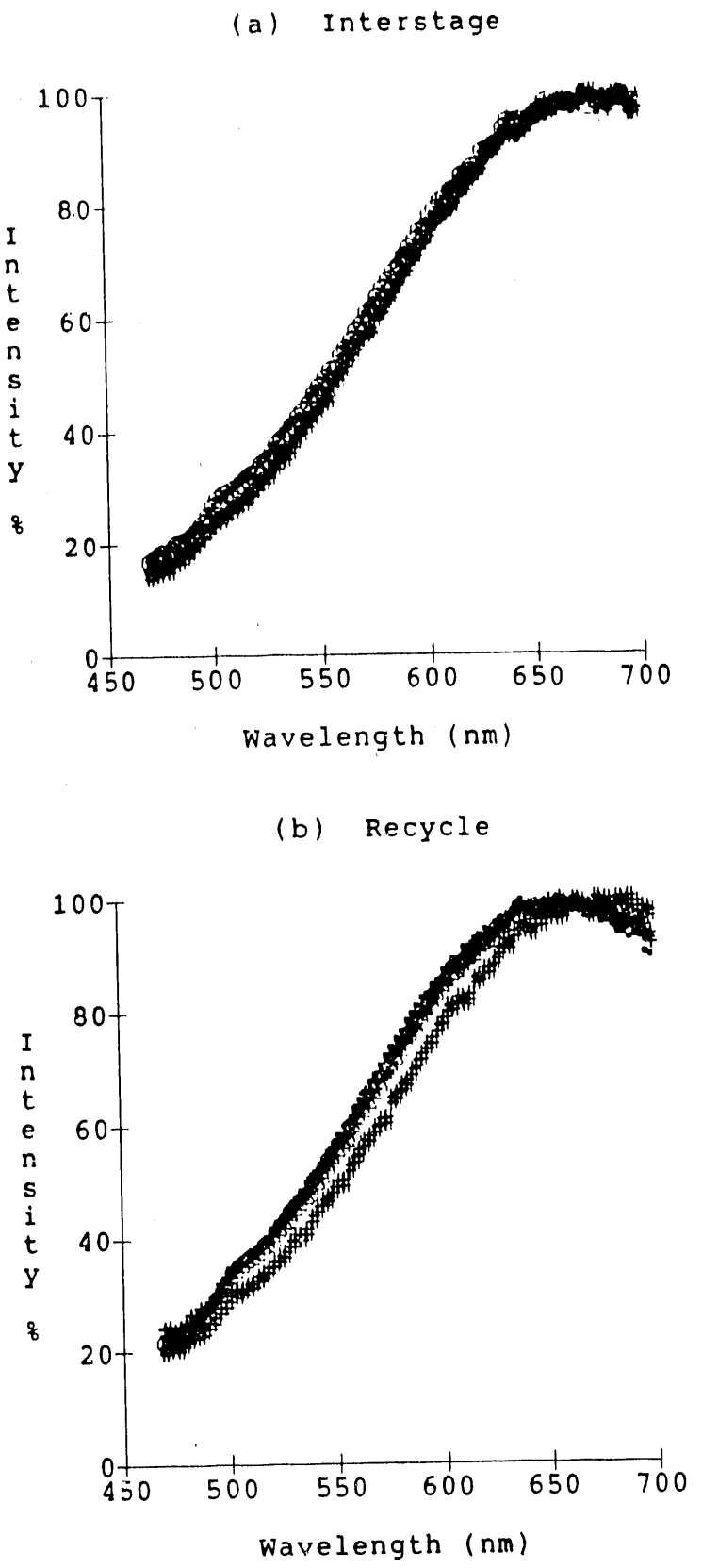

Figure 14. Corrected fluorescence spectra for Run 250 resids

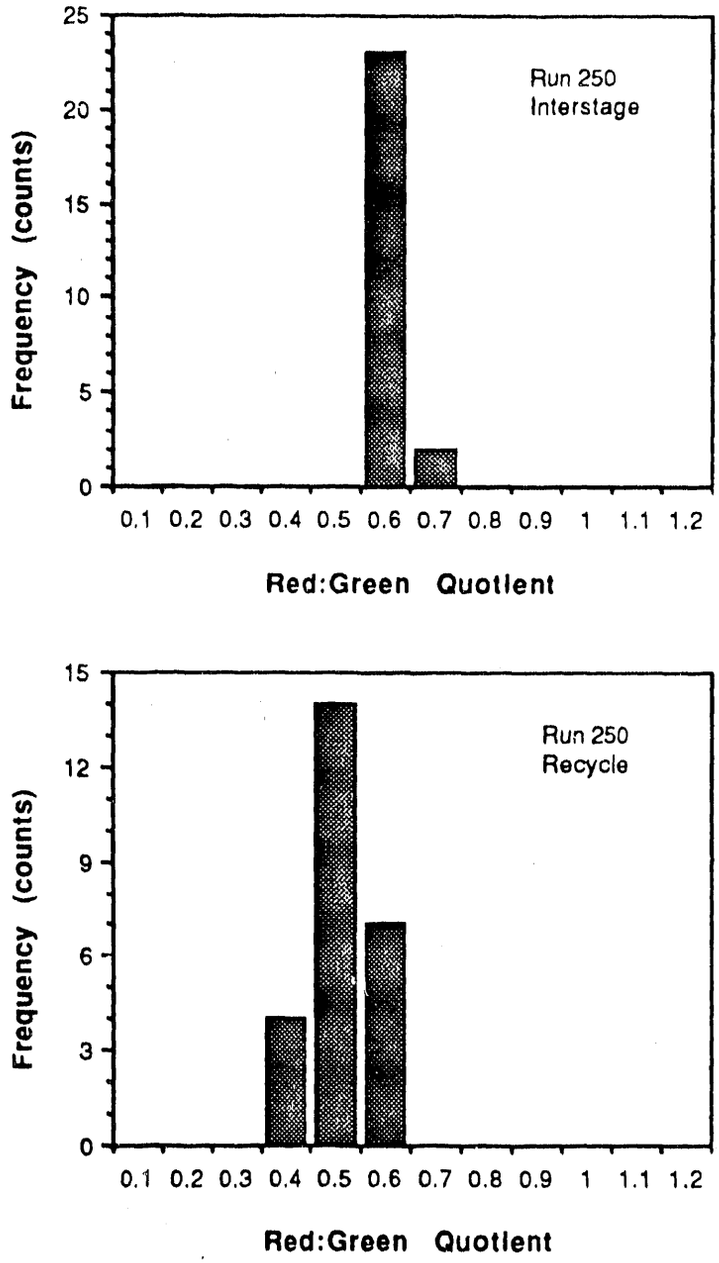

Figure 15. Red:Green quotient histograms for Run 250 resids

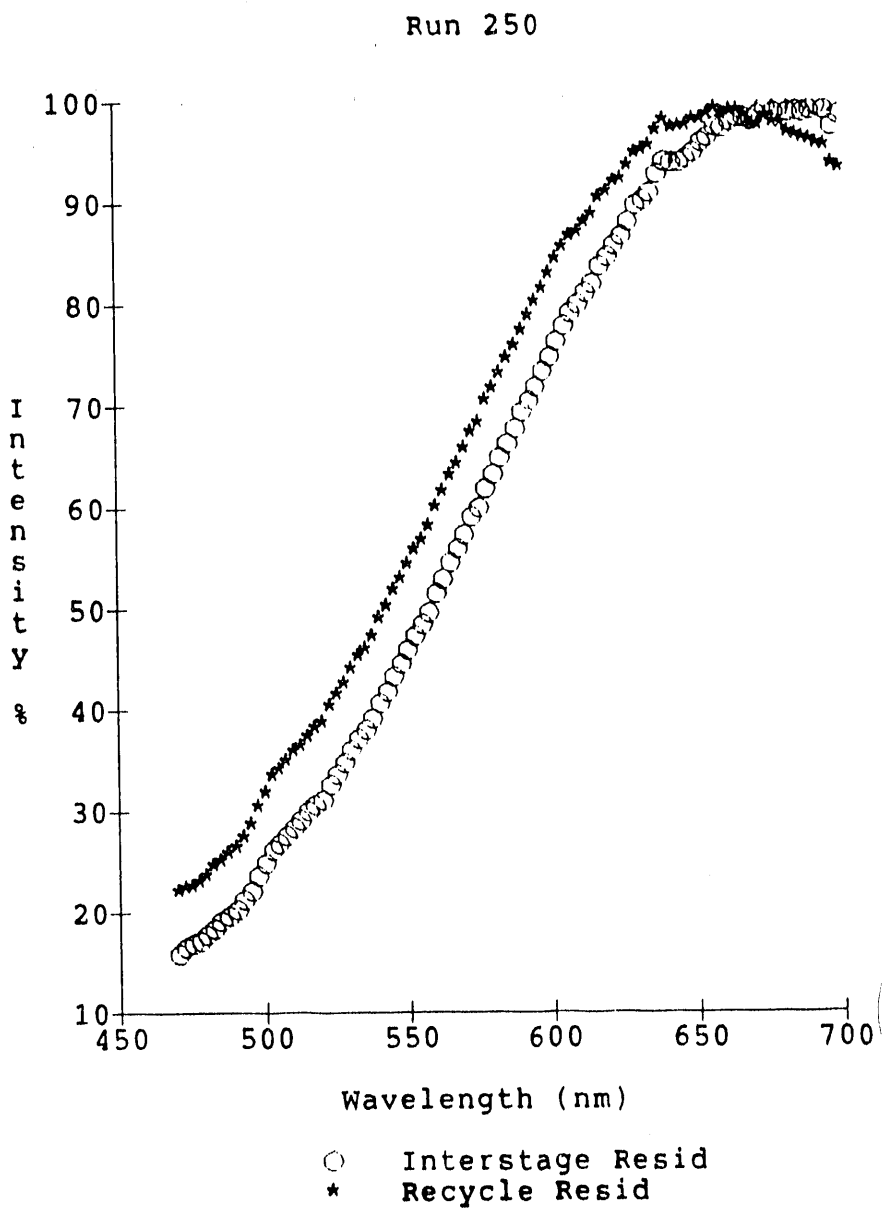

Figure 16. Averaged corrected spectra for Run 250 resids

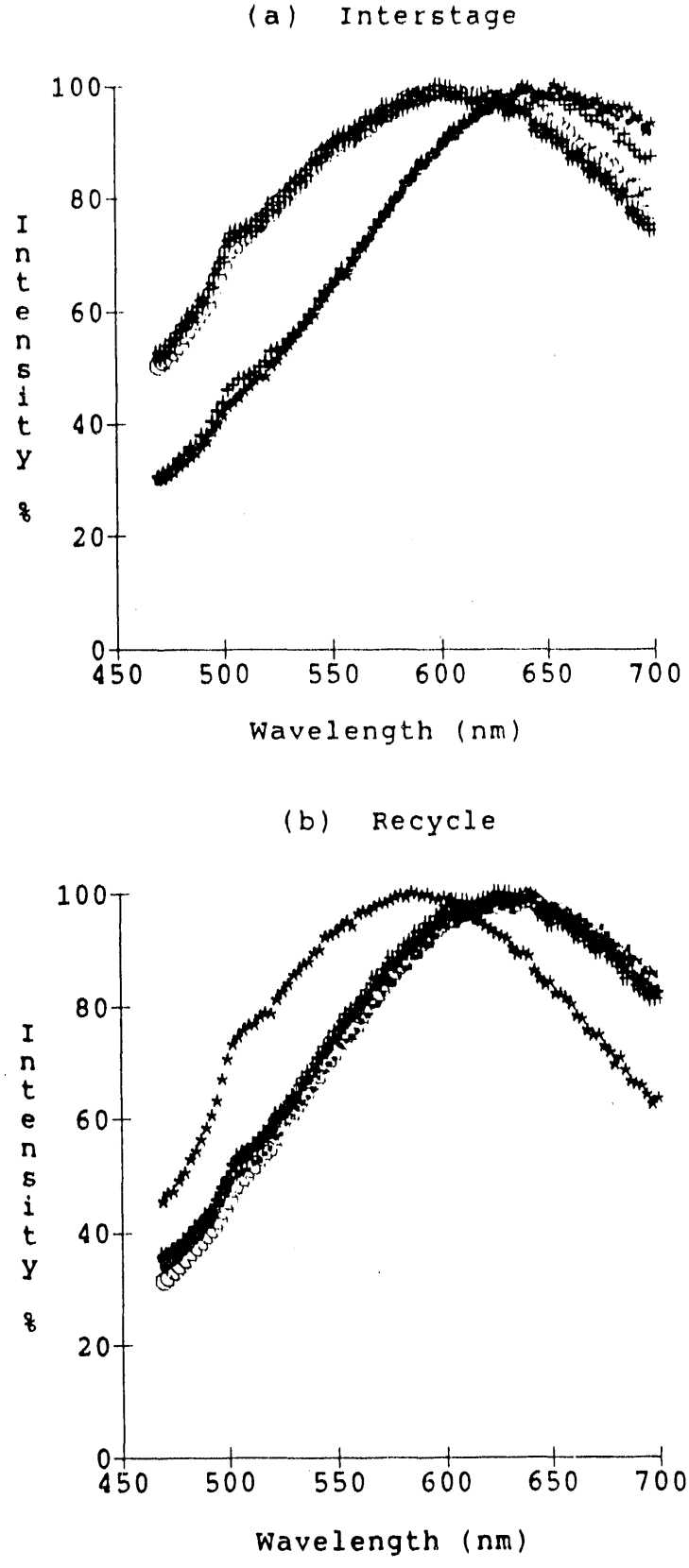

Figure 17. Corrected fluorescence spectra for Run 257 resids

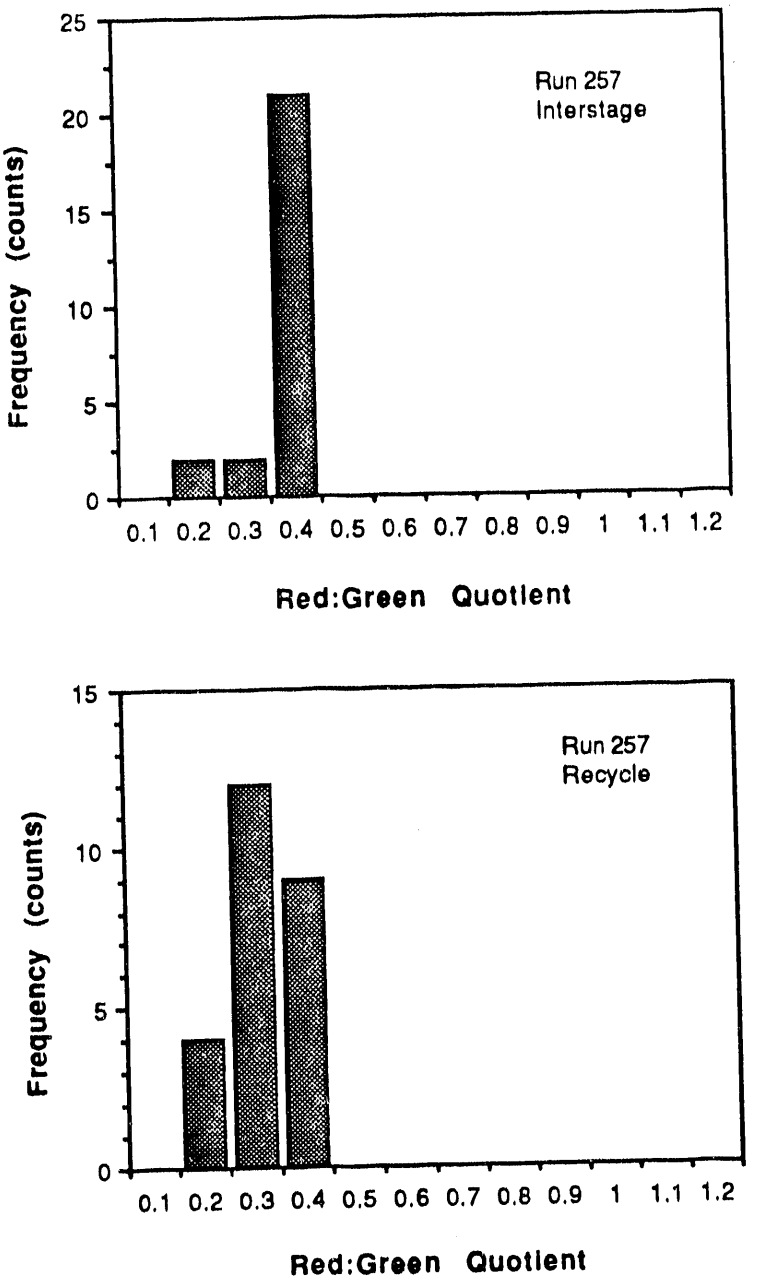

Figure 18. Red:Green quotient histograms for Run 257 resids

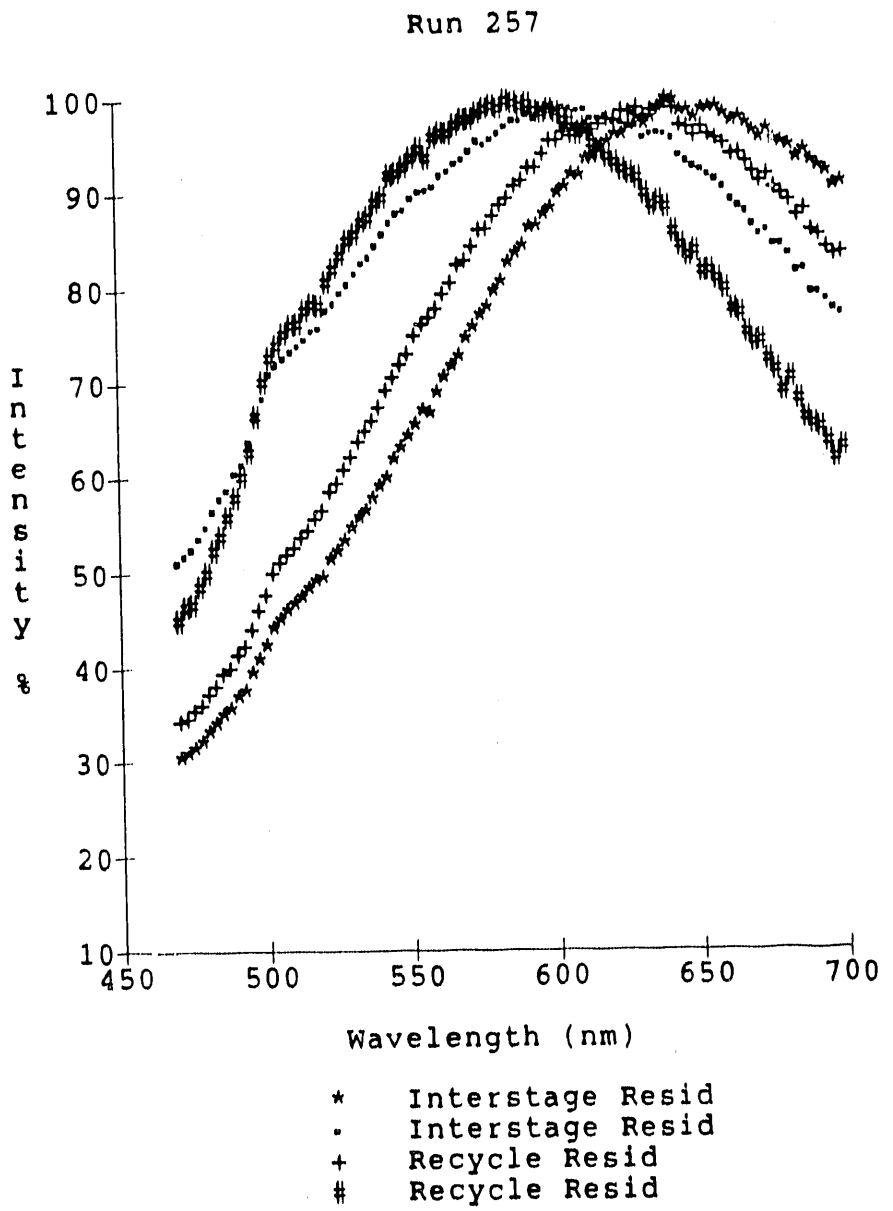

Figure 19. Averaged corrected spectra for Run 257 resids. Recycle resid spectrum denoted by # represents only one (1) spectrum, not an average of multiple spectra.

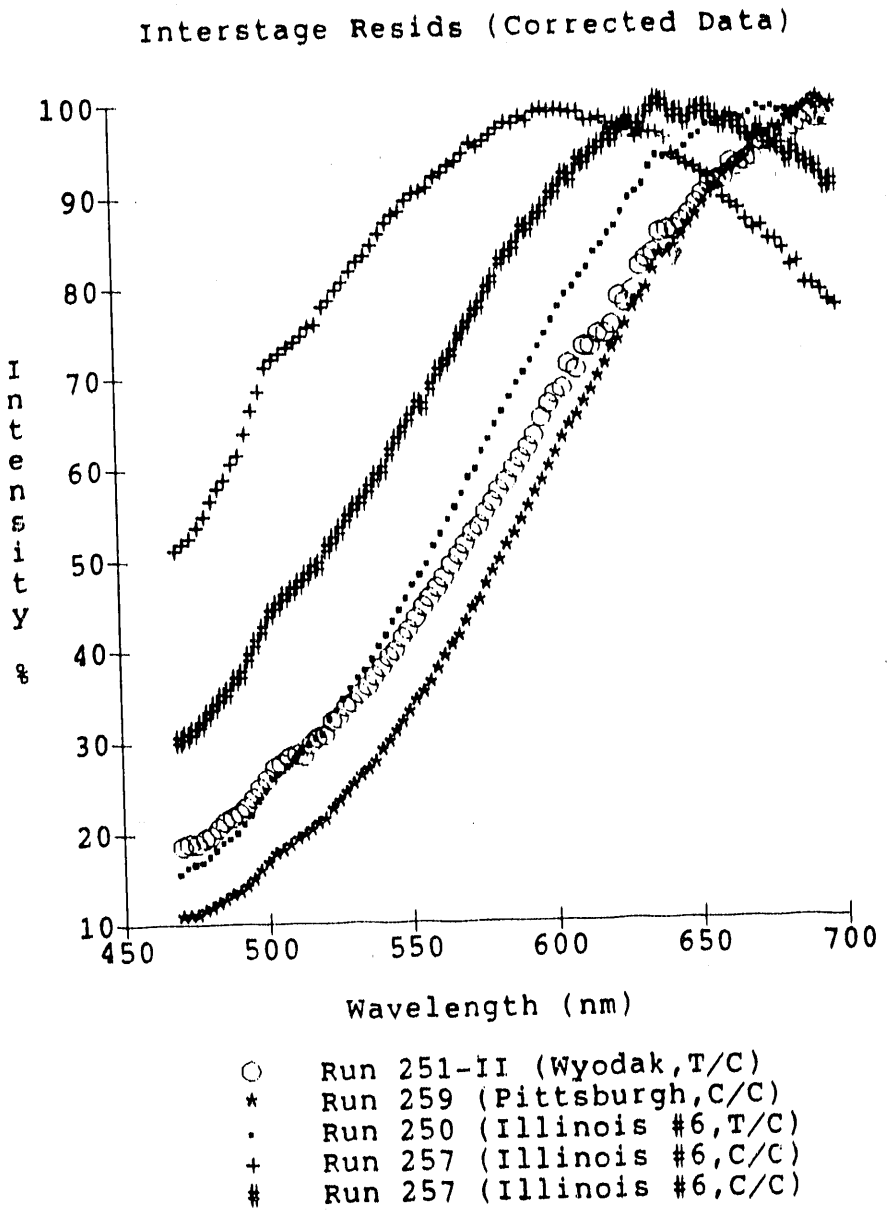

Figure 20. Averaged corrected fluorescence spectra for Wilsonville interstage resid samples

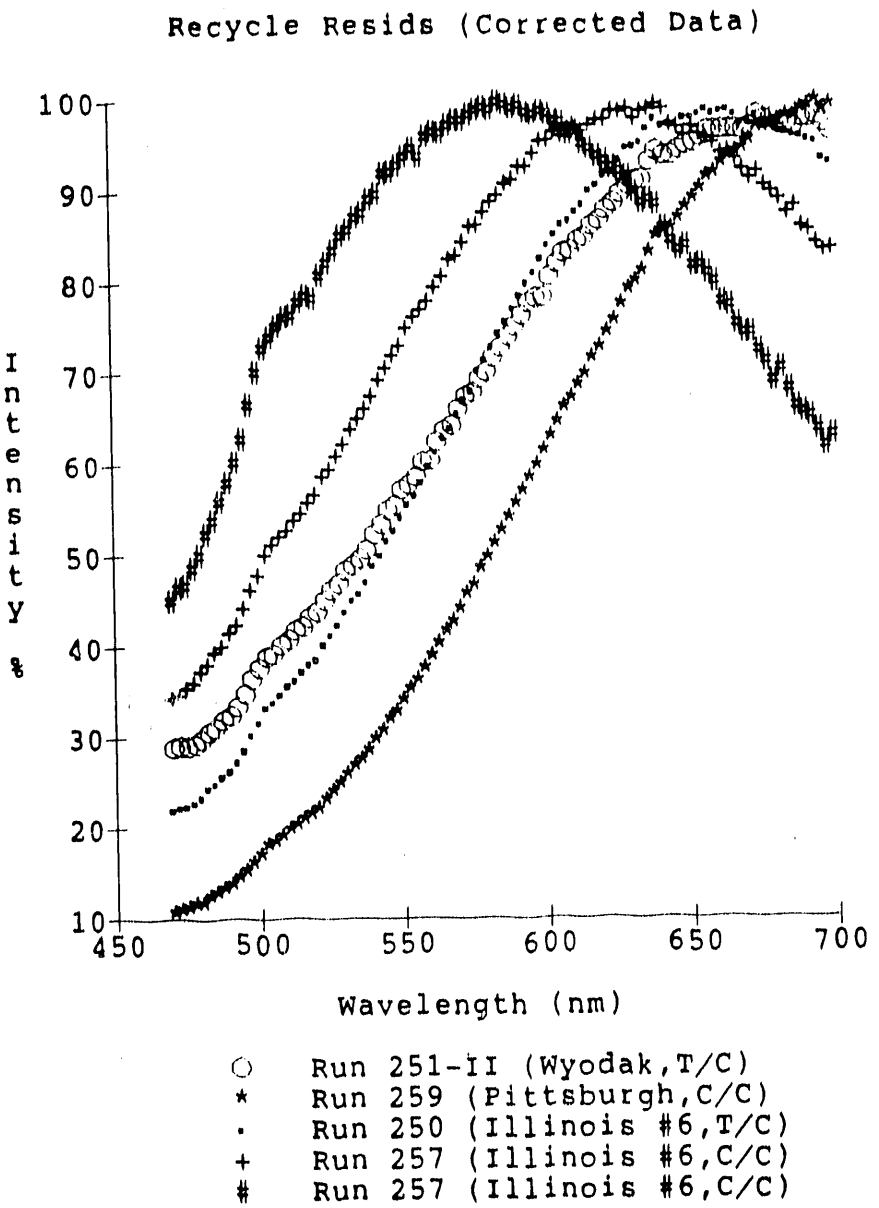

Figure 21. Averaged corrected fluorescence spectra for Wilsonville recycle resid samples

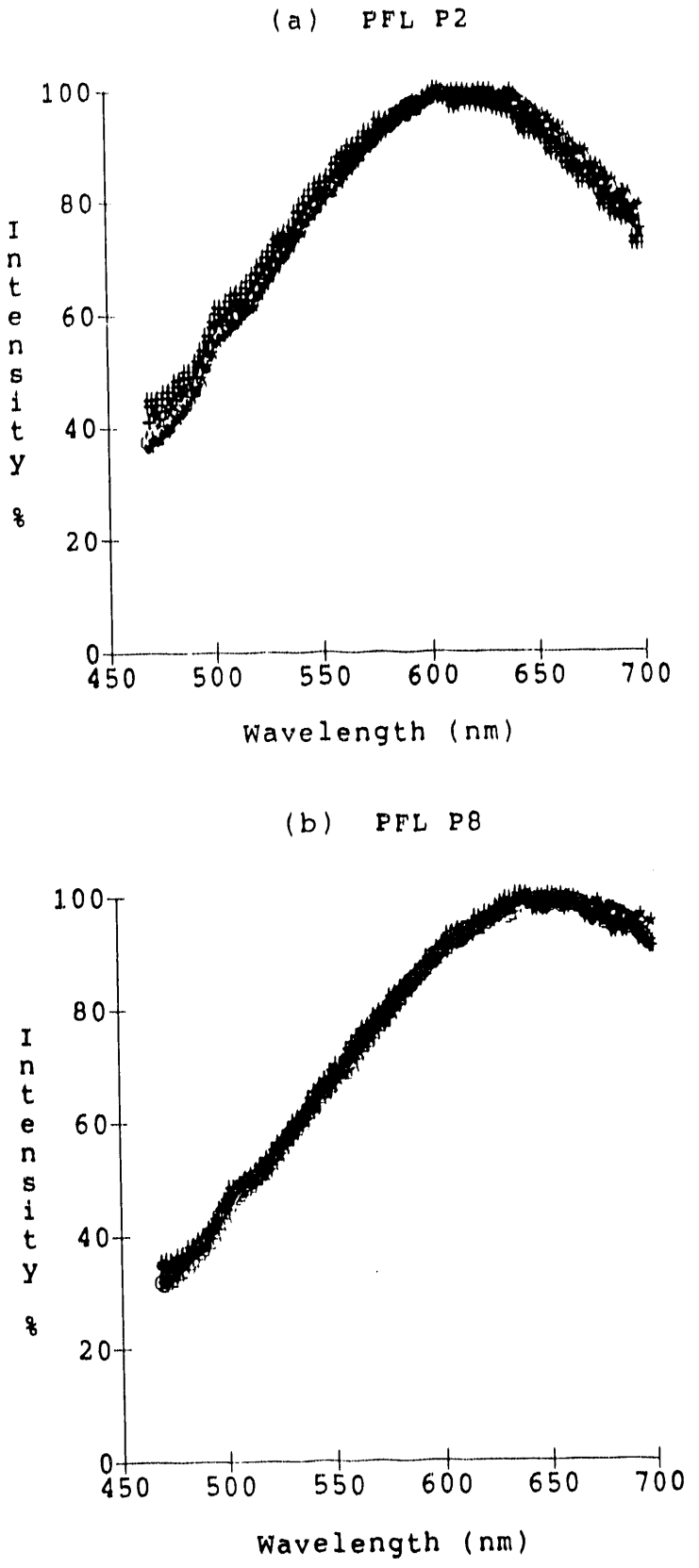

Figure 22. Corrected fluorescence spectra for HRI Run I-27 PFL resids

(c) PFL P18

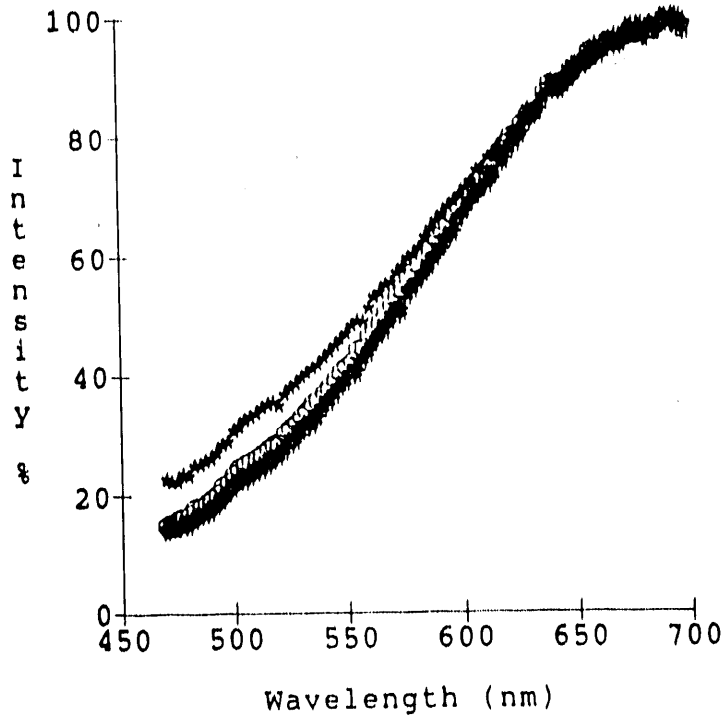

(d) PFL P25

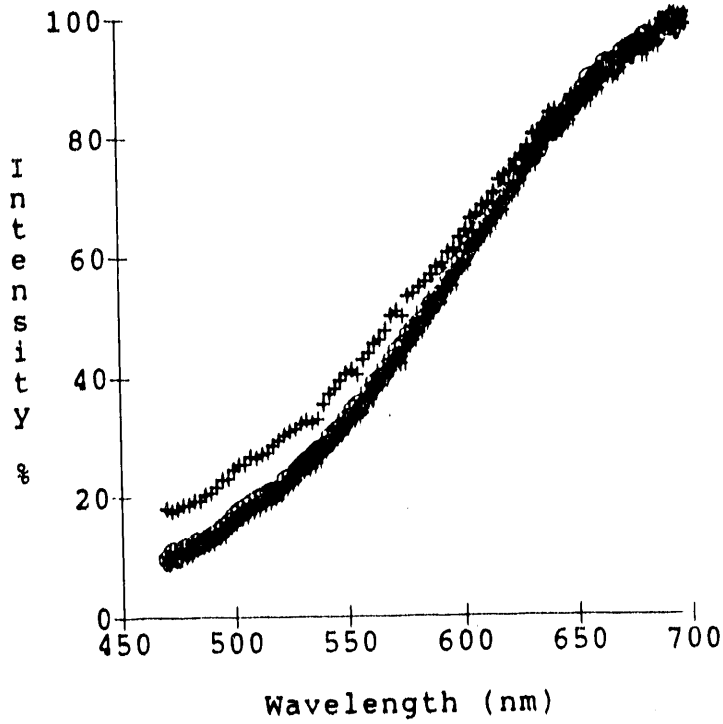

Figure 22. (continued)

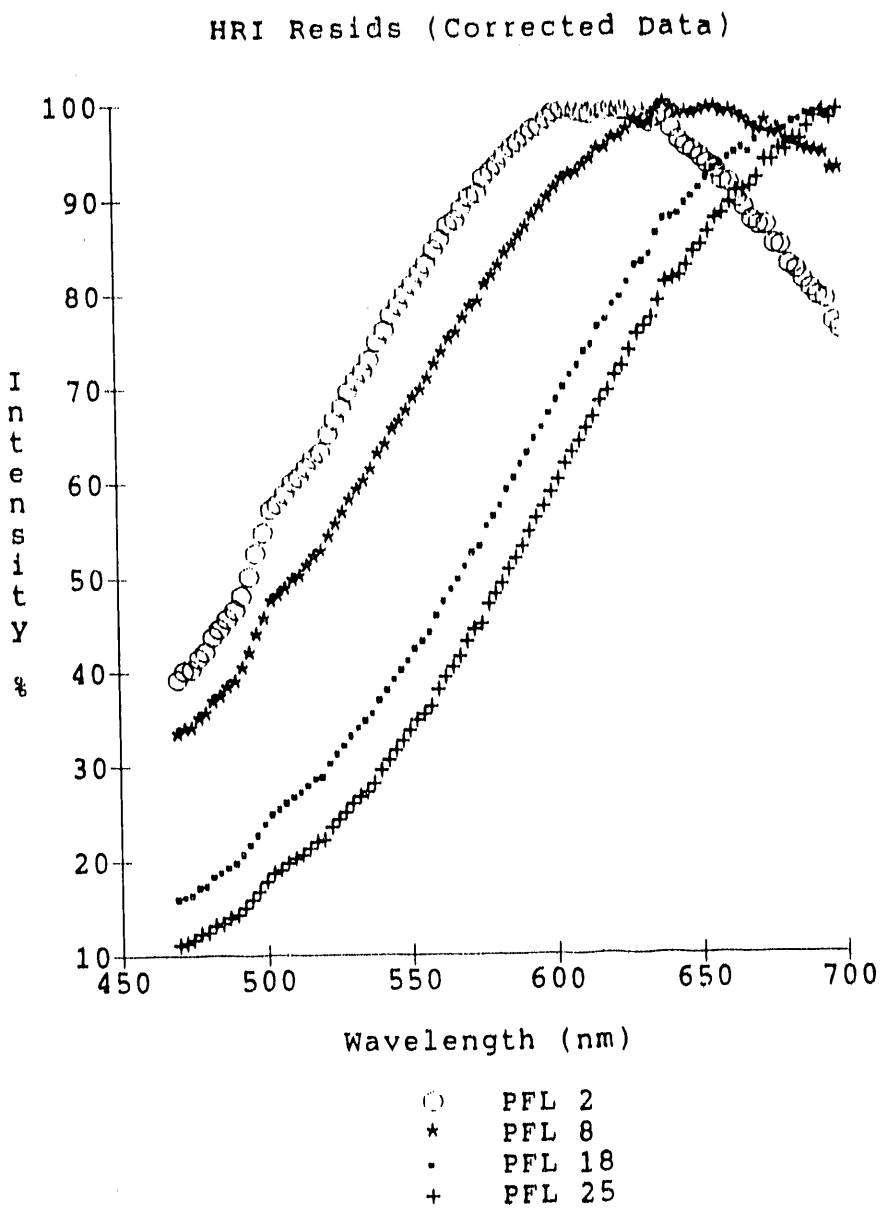

Figure 23. Averaged corrected fluorescence spectra for HRI Run I-27 PFL resids

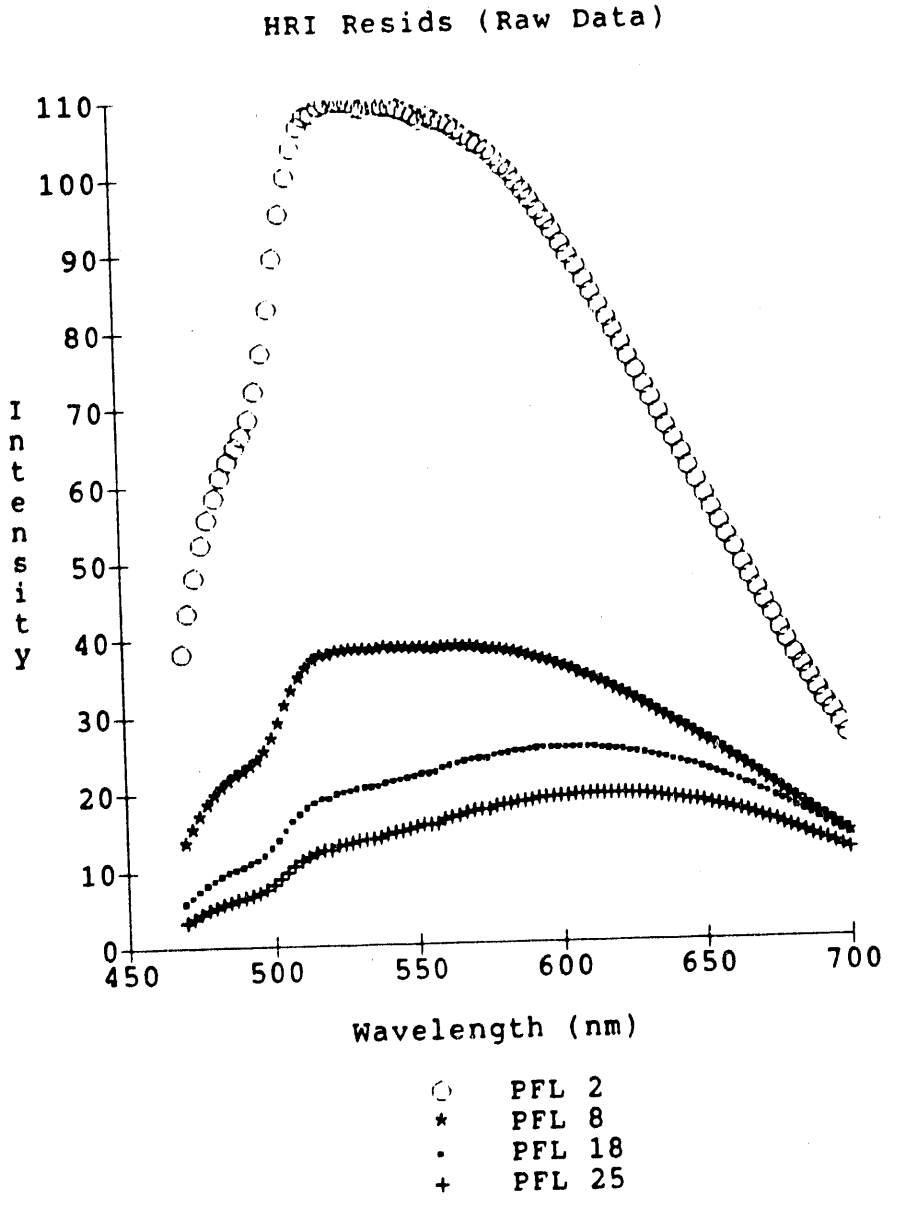

Figure 24. Averaged raw (uncorrected) fluorescence spectra of HRI Run I-27 PFL resids. Arbitrary intensity units are computer counts; intensities of different resids can be directly compared e.g. PFL 2 is the most intensely fluorescing HRI resid.

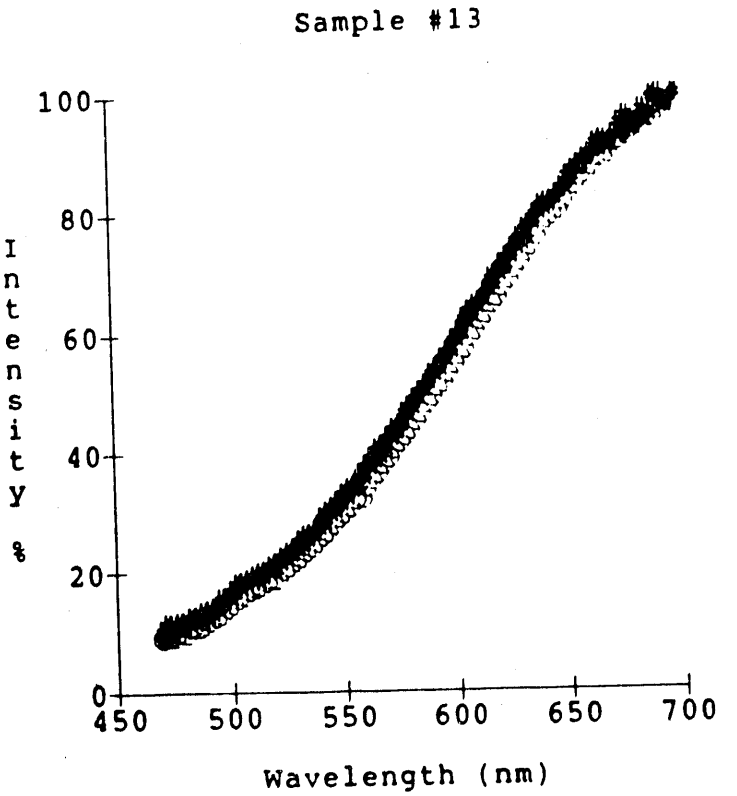

(d) PFL P25

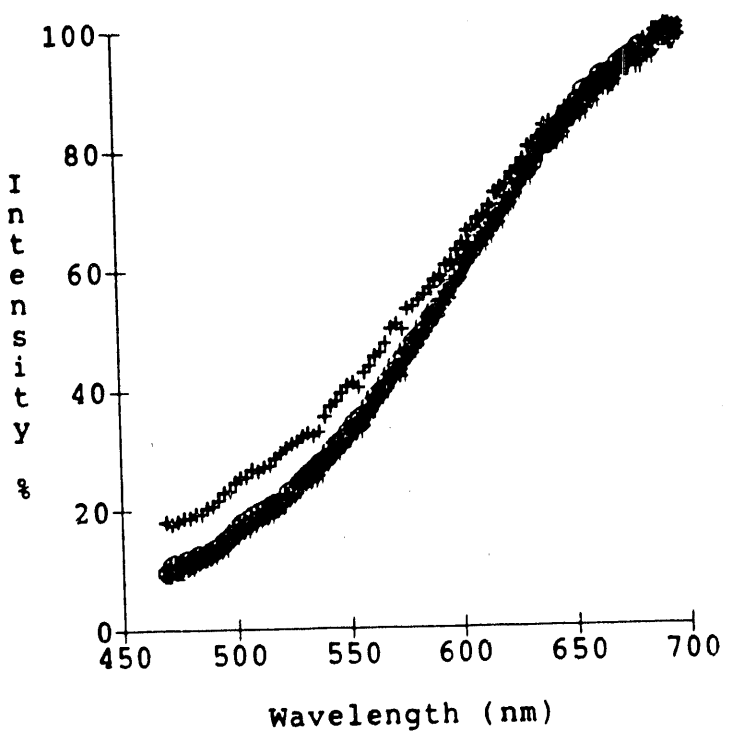

Figure 25. Corrected fluorescence spectra of sample ref. #13 (top), and HRI Run I-27 PFL 25 resid (bottom)

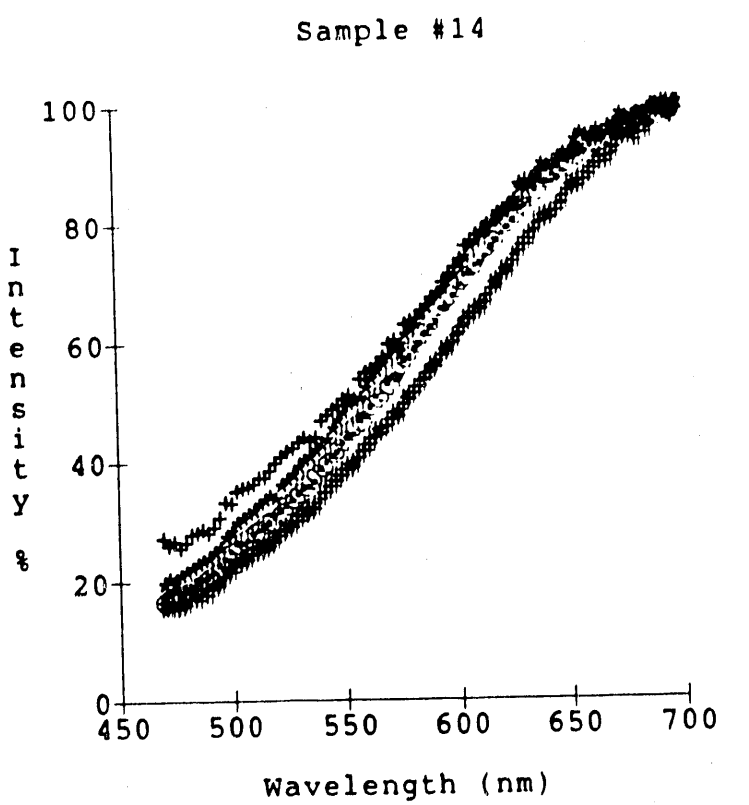

(a) Interstage

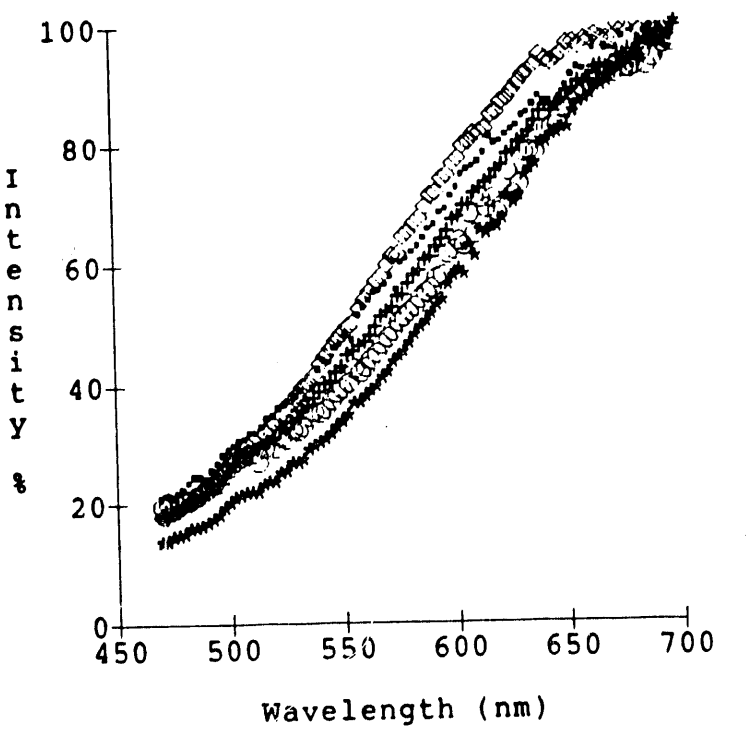

Figure 26. Corrected fluorescence spectra of sample ref. #14 (top), and Run 251-II interstage resid (bottom)

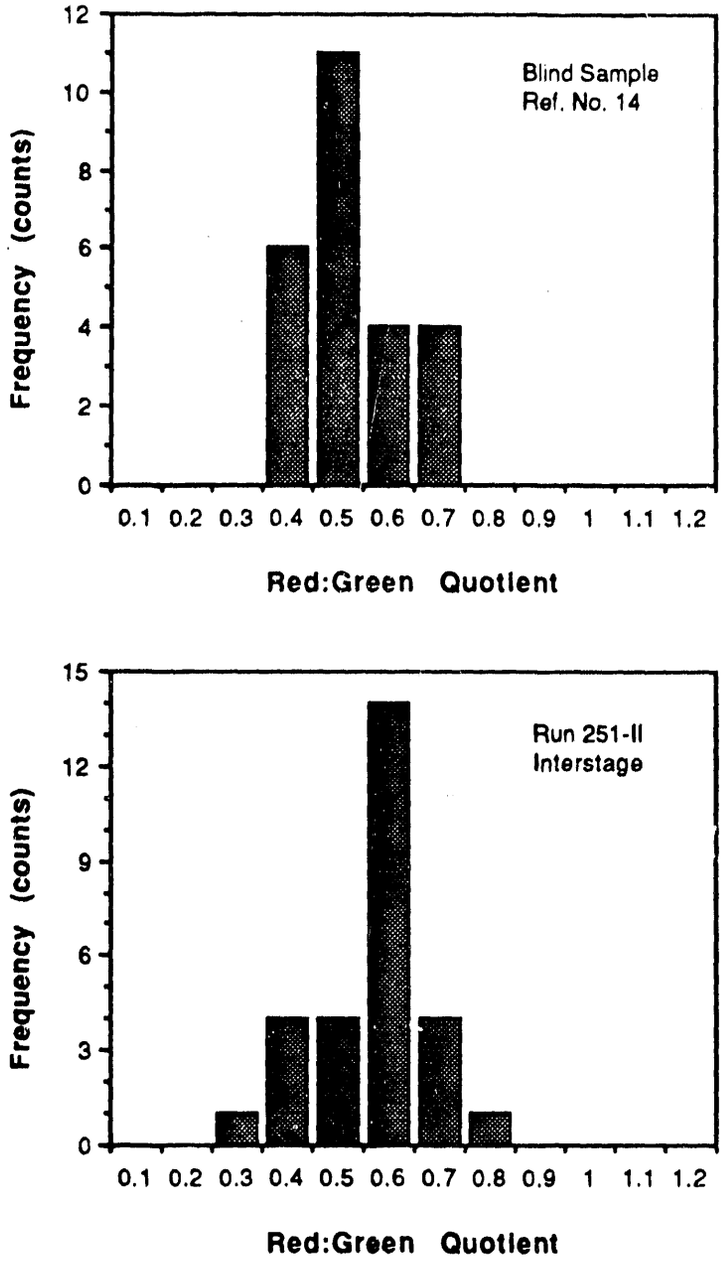

Figure 27. Red:Green quotient histograms for sample ref. # 14 and Run 251-II interstage resids

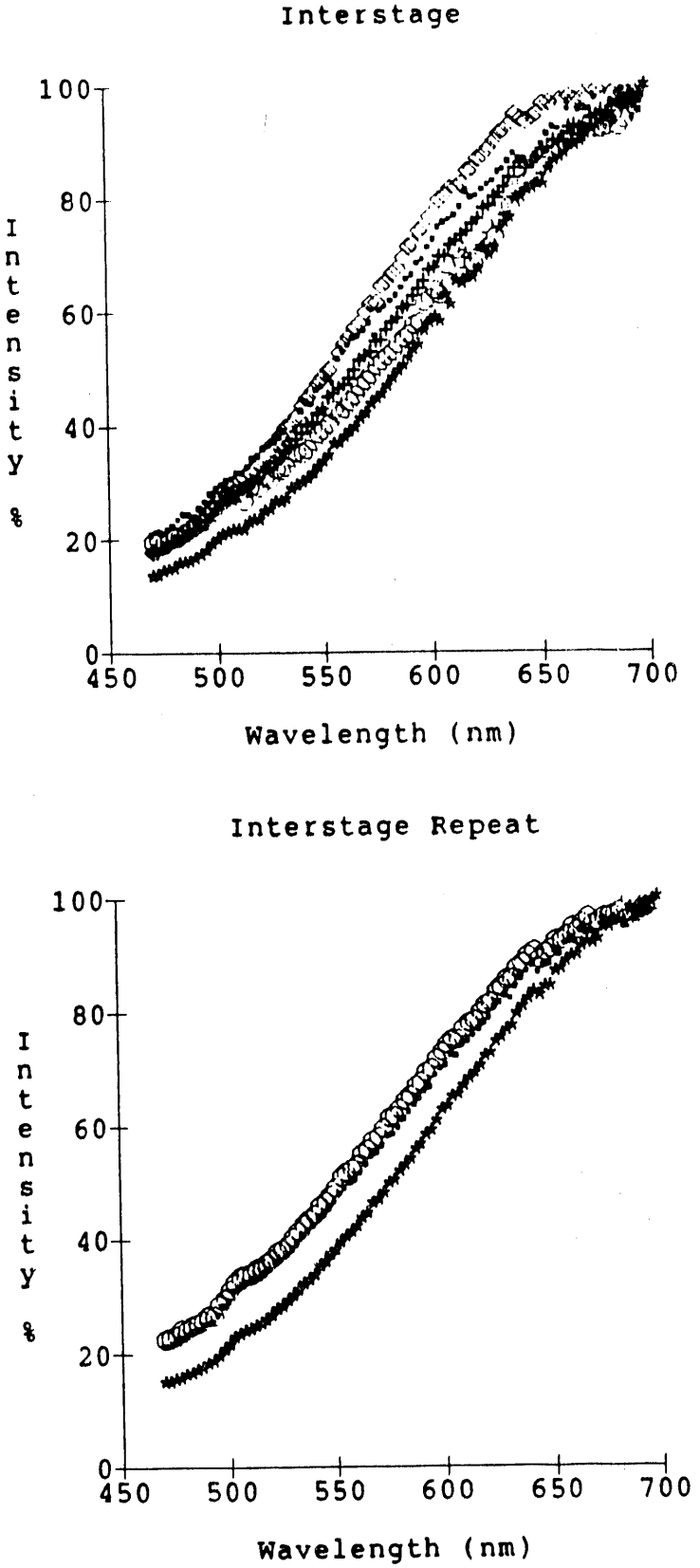

Figure 28. Corrected fluorescence spectra for Run 251-II interstage resid (top), and replicate analysis (bottom)

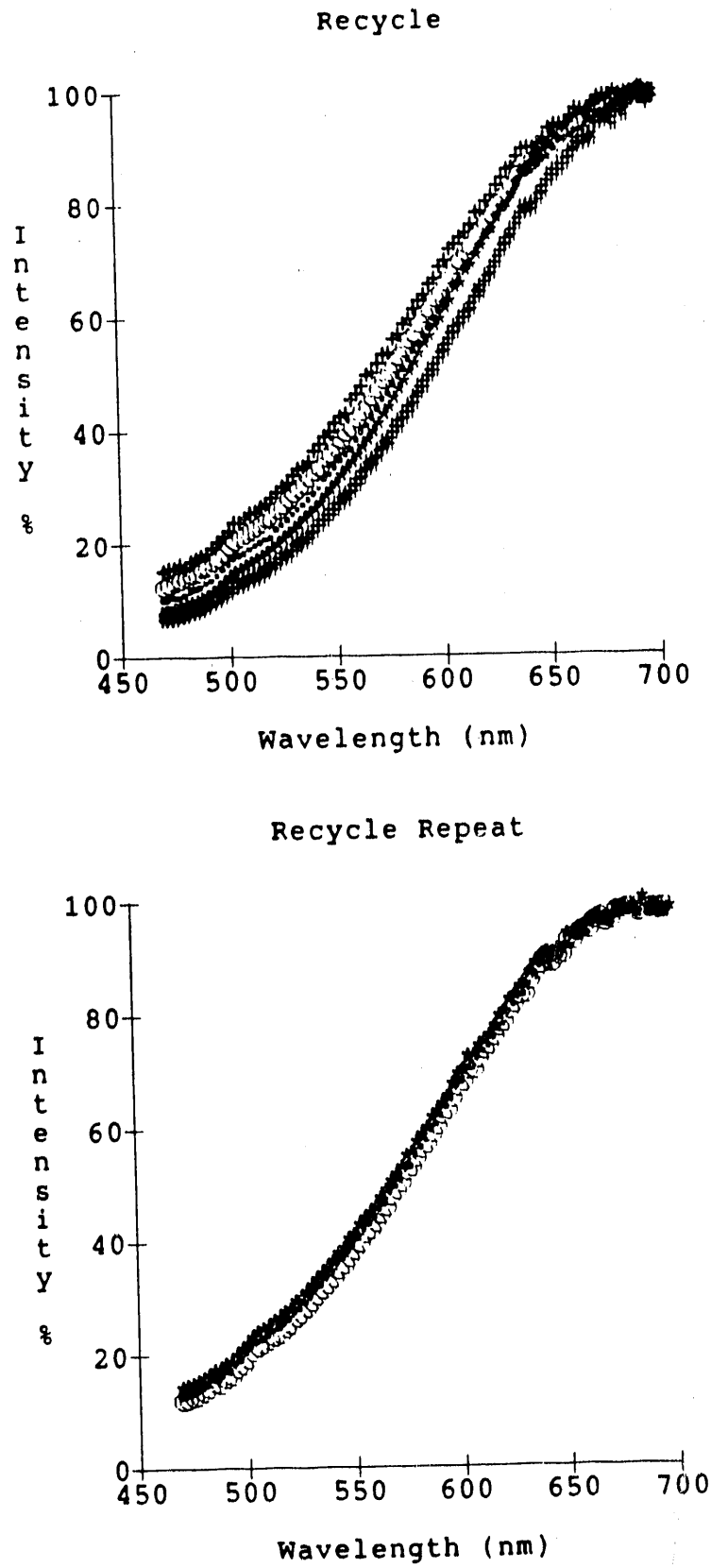

Figure 29. Same as figure 28, except for Run 259 recycle resid

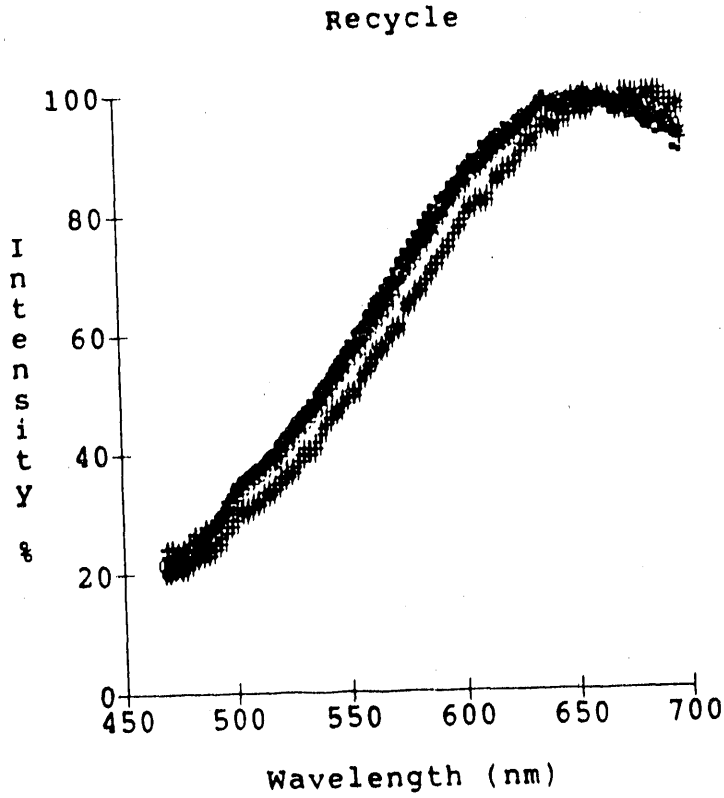

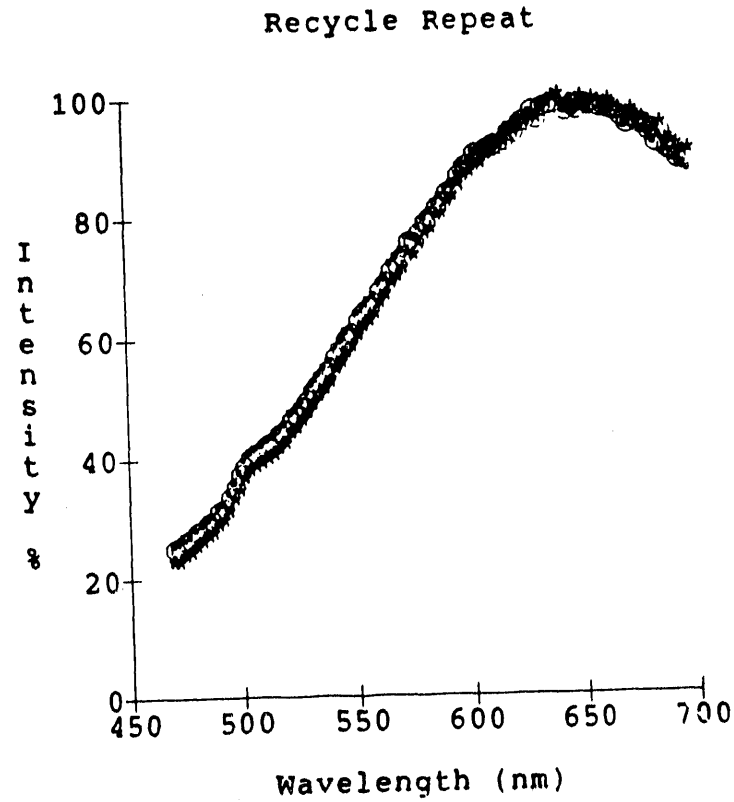

Figure 30. Same as figure 28, except for Run 250 recycle resid

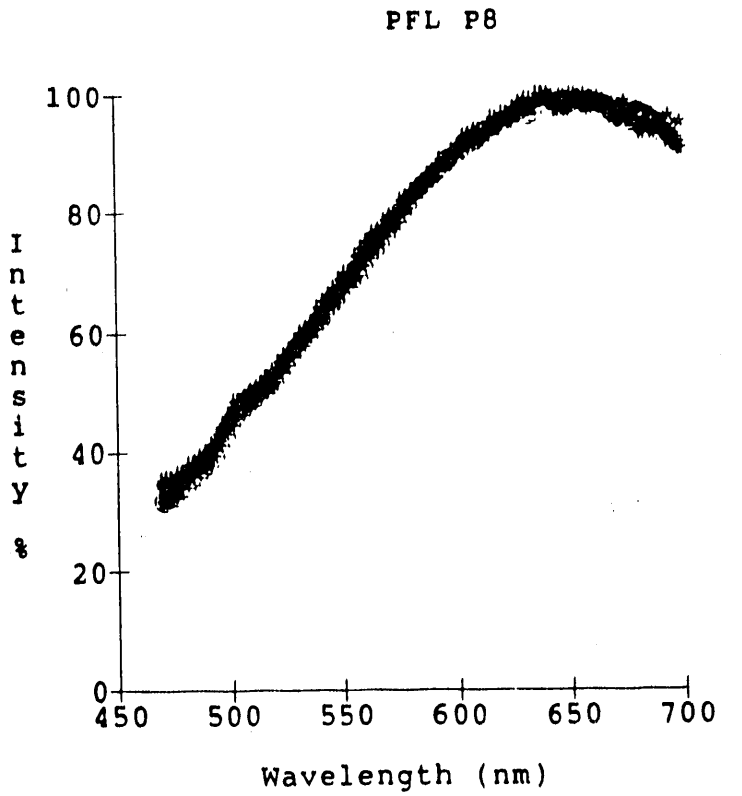

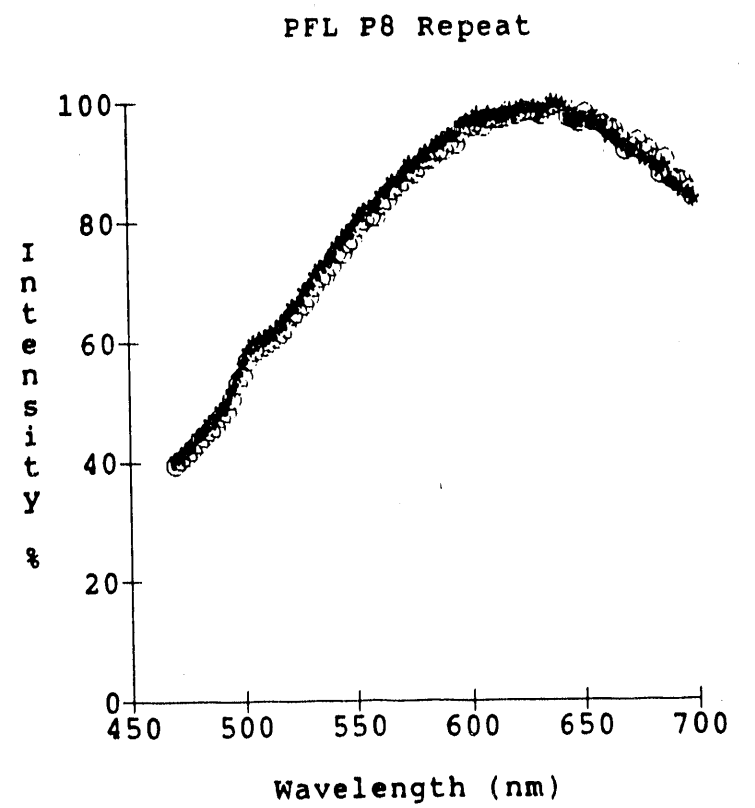

Figure 31. Same as figure 28, except for HRI Run I-27, PFL 8

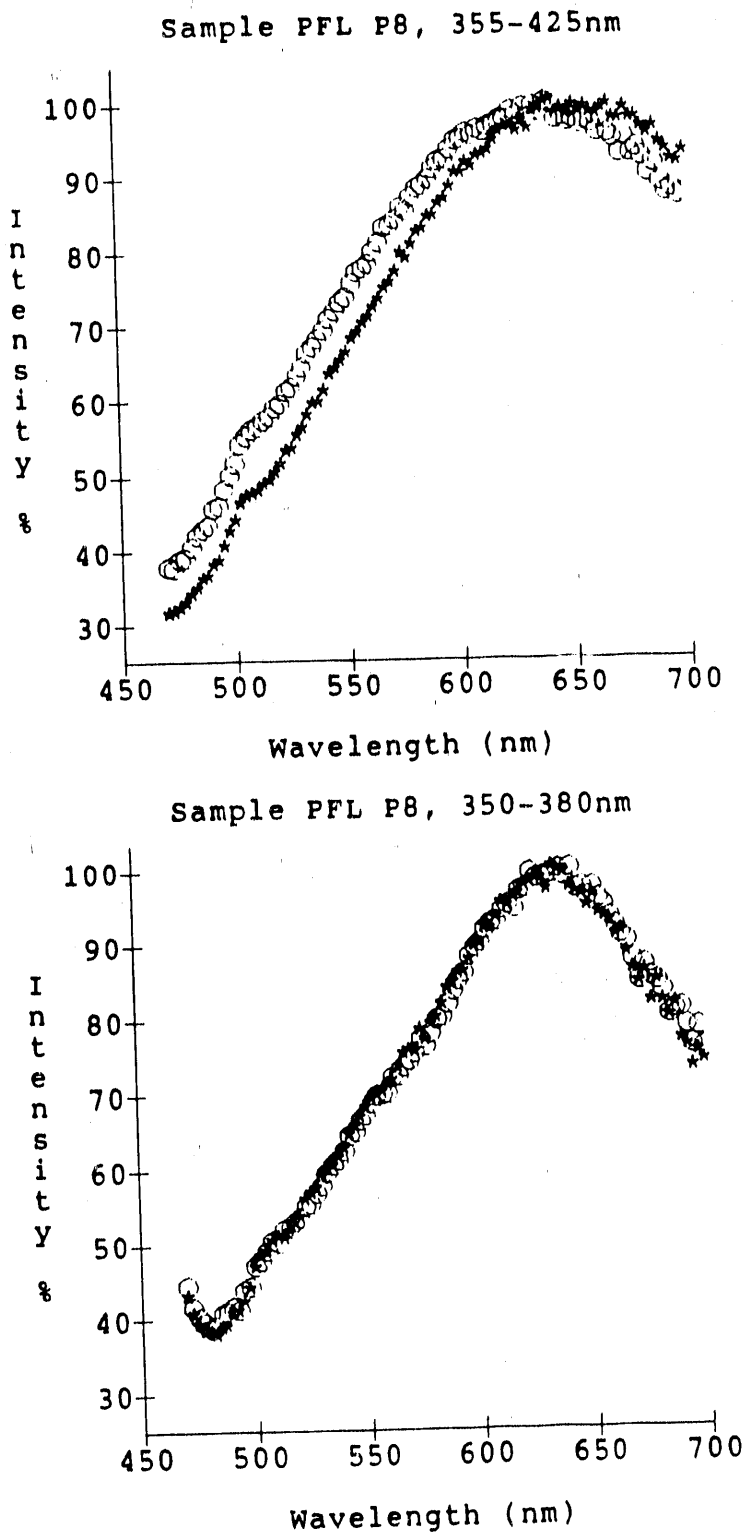

Figure 32. Corrected fluorescence spectra of HRI Run I-27 PFL P8 resid, using different mercury arc bulbs, and excitation filters. Top spectra were acquired with uv-violet excitation, whereas the bottom spectra were obtained with uv excitation.

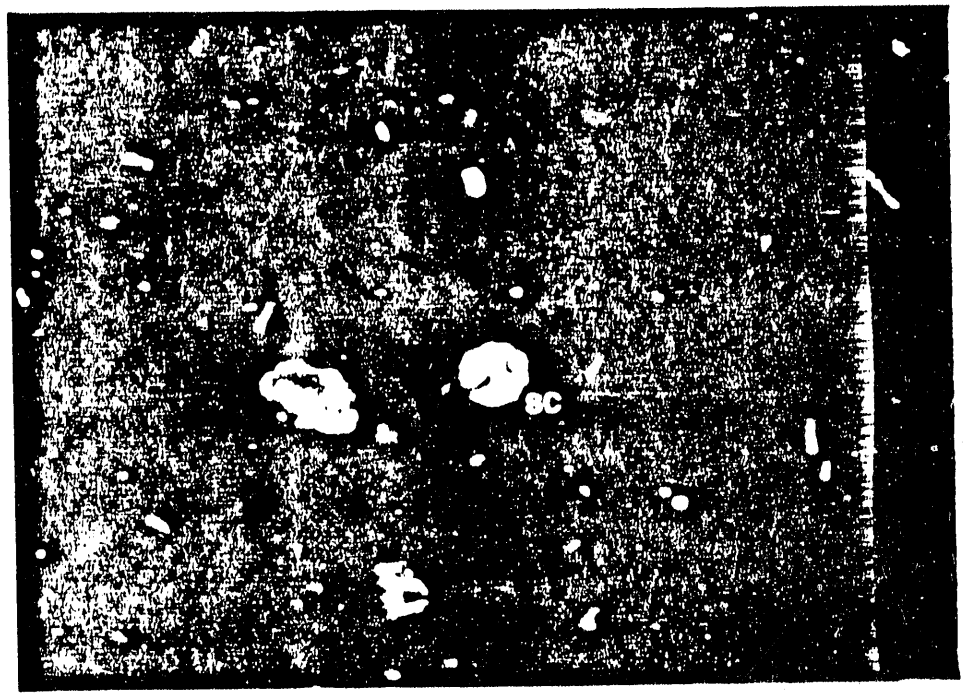

a

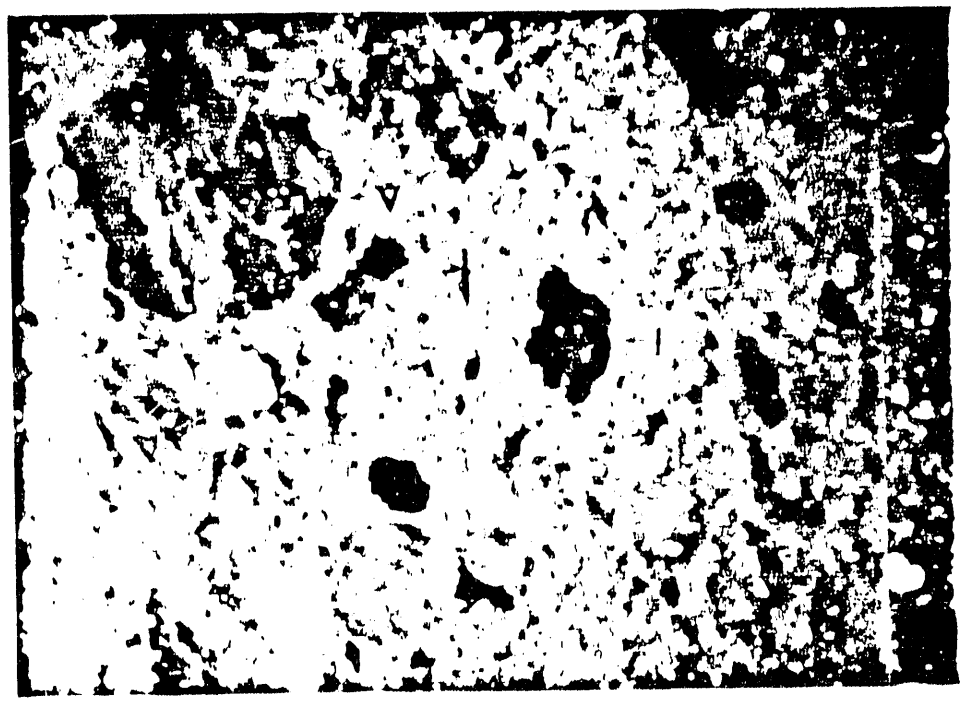

b

Plate I

a. Run 251-II. Anisotropic semi-coke sphere, observed with polarizers crossed, displaying isogyres (black, curved structures) indicative of biaxial anisotropy. White light illumination, width is approx. 250 microns.

b. Interstage resid composite from Run 251-II in uv-violet illumination. Orange fluorescing material is resid (coal liquid), bright fluorescing specks and fragments are liptinites. V = unreacted vitrinite, I = inertinite. Width is approx. 250 microns.

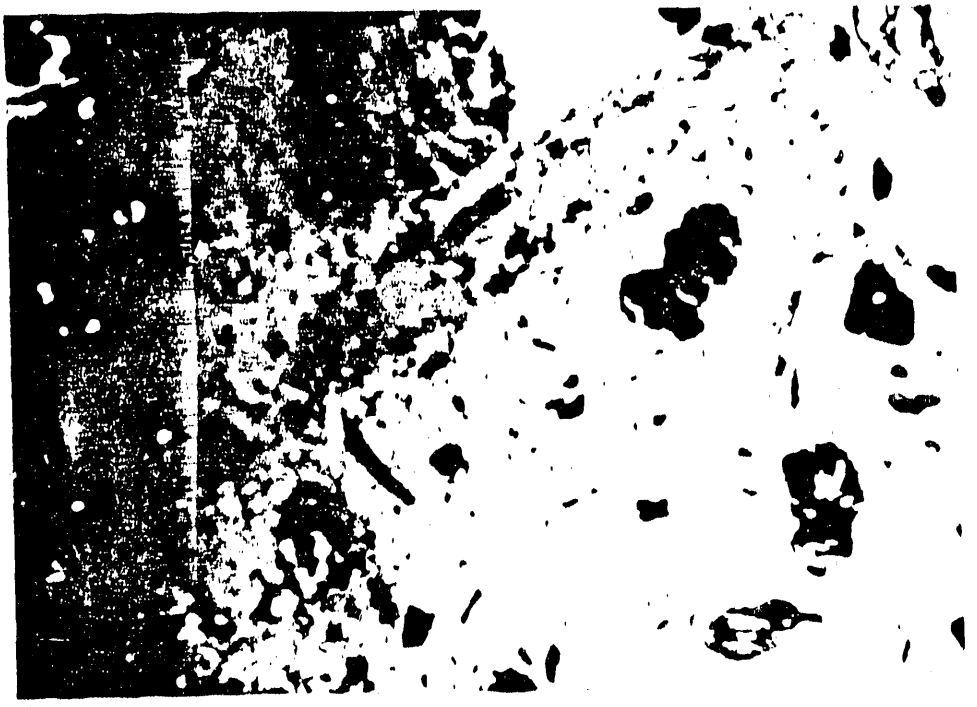

a

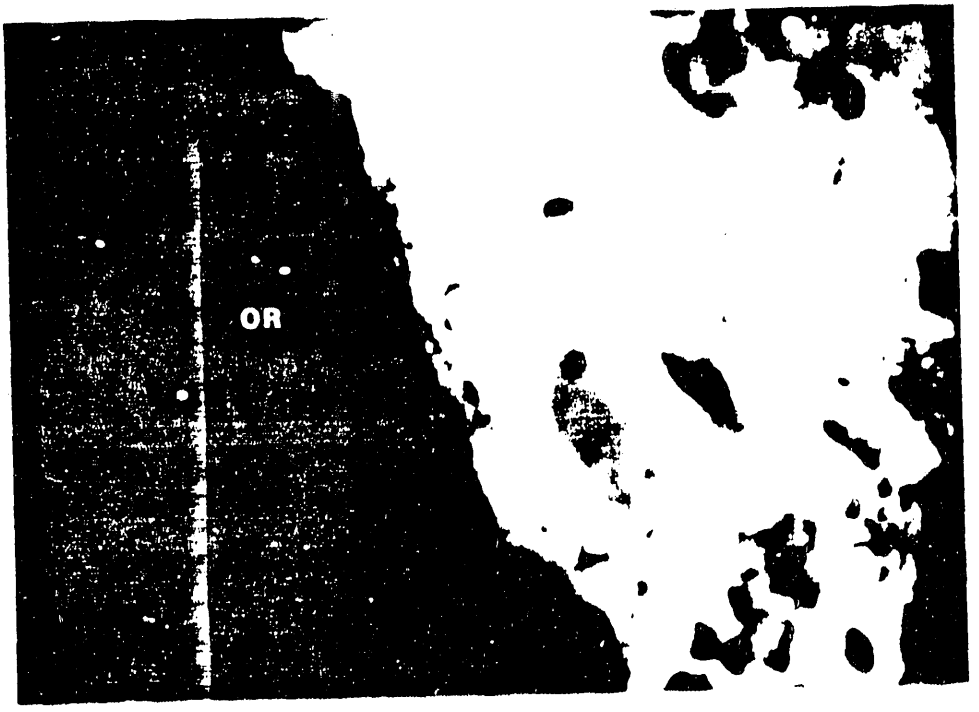

b

Plate II

a. Recycle resid composite from Run 251-II in uv-violet illumination, showing intensely yellow fluorescing resid, grading to dark, brownish orange fluorescing resid. Width = approx. 250 microns.

b. Pecycle resid composite from Run 251-II in uv-violet illumination. Similar description as IIa, except the boundary between orange fluorescing resid (or) and yellow fluorescing resid is well defined. Width = approx. 250 microns.

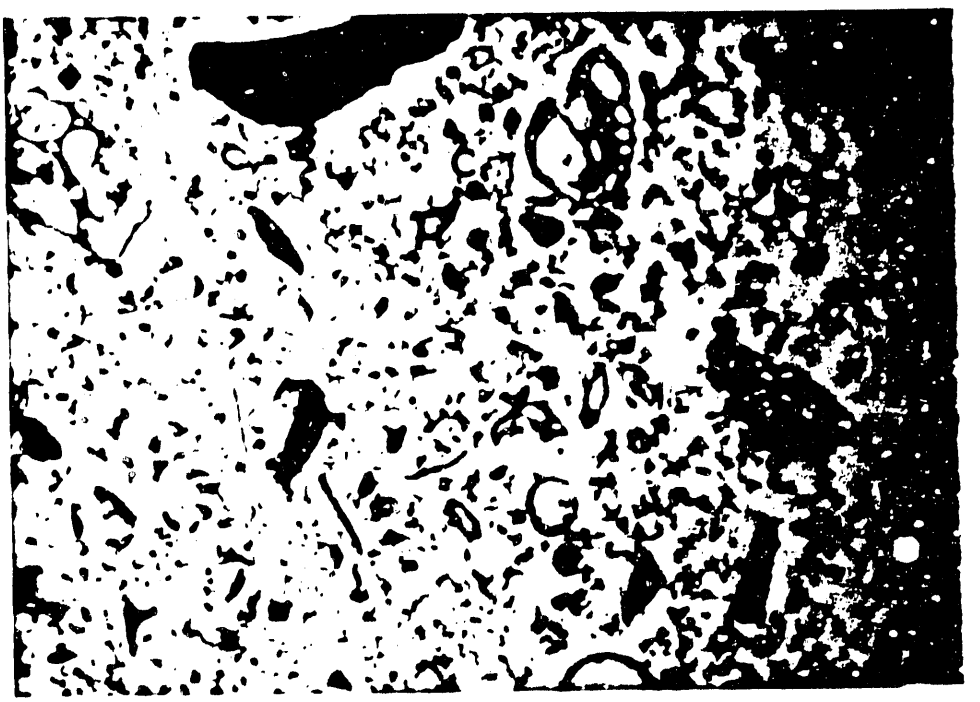

- a -

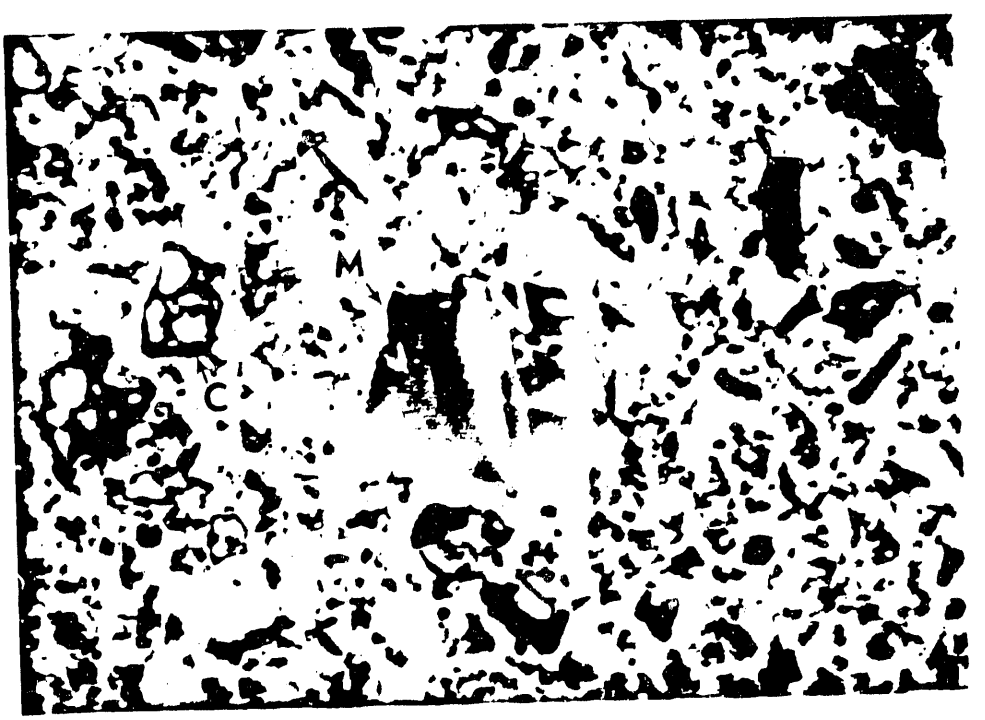

- b -

Plate III

a. Interstage resid from Run 257 in uv-violet illumination. Note gradation (left to right) in fluorescence intensity. C = cenosphere, I = inertinite. Width = approx. 250 microns.

b. Same sample as IIIa, except that resid fluorescence is greenish yellow (color of photomicrograph is not entirely representative of the observed fluorescence color). C = cenosphere, M = mineral, probably a carbonate. Approximate width of photo is 200 microns.

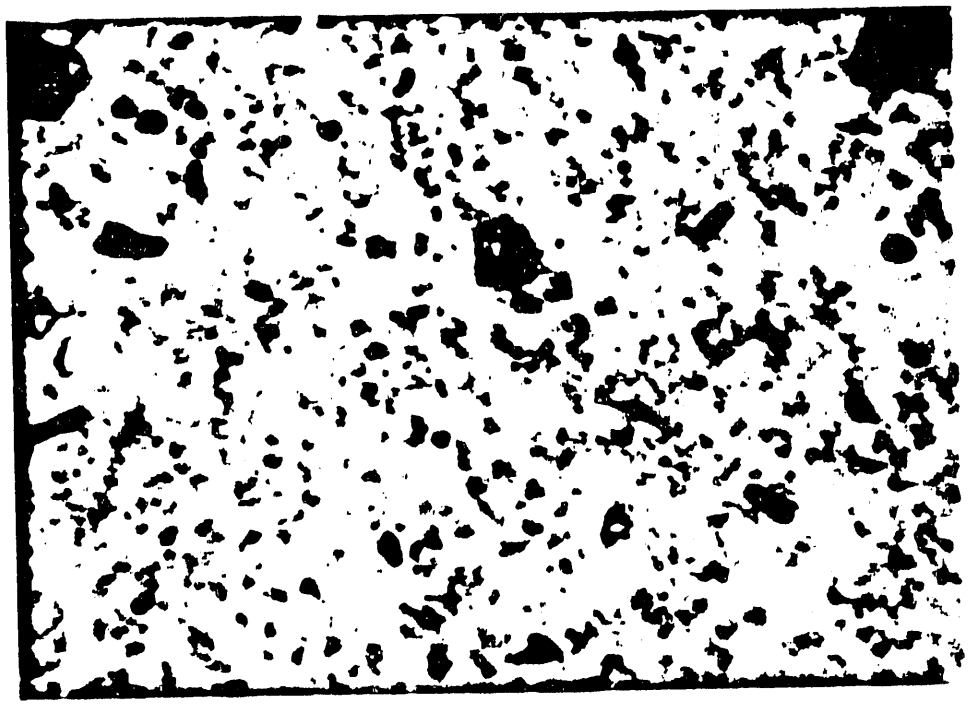

-a-

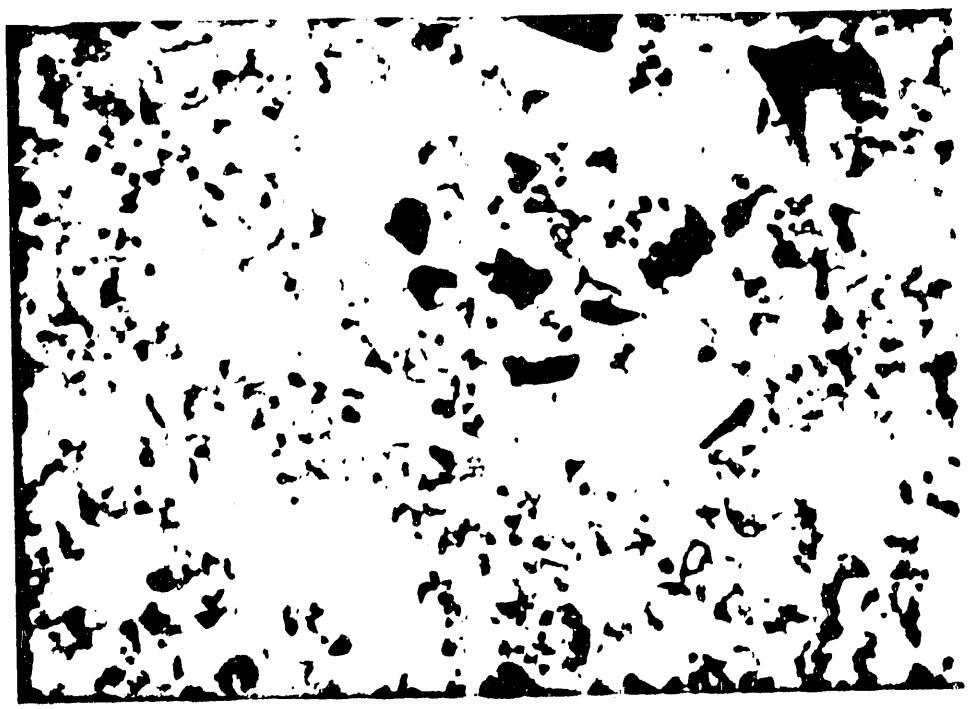

-b-

Plate IV

a. Recycle resid from Run 257 in uv-violet illumination. Orange material is resid, dark particles are mainly inertinites and cenospheres wall fragments. Width is approx. 250 microns.

b. Same sample and illumination as IVa. Despite color of photomicrograph, resid fluoresced yellowish-green. Dark particles are inertinites and cenosphere wall fragments. Width = approx. 250 microns.

Appendix I

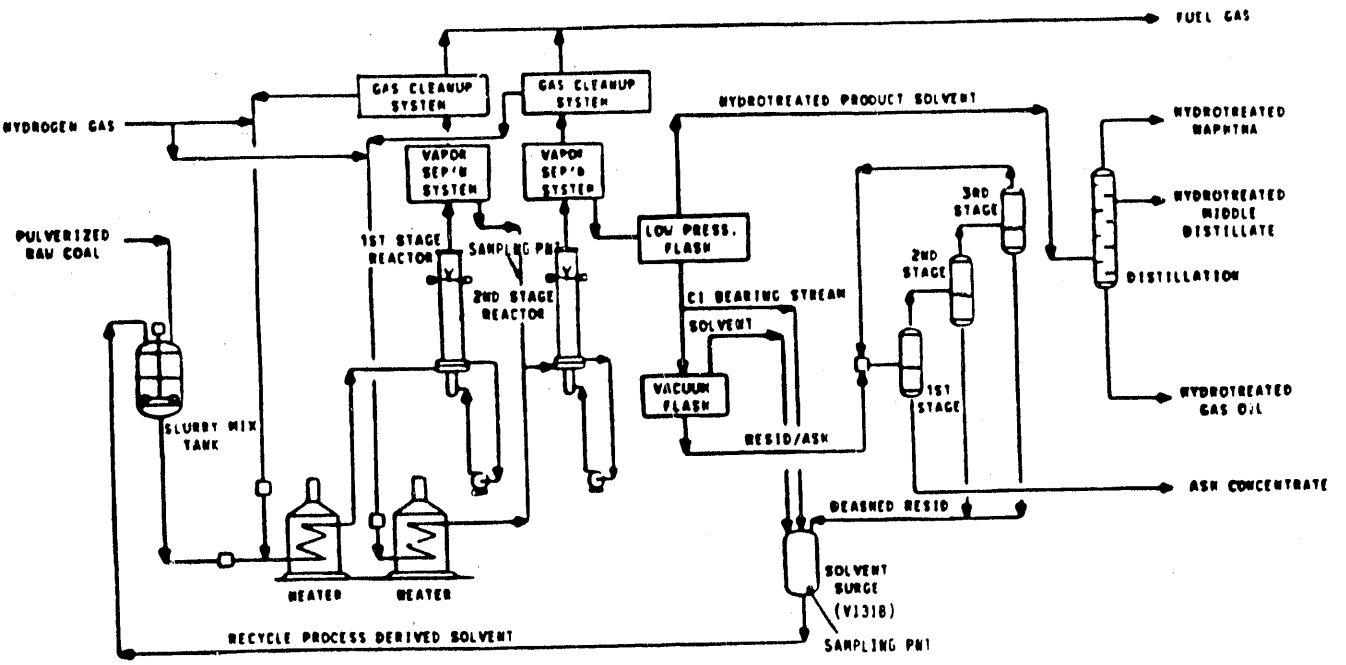

Generalized Flow Sheet

Close-Coupled Integrated Two-Stage Liquefaction System
(Wilsonville Facility, as Configured for Run 252)

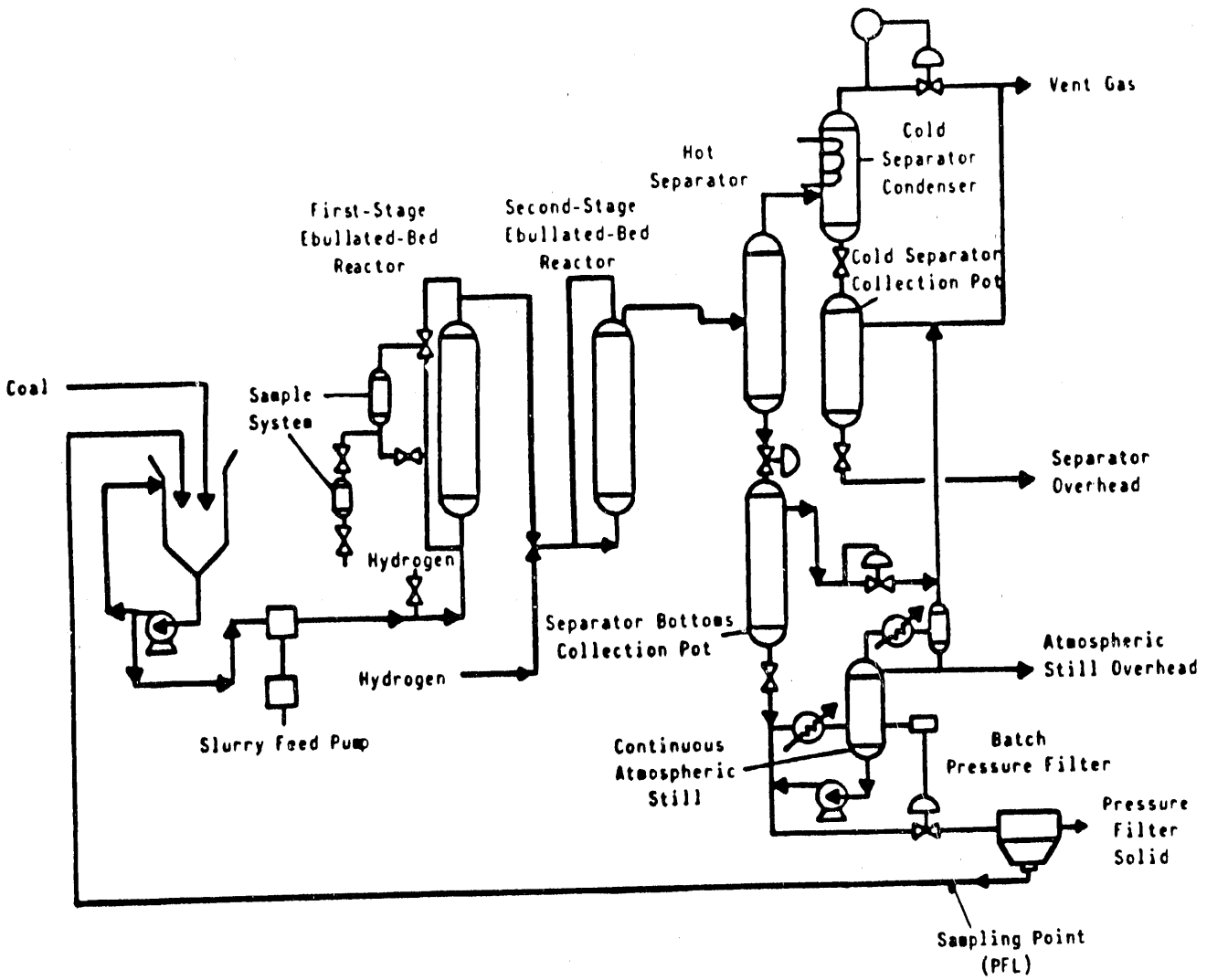

HRI Ebullated-Bed Bench Unit 227
(Excludes Solvent Inventory Tank)

Appendix II

CONDITIONS AND YIELDS FOR MATERIAL BALANCE PERIODS
Wilsonville Run 251-II

	251-11A	251-11B	251-11C	251-11D
Operating Period				
Days, 1986	7/28,29	8/2-5	8/7,8,10,11	8/14,15,17,18
Coal feed rate, MF lb/hr	352	353	354	249
Coal conc. in slurry, wt % MF	32.6	33.0	33.1	33.3
Process Solvent, wt %				
Resid (a)	25 (33)	25 (33)	26 (34)	26 (34)
Cl	23	24	24	24
First Stage				
Reaction temp., °F (avg)	819	819	818	807
Inlet H_2 part. press., psia	2530	2510	2530	2530
Space velocity, hr^{-1}	-	-	-	-
Catalyst type	-	-	-	-
Catalyst age, lb (res+Cl)/lb cat	-	-	-	-
Fe_2O_3 addition, wt % MF coal	1.0	0.8	1.5	1.5
Coal space rate, MF lb/hr/ft^3 (>700°F)	23.8	23.7	23.9	16.8
Second Stage				
Reaction temp., °F (avg)	719	743	745	745
Inlet H_2 part. press., psia	2540	2550	2560	2580
Space velocity, hr^{-1}	2.84	2.79	2.79	1.99
Catalyst type	Am. 1C	Am. 1C	Am. 1C	Am. 1C
Catalyst age, lb (res+Cl)/lb cat	725-762	915-1028	1105-1254	1339-1443
H_2 Consumption, wt % MAF	5.9 ±0.2	6.3 ±0.1	6.0 ±0.1	6.3 ±0.1
Energy Rejection, %	14.6 ±1.7	12.7 ±0.7	13.7 ±1.2	12.6 ±0.6
Yield, wt % MAF Coal				
Water	14.1 ±1.0	13.6 ±1.1	13.0 ±0.7	14.1 ±0.5
H_2S, CO, CO_2, NH_3	10.0 ±0.2	10.1 ±0.4	10.4 ±0.8	8.2 ±0.5
C_1-C_3 gas	7.4 ±0.4	8.1 ±0.3	7.0 ±0.4	6.0 ±0.8
C_4+ distillate	60.1 ±0.1	61.0 ±1.3	58.4 ±1.6	60.7 ±1.8
C_4+ naphtha	18.6 ±0.3	19.7 ±1.1	19.3 ±1.4	18.9 ±1.1
Middle distillate	10.3 ±0.1	10.3 ±0.6	11.4 ±0.7	11.0 ±0.4
Distillate solvent	31.3 ±0.4	31.1 ±1.9	27.6 ±0.9	30.8 ±3.0
Resid (b)	3.7 ±0.8	3.9 ±2.2	7.3 ±1.8	7.9 ±1.7
Ash Concentrate	10.2 ±0.7	9.4 ±0.8	9.3 ±1.0	8.7 ±0.3
H_2 Efficiency				
lb C_4+ dist/lb H_2 cons.	10.3 ±0.3	9.7 ±0.1	9.7 ±0.3	9.7 ±0.3
C_1-C_3 Selectivity (x100)				
To C_4+ distillate	13.0 ±1.0	13.0 ±1.0	12.0 ±1.0	10.0 ±2.0
Coal Conversion, wt % MAF (c)				
First stage	92.2 ±3.4	94.2 ±0.8	94.7 ±1.1	94.4 ±1.0
First and second stage	95.4 ±0.4	95.4 ±0.8	95.7 ±0.4	96.0 ±0.3
Two-stage	95.3 ±0.1	95.4 ±1.3	95.3 ±0.4	94.7 ±0.7
(Resid + UC) Conversion, wt % feed (d)				
First stage (e)	34.4 ±0.9 (61.2 ±2.8)	34.8 ±1.1 (61.0 ±1.8)	35.6 ±1.7 (62.3 ±3.1)	37.0 ±1.4 (64.1 ±1.8)
Second stage	21.6 ±2.7 (25.4 ±2.8)	23.4 ±1.3 (27.2 ±1.4)	17.8 ±2.1 (20.1 ±2.7)	18.4 ±1.7 (20.2 ±2.3)

(a) Data in parentheses on Cl-free basis.
(b) Includes TSL system UC accumulation.
(c) Cresol solubles.
(d) Data in parentheses are based on MAF coal.
(e) MAF coal as 100 wt % UC.

SUMMARY OF OPERATING CONDITIONS AND OVERALL TSL YIELDS
Wilsonville Run 259

Representative Operating Period	259B (transitional)	259C	259D	259E	259F	259G
Date, 1990	Mar 26-28	Apr 1,2,4,5,6	Apr 9-13	Apr 16-20	Apr 22,23,24,26	Apr 30, May 1,2,3,4
Operation Days	41-43	47,48,50,51,52	55-59	62-66	68,69,70,72	76-80
Coal						
Feed rate, MF lb/hr	301.6	305.4	300.5	298.7	297.5	230.0
Ash, wt % MF	4.5	4.6	4.6	4.4	4.5	4.4
Conc. in slurry, MF wt %	30.0	30.0	30.0	30.0	30.0	30.0
Process solvent, wt %						
Resid	50.9	49.3	49.9	50.4	50.5	40.3
Cl	5.9	12.0	12.0	12.0	11.6	12.0
1st stage						
Reaction temp., °F (average)	810	810	825	825	824	825
Inlet H_2 part. press., psia	2,640	2,650	2,610	2,650	2,690	2,710
Space velocity,						
lb feed/hr-lb cat	2.3	2.4	2.3	2.1	2.1	1.8
lb MF coal/hr-ft^3 cat	37.0	37.5	36.9	32.7	32.8	28.2
Catalyst type	Shell 324	Shell 324	Shell 324	Shell 324	Shell 324	Shell 324
Catalyst age, lb(resid+Cl)/lb cat	895±39	1122±23	1135±21	1115±55	1157±16	1141±16
lb MF coal/lb cat	385±13	475±8	479±8	485±6	484±7	487±6
Catalyst replacement rate, lb/ton MF coal	0.0	4.0**	4.0	4.0	4.0	4.0
2nd stage						
Reaction temp., °F (average)	790	790	790	790	790	790
Inlet H_2 part. press., psia	2,510	2,490	2,500	2,490	2,490	2,500
Space velocity,						
lb feed/hr-lb cat	2.3	2.3	2.2	1.9	1.9	1.7
lb MF coal/hr-ft^3 cat	37.0	37.5	36.9	32.7	32.8	28.2
Catalyst type	Shell 324	Shell 324	Shell 324	Shell 324	Shell 324	Shell 324
Catalyst age, lb(resid+Cl)/lb cat	718±33	825±27	959±18	966±24	940±15	924±13
lb MF coal/lb cat	385±13	487±12	494±8	488±6	490±7	490±6
Catalyst replacement rate, lb/ton MF coal	0.0	4.0**	4.0	4.0	4.0	4.0
ROSE-SR™						
DAS type	2704	2704	2704	2664	2674	2644
Yield, wt % MAF coal						
H_2	-5.9±0.3	-6.1±0.2	-6.6±0.2	-6.8±0.1	-6.3±0.4	-6.8±0.1
Water	6.4±0.3	6.4±0.5	6.7±0.5	6.7±0.8	7.1±0.4	6.5±0.6
H_2S, CO, CO_2, NH_3	4.4±0.1	4.3±0.1	4.3±0.1	4.7±0.2	4.5±0.1	4.7±0.1
C_1-C_3 gas	5.5±0.2	6.4±0.5	6.8±0.7	8.3±0.1	8.6±0.3	8.9±0.2
C_4+ distillate	75.1±3.8	65.3±3.2	69.8±1.6	73.9±2.5	63.0±3.4	73.7±2.9
C_4+ naphtha	20.1±2.0	20.7±2.8	24.0±1.7	23.9±2.7	23.8±2.1	22.7±0.7
Middle distillate	9.5±0.7	9.3±0.5	10.5±0.3	12.1±1.3	9.4±0.2	10.3±0.4
Distillate solvent	45.5±3.7	35.2±4.9	35.2±2.8	38.0±3.4	29.9±1.5	40.7±3.0
Resid*	1.1±4.1	12.9±2.3	7.6±1.5	4.3±2.2	13.4±2.6	4.0±2.1
Ash concentrate (ash-free)	13.2±0.5	10.8±1.0	9.4±0.3	8.9±0.6	9.7±1.6	8.9±0.5
H_2 efficiency						
lb C_4+ dist/lb H_2 cons	12.7±1.1	10.7±0.5	10.6±0.2	10.9±0.5	10.0±0.5	10.9±0.5
C_1-C_3 selectivity						
lb C_4+ distillate (X100)	7.3±0.6	9.8±0.7	12.6±1.0	11.2±0.4	13.6±1.0	12.0±0.7
Coal conversion, wt % MAF						
1st stage	93.4±2.9	93.3±0.6	91.8±0.4	92.8±1.0	93.8±0.7	93.1±0.6
1st and 2nd stage	94.8±0.2	95.3±0.1	95.5±0.1	95.7±0.1	95.7±0.2	95.7±0.1
Overall TSL	93.7±0.1	94.3±0.2	94.8±0.3	95.2±0.3	95.3±0.2	95.1±0.1
Resid + UC conversion, wt % feed						
1st stage	18.5±1.2	16.3±1.4	21.9±0.7	22.6±1.7	20.7±1.2	25.5±1.1
2nd stage	22.1±1.1	19.2±1.4	16.9±1.5	17.4±1.8	20.0±2.5	20.6±1.9

*UC accumulation included.
**Catalyst addition/withdrawal started April 3 and 4 in 1st and 2nd stages, respectively.

(Continued)

SUMMARY OF OPERATING CONDITIONS AND OVERALL TSL YIELDS
Wilsonville Run 259

Representative Operating Period	259I	259J
Date, 1990	May 28-31	June 5-8
Operation Days	102-105	110-113
Coal		
Feed rate, MF lb/hr	268.0	265.5
Ash, wt % MF	4.6	4.5
Conc. in slurry, MF wt %	30.2	30.0
Process solvent, wt %		
Resid	48.9	49.2
CI	12.0	11.9
1st stage		
Reaction temp., °F (average)	825	824
Inlet H_2 part. press., psia	2676	2684
Space velocity,		
lb feed/hr-lb cat	2.1	2.1
lb MF coal/hr-ft^3 cat	32.9	32.6
Catalyst type	Shell 324	Shell 324
Catalyst age, lb (resid+CI)/lb cat	1834±46	1918±46
lb MF coal/lb cat	684±16	800±16
Catalyst replacement rate, lb/ton MF coal	0**	0
2nd stage		
Reaction temp., °F (average)	791	791
Inlet H_2 part. press., psia	2513	2,510
Space velocity,		
lb feed/hr-lb cat	1.9	1.9
lb MF coal/hr-ft^3 cat	32.9	32.6
Catalyst type	Shell 324	Shell 324
Catalyst age, lb(resid+CI)/lb cat	1292±38	1529±38
lb MF coal/lb cat	673±16	765±16
Catalyst replacement rate, lb/ton MF coal	0	0
ROSE-SR^{SM}		
DAS type	2644	2684
Yield, wt % MAF coal		
H_2	-6.5±0.2	-6.0±0.1
Water	5.1±0.6	6.1±0.3
H_2S, CO, CO_2, NH_3	4.2±0.1	3.9±0.1
C_1-C_3 gas	8.4±0.3	8.2±0.3
C_4+ distillate	64.5±1.3	57.0±2.3
C_4+ naphtha	19.3±1.6	19.6±0.9
Middle distillate	8.9±0.4	8.4±0.2
Distillate solvent	36.2±1.4	28.9±1.9
Resid*	15.3±1.6	20.4±1.4
Ash concentrate (ash-free)	9.1±0.4	10.3±0.6
H_2 efficiency		
lb C_4+ dist/lb H_2 cons	9.9±0.2	9.6±0.4
C_1-C_3 selectivity		
to C_4+ ditillate (X100)	13.1±0.3	14.5±1.1
Coal conversion, wt % MAF		
1st stage	93.8±0.9	92.2±1.0
1st and 2nd stage	96.0±0.1	95.4±0.1
Overall TSL	95.4±0.2	94.6±0.3
Resid + UC conversion, wt % feed		
1st stage	19.3±1.7	17.7±0.7
2nd stage	16.8±1.9	14.5±1.3

*UC accumulation included.
**Batch deactivation started on May 22.

OPERATING CONDITIONS AND YIELD STRUCTURES
Wilsonville Run 250, Periods A-E

Operating Period	250A	250B	250C	250D	250E
Catalyst Type	Shell 324M	Shell 324M	Amocat 1C	Amocat 1C	Amocat 1C
Interstage HP Vent Separator	No	No	Yes	Yes	Yes
Ash Recycle	No	No	No	No	No
Coal Feed Rate (lb MF/hr)	190	180	180	280	340
TLU					
Reaction Temp., °F (Avg)	818	809	809	824	829
Solvent-to-Coal (MF) Ratio(a)	1.8	1.8	1.8	1.8	1.8
Volume in Use, %	50	50	50	50	50
Resid in Process Solvent, wt %(a)	49-52	48-49	48	50	49
Hydrogen Purity in Feed Gas, %	--	100	85	85	85
HTR					
Reaction Temp., °F (Avg)	728	724	703	742	750
Space Rate, WHSV, hr	1.13	0.95	1.34	2.06	2.59
Cat Age lb (resid+ash+UC)/lb cat	1289-1304	1432-1470	302-396	697-786	1040-1191
H_2 Consumption, % MAF coal	6.9±0.1	6.5 ±0.2	5.6 ±0.1	6.1 ±0.1	5.7 ±0.1
Energy Rejection, %	19.4±0.6	19.8 ±0.4	23.7 ±0.1	22.9 ±1.0	21.7 ±0.6
Yield, % MAF Coal					
Water	11.9±1.5	9.8±0.7	9.6±0.5	9.5±1.5	9.3±0.6
H_2S, CO, CO_2, NH_3	5.2±0.2	5.0±0.1	5.6±0.2	5.2±0.1	5.4±0.3
C_1-C_3 gas	7.3±0.1	6.2±0.2	5.2±0.6	7.0±0.2	6.3±0.1
C_4+ Distillate	64.6±2.6	61.0±2.3	60.5±3.2	63.9±1.6	57.9±1.8
C_4+ Naphtha	18.2±1.6	15.1±0.8	10.8±0.7	13.3±1.1	14.2±0.0
Middle Distillate	7.5±0.2	6.3±0.2	6.7±0.5	7.1±0.1	7.4±0.2
Distillate Solvent	39.9±0.9	39.6±2.7	43.0±2.9	43.5±2.7	36.3±1.6
Resid	-2.0±1.1	6.1±1.7	2.3±2.7	-1.7±1.9	7.4±1.8
Ash Concentrate	19.8±2.3	18.3±1.4	22.4±0.8	22.2±0.4	19.4±1.5
H_2 Efficiency					
lb C_4+ Dist/lb H_2 Cons	9.4±0.5	9.5±0.3	10.9±0.6	10.5±0.3	10.2±0.2
C_1-C_3 Selectivity (X100)					
to C_4+ Distillate	12.0±1.0	10.0±0.0	9.0±1.0	11.0±1.0	11.0±0.0
Coal Conversion, % MAF(b)					
TLU	NA	93.1±0.7(c)	92.1±0.5	92.8±0.3	93.2±0.3
TLU + HTR	92.9±0.1	93.4±0.5	92.9±0.3	92.3±0.2	92.8±0.5
HTR Conversion, % Feed					
Resid	NA	28.5±1.6(c)	21.8±1.7	25.6±1.1	23.9±0.1
Resid + UC	NA	27.5±1.7(c)	20.9±1.6	23.7±1.0	22.5±0.4

(a) Data in parentheses are based on Cl-free analyses of process solvent.
(b) Cresol solubles.
(c) By the forced ash balance method.

OPERATING CONDITIONS AND YIELDS
Wilsonville Run 257

Operating Period	257A	257B	257C	257D	257E	257F
Date	12/9-12/88	12/18-21/88	12/26-31/88 & 1/1/89	1/9-12/89	1/16-18/89	2/2-6/89
Coal						
Feed rate, MF lb/hr	476	483	531	423.4	402.3	345.3
Ash, wt % MF	11.5	11.4	11.3	11.2	11.4	11.4
Conc. in slurry, wt % MF	29.9	33.2	33.2	33.2	33.2	33.4
Process Solvent, wt %						
Resid	48.1	48.8	49.3	49.8	49.9	39.8
Cl	12.2	12.0	12.1	12.0	12.1	12.1
1st Stage						
Reaction temp., °F (avg)	790	790	792	791	791	790
Inlet H_2 part. pressure, psia	2680	2666	2679	2660	2658	2664
Space velocity, hr^{-1}	5.6	5.2	5.6	4.5	4.3	3.7
lbs MF coal/hr-ft³ cat	57.11±0.91	58.31±0.40	64.10±0.41	51.14±0.48	48.58±0.63	41.70±0.08
Catalyst type	Amocat 1C	Amocat 1C	Amocat 1C	Amocat 1C	Amocat 1C	Amocat 1C
Cat. age, lb (resid+Cl)/lb cat	926	1478	1440	1454	1434	1409
lb MF coal/lb cat	383	616	622	636	630	645
Cat. addition rate lbs/ton	0.0	3.0	3.0	3.0	3.0	3.0
2nd Stage						
Reaction temp., °F (avg)	760	761	760	760	760	760
Space velocity, hr^{-1}	5.6	5.2	5.6	4.6	4.3	3.7
lbs MF coal/hr-ft³ cat	57.11±0.91	58.31±0.40	64.10±0.41	51.14±0.48	48.58±0.63	41.70±0.08
Catalyst type	Amocat 1C	Amocat 1C	Amocat 1C	Amocat 1C	Amocat 1C	Amocat 1C
Cat. age, lb (resid+Cl)/lb cat	727	1404	2126	2314	2313	2228
lb MF coal/lb cat	379	727	1137	1259	1270	1277
Cat. addition rate lbs/ton	0.0	0.0	0.0	1.5	1.5	1.5
Yield, wt % MAF Coal						
H_2	-6.00±0.13	-5.58±0.07	-5.68±0.20	-6.41±0.18	-6.04±0.14	-6.29±0.11
Water	9.56±0.24	9.49±0.17	10.00±0.39	10.97±0.48	9.51±0.87	9.89±0.26
H_2S, CO, CO_2, NH_3	4.19±0.11	4.38±0.06	4.21±0.09	4.43±0.13	4.42±0.08	4.49±0.20
C_1-C_3 gas	4.44±0.36	4.43±0.21	4.76±0.25	4.41±0.30	4.68±0.17	4.80±0.21
C_4^+ distillate	63.14±3.16	58.90±1.86	59.08±2.37	65.82±3.04	66.47±1.62	62.88±2.90
C_4^+ naphtha	15.78±1.27	15.91±2.56	15.26±1.85	16.58±1.69	15.77±0.41	17.49±1.85
Middle distillate	6.35±0.47	6.13±0.37	6.10±0.46	6.84±0.55	7.01±0.51	6.95±0.61
Distillate solvent	41.01±2.22	36.86±2.87	37.72±1.27	42.40±3.40	43.69±1.01	38.44±5.42
Resid	3.27±2.32	7.84±1.86	8.68±2.23	2.02±2.82	2.14±1.30	5.60±2.45
Ash concentrate	21.40±0.23	20.55±0.99	18.96±0.52	18.77±0.85	18.81±0.53	18.63±0.82
Coal Conversion, wt % MAF						
1st and 2nd stages	91.9	92.2	93.7	92.9	93.0	91.9
Overall TSL	91.1	91.4	90.6	91.7	92.6	91.5
Resid + UC Conversion, wt % Feed						
1st stage	19.88	22.52	21.32	23.87	26.40	28.12
2nd stage	12.16	11.41	7.97	14.24	12.07	14.71

OPERATING CONDITIONS (2)
HRI CTSL Run I-27

Feed Coal: Illinois 6 (Burning Star No. 2 mine), cleaned by Bituminous Coal Research, Inc. to 5.77% ash.

Start-up Oils: Wilsonville distillate recycled during past start-ups used for heat-up and catalyst presulfiding. Coal start-up used initial solvent inventory tank blend of 50% VSOH and 50% L-720 produced in Run I-25.

Pressure: 2500 psig

Coal Space Velocity: 44.5 lbs/hr/ft^3 on a settled catalyst volume basis (each stage)

Catalyst: Shell S-317 (Ni/Mo on alumina), 1/32" extrudates

Periods	Temperature, °F		Distillate Product End-Point, °F (a)	Solvent/Coal Ratio (b)
	1st Stage	2nd Stage		
1-3	740-750	780-800	715	1.6
4-5	740-750	780-800	715	1.3
6	751-755	802-810	730	1.3
7-10	751-755	802-810	730	1.1
11-15	756-760	811-815	740	1.1
16-20	761-765	816-820	750	1.1
21-26 (c)	766-771	821-825	760	1.1

(a) Approximate end-point by ASTM D-86 of combined overhead products. Closely related to initial boiling-point of recycled pressure-filter liquid.

(b) Pressure-filter liquid to coal ratio in feed slurry. Solvent inventory tank liquid added through buffer pumps increases overall solvent/coal ratio by 0.3 to 0.4.

(c) Periods 24 through 26 used a first-stage hydrogen flow 50% greater than the other periods.

ANALYSIS OF COMPOSITED RESIDS

Reference No. 1
Plant: Wilsonville
Run Number: 251-II
Sample Designator: V1258
Sampling Point: Interstage
Feed Coal: Clovis Point Mine, Wyodak Seam

Ultimate:	
Ash, wt % as determined	25.22
C, wt % ash free	88.27
H, wt % ash free	6.07
N, wt % ash free	1.23
S, wt % ash free	1.85
O (diff) wt % ash free	2.58
Ash Elementals:	
Na_2O	
K_2O	
CaO	
MgO	
Fe_2O_3	
TiO	
P_2O_5	
SiO_2	
Al_2O_3	
SO_3	
Unaccounted	
Proton Distribution:	
Condensed Aromatics	26.8
Uncondensed Aromatics	6.4
Cyclic Alpha	20.2
Alkyl Alpha	8.9
Cyclic Beta	13.1
Alkyl Beta	16.5
Gamma	8.0
Phenolic -OH Concentration, meq/g	1.10
Phenol Peak Location, cm^{-1}	3294
Heating Value, Ash Free, Btu/lb	15653
Insoluble Organic Matter, IOM, wt %	16.0

ANALYSIS OF COMPOSITED RESIDS

Reference No. 2
Plant: Wilsonville
Run Number: 251-II
Sample Designator: V131B
Sampling Point: Recycle
Feed Coal: Clovis Point Mine, Wyodak Seam

Ultimate:	
Ash, wt % as determined	27.01
C, wt % ash free	87.81
H, wt % ash free	6.85
N, wt % ash free	0.97
S, wt % ash free	2.32
O (diff) wt % ash free	2.06
Ash Elementals:	
Na_2O	
K_2O	
CaO	
MgO	
Fe_2O_3	
TiO	
P_2O_5	
SiO_2	
Al_2O_3	
SO_3	
Unaccounted	
Proton Distribution:	
Condensed Aromatics	22.2
Uncondensed Aromatics	4.6
Cyclic Alpha	19.7
Alkyl Alpha	8.7
Cyclic Beta	15.4
Alkyl Beta	20.0
Gamma	9.4
Phenolic -OH Concentration, meq/g	0.74
Phenol Peak Location, cm^{-1}	3298
Heating Value, Ash Free, Btu/lb	16125
Insoluble Organic Matter, IOM, wt %	13.4

ANALYSIS OF COMPOSITE RESIDS

Ref. No. 3
Plant:Wilsonville
Run Number:259
Sample Designator:R1235
Sampling Point:Interstage
Feed Coal:Pittsburgh Seam
Ireland Mine

Ultimate:	
Ash, wt% as det.	8.74
C, wt % MAF	90.12
H, wt % MAF	6.19
N, wt % MAF	1.15
S, wt % MAF	1.50
O (dif), wt % MAF	1.04
Ash Elementals:	
Na_2O	0.52
K_2O	1.63
CaO	2.62
MgO	0.84
Fe_2O_3	20.67
TiO_2	0.91
P_2O_5	0.15
SiO_2	44.30
Al_2O_3	24.77
SO_3	1.46
Unaccounted	2.13
Proton Distribution:	
Condensed Aromatics	30.7
Uncondensed Aromatics	2.6
Cyclic Alpha	20.9
Alkyl Alpha	10.2
Cyclic Beta	13.8
Alkyl Beta	13.4
Gamma	8.4

Phenolic -OH Concentration (meq/g): 0.92

Heating Value (Btu/lb), ash free: 14896

Insoluble Organic Matter (IOM) wt%:

ANALYSIS OF COMPOSITE RESIDS

Ref. No. 4
Plant:Wilsonville
Run Number:259
Sample Designator:V131B
Sampling Point:Recycle
Feed Coal:Pittsburgh Seam
Ireland Mine

Ultimate:	
Ash, wt% as det.	8.51
C, wt % MAF	91.01
H, wt % MAF	6.50
N, wt % MAF	1.04
S, wt % MAF	1.25
O (dif), wt % MAF	0.20
Ash Elementals:	
Na_2O	0.52
K_2O	1.65
CaO	2.97
MgO	0.87
Fe_2O_3	20.76
TiO_2	0.93
P_2O_5	0.15
SiO_2	44.01
Al_2O_3	25.29
SO_3	1.09
Unaccounted	1.76
Proton Distribution:	
Condensed Aromatics	26.1
Uncondensed Aromatics	5.4
Cyclic Alpha	18.9
Alkyl Alpha	9.4
Cyclic Beta	14.8
Alkyl Beta	14.6
Gamma	10.8

Phenolic -OH Concentration (meq/g): 0.69

Heating Value (Btu/lb), ash free: 15177

Insoluble Organic Matter (IOM) wt%:

ANALYSIS OF COMPOSITED RESIDS

Reference No. 5
Plant: Wilsonville
Run Number: 250
Sample Designator: R1236
Sampling Point: Interstage
Feed Coal: Burning Star 2 Mine, Illinois No. 6 Seam

Ultimate:	
Ash, wt % as determined	6.13
C, wt % ash free	89.65
H, wt % ash free	6.33
N, wt % ash free	1.27
S, wt % ash free	1.02
O (diff) wt % ash free	1.73
Ash Elementals:	
Na_2O	0.26
K_2O	1.84
CaO	5.45
MgO	0.91
Fe_2O_3	17.78
TiO	0.90
P_2O_5	0.35
SiO_2	47.45
Al_2O_3	18.79
SO_3	4.57
Unaccounted	1.70
Proton Distribution:	
Condensed Aromatics	29.3
Uncondensed Aromatics	5.2
Cyclic Alpha	20.8
Alkyl Alpha	9.5
Cyclic Beta	13.9
Alkyl Beta	13.6
Gamma	7.8
Phenolic -OH Concentration, meq/g	1.07
Phenol Peak Location, cm^{-1}	3292
Heating Value, Ash Free, Btu/lb	16255
Insoluble Organic Matter, IOM, wt %	4.6

ANALYSIS OF COMPOSITED RESIDS

Reference No. 6
Plant: Wilsonville
Run Number: 250
Sample Designator: V131B
Sampling Point: Recycle
Feed Coal: Burning Star 2 Mine, Illinois No. 6 Seam

Ultimate:	
Ash, wt % as determined	0.20
C, wt % ash free	89.73
H, wt % ash free	7.43
N, wt % ash free	1.00
S, wt % ash free	0.28
O (diff) wt % ash free	1.56
Ash Elementals:	
Na_2O	0.48
K_2O	1.98
CaO	8.96
MgO	1.56
Fe_2O_3	17.70
TiO	1.85
P_2O_5	0.87
SiO_2	46.51
Al_2O_3	18.81
SO_3	
Unaccounted	1.29
Proton Distribution:	
Condensed Aromatics	20.2
Uncondensed Aromatics	5.9
Cyclic Alpha	19.1
Alkyl Alpha	9.6
Cyclic Beta	16.6
Alkyl Beta	18.2
Gamma	10.4
Phenolic -OH Concentration, meq/g	0.74
Phenol Peak Location, cm^{-1}	3299
Heating Value, Ash Free, Btu/lb	16537
Insoluble Organic Matter, IOM, wt %	0.2

ANALYSIS OF COMPOSITED RESIDS

Reference No. 7
Plant: Wilsonville
Run Number: 257
Sample Designator: R1235
Sampling Point: Interstage
Feed Coal: Burning Star 2 Mine, Illinois No. 6 Seam

Ultimate:	
Ash, wt % as determined	12.52
C, wt % ash free	88.05
H, wt % ash free	7.70
N, wt % ash free	0.86
S, wt % ash free	1.34
O (diff) wt % ash free	2.05
Ash Elementals:	
Na_2O	
K_2O	
CaO	
MgO	
Fe_2O_3	
TiO	
P_2O_5	
SiO_2	
Al_2O_3	
SO_3	
Unaccounted	
Proton Distribution:	
Condensed Aromatics	18.1
Uncondensed Aromatics	3.7
Cyclic Alpha	19.6
Alkyl Alpha	9.2
Cyclic Beta	19.2
Alkyl Beta	19.9
Gamma	10.4
Phenolic -OH Concentration, meq/g	0.68
Phenol Peak Location, cm^{-1}	3300
Heating Value, Ash Free, Btu/lb	16708
Insoluble Organic Matter, IOM, wt %	21.3

ANALYSIS OF COMPOSITED RESIDS

Reference No. 8
Plant: Wilsonville
Run Number: 257
Sample Designator: V131B
Sampling Point: Recycle
Feed Coal: Burning Star 2 Mine, Illinois No. 6 Seam

Ultimate:	
Ash, wt % as determined	9.28
C, wt % ash free	88.64
H, wt % ash free	8.08
N, wt % ash free	0.78
S, wt % ash free	1.79
O (diff) wt % ash free	1.71
Ash Elementals:	
Na_2O	
K_2O	
CaO	
MgO	
Fe_2O_3	
TiO	
P_2O_5	
SiO_2	
Al_2O_3	
SO_3	
Unaccounted	
Proton Distribution:	
Condensed Aromatics	16.8
Uncondensed Aromatics	3.1
Cyclic Alpha	19.1
Alkyl Alpha	8.9
Cyclic Beta	20.7
Alkyl Beta	20.7
Gamma	10.6
Phenolic -OH Concentration, meq/g	0.50
Phenol Peak Location, cm^{-1}	3302
Heating Value, Ash Free, Btu/lb	17056
Insoluble Organic Matter, IOM, wt %	14.8

ANALYSIS OF DAILY RESID SAMPLES

Ref. No. 9
Plant:HRI
Run Number:I-27
Sample Designator:PFL
Day Generated: Day 2
Feed Coal:Illinois No.6
Burning Star #2

Ultimate:

Ash, wt% as det.	
C, wt% as det.	88.06
H, wt% as det.	9.14
N, wt% as det	0.48
S, wt% as det.	0.03
O (dif), wt% as det.	

Proton Distribution:

Condensed Aromatics	12.0
Uncondensed Aromatics	2.5
Cyclic Alpha	18.9
Alkyl Alpha	9.2
Cyclic Beta	23.9
Alkyl Beta	22.5
Gamma	10.9

Solubility Fractions (wt%):

Oils	90.6
Asphaltenes	9.2
Preasphaltenes	0.2

Phenolic -OH Concentration (meq/g): 0.25

Phenol Peak Location (cm^{-1}):3305

ANALYSIS OF DAILY RESID SAMPLES

Ref. No. 10
Plant:HRI
Run Number:I-27
Sample Designator:PFL
Day Generated: Day 8
Feed Coal:Illinois No.6
Burning Star #2

Ultimate:

Ash, wt% as det.	
C, wt% as det.	88.25
H, wt% as det.	8.18
N, wt% as det	0.59
S, wt% as det.	0.06
O (dif), wt% as det.	

Proton Distribution:

Condensed Aromatics	17.8
Uncondensed Aromatics	2.9
Cyclic Alpha	19.6
Alkyl Alpha	8.7
Cyclic Beta	20.0
Alkyl Beta	19.8
Gamma	11.2

Solubility Fractions (wt%):

Oils	83.0
Asphaltenes	12.9
Preasphaltenes	4.1

Phenolic -OH Concentration (meq/g): 0.41

Phenol Peak Location (cm^{-1}):3301

ANALYSIS OF DAILY RESID SAMPLES

Ref. No. 11
Plant:HRI
Run Number:I-27
Sample Designator:PFL
Day Generated: Day 18
Feed Coal:Illinois No. 6
Burning Star #2

Ultimate:

Ash, wt% as det.	
C, wt% as det.	89.58
H, wt% as det.	7.12
N, wt% as det	0.90
S, wt% as det.	0.15
O (dif), wt% as det.	

Proton Distribution:

Condensed Aromatics	25.3
Uncondensed Aromatics	3.9
Cyclic Alpha	20.8
Alkyl Alpha	9.4
Cyclic Beta	16.5
Alkyl Beta	15.2
Gamma	8.8

Solubility Fractions (wt%):

Oils	78.2
Asphaltenes	18.5
Preasphaltenes	3.7

Phenolic -OH Concentration (meq/g): 0.66

Phenol Peak Location (cm^{-1}):3297

ANALYSIS OF DAILY RESID SAMPLES

Ref. No. 12
Plant:HRI
Run Number:I-27
Sample Designator:PFL
Day Generated: Day 25
Feed Coal:Illinois No.6
Burning Star #2

Ultimate:

Ash, wt% as det.	
C, wt% as det.	90.31
H, wt% as det.	6.50
N, wt% as det	1.09
S, wt% as det.	0.16
O (dif), wt% as det.	

Proton Distribution:

Condensed Aromatics	33.5
Uncondensed Aromatics	4.8
Cyclic Alpha	19.7
Alkyl Alpha	9.1
Cyclic Beta	13.9
Alkyl Beta	11.8
Gamma	7.1

Solubility Fractions (wt%):

Oils	79.0
Asphaltenes	18.1
Preasphaltenes	3.0

Phenolic -OH Concentration (meq/g): 0.71

Phenol Peak Location (cm^{-1}):3296

END

DATE
FILMED
4 128192